Summer 8-12-2011

High Throughput Screening for the Enhancement of Adeno-Associated Virus Type 2 Transduction

Alexis J. Wallen
University of Pennsylvania, wallenaj@seas.upenn.edu

High Throughput Screening for the Enhancement of Adeno-Associated Virus Type 2 Transduction

Abstract
Adeno-associated virus (AAV) is a promising vector for human gene therapy. Although more effective than non-viral vectors, AAV still requires improvement in efficacy in order to become a successful gene therapy vector. With this in mind, we have sought to identify and examine identified enhancers of adeno-associated virus type 2 (AAV2) transduction. Using a high throughput screening system with recombinant AAV2 carrying the luciferase reporter gene (AAV2-Luc), we found siRNA sequences and chemical compounds which increase AAV2 reporter gene expression. We specifically identified a hexamer seed region 5'-UGUUUC-3' which facilitated AAV2 transduction. Chemical compound enhancers included ellagic acid, 1,10-phenanthroline, EGFR tyrosine kinase inhibitors, nucleoside analogs, and DNA alkylating agents. Although several of these compounds, such as EGFR tyrosine kinase inhibitors and DNA alkylating agents, were known enhancers of AAV transduction, compounds such as ellagic acid and 1,10-phenanthroline were newly identified as facilitating AAV2 transduction. After identifying these enhancers, we have further sought to understand a mechanistic basis for them through studies which individually quantified enhancement at stages including the virus-receptor interaction, the viral DNA introduction into the cell, reporter gene RNA transcription, and the production of protein from the transgene. The identification of siRNAs and chemical compounds which enhance transduction can lead to a better understanding of AAV2 biology and may provide a foundation for the engineering of novel AAV formulations, delivery systems, or vectors.

Degree Type
Dissertation

Degree Name
Doctor of Philosophy (PhD)

Graduate Group
Chemical and Biomolecular Engineering

First Advisor
Scott L. Diamond

Keywords
adeno-associated virus, high throughput screening, siRNA, gene delivery, gene therapy

Subject Categories
Biochemical and Biomolecular Engineering

HIGH THROUGHPUT SCREENING FOR THE ENHANCEMENT OF ADENO-ASSOCIATED VIRUS TYPE 2 TRANSDUCTION

Alexis Jessica Wallen

A DISSERTATION

in

Chemical and Biomolecular Engineering

Presented to the Faculties of the University of Pennsylvania

in

Partial Fulfillment of the Requirements for the

Degree of Doctor of Philosophy

2011

Supervisor of Dissertation

_____

Scott L. Diamond

Professor of Chemical and Biomolecular Engineering

Graduate Group Chairperson

_____

Raymond J. Gorte

Professor of Chemical and Biomolecular Engineering

Dissertation Committee

Matthew J. Lazzara, Assistant Professor of Chemical and Biomolecular Engineering

Daniel A. Hammer, Professor of Bioengineering

Sara A. Cherry, Assistant Professor of Microbiology

HIGH THROUGHPUT SCREENING FOR THE ENHANCEMENT OF ADENO-ASSOCIATED VIRUS TYPE 2 TRANSDUCTION

Acknowledgments

John Donne said that "No man is an island," likewise, no PhD is produced without the assistance of many others. The work presented here is due to an entire cast of supporting characters.

First, I would like to thank my advisor, Scott Diamond. Your guidance and advice have been invaluable throughout the duration of this project. I would also like to thank my thesis committee, Matthew Lazzara, Daniel Hammer, and Sara Cherry, for their thoughtful suggestions. Maria Limberis and the Penn Vector Core provided the viral vectors used in my work, as well as advice for assay troubleshooting.

I have relied upon the support of many members of the Diamond lab. Gregory Barker's dissertation work provided a strong foundation upon which this work was based. His work included the initial optimization and set-up of high throughput screening for siRNA in our lab, as well as the primary screen for siRNA for enhancement of adenovirus and adeno-associated virus transduction. Songtao Zhou's assistance was invaluable, specifically for his help generating chemical compound data and for initial second-strand assay development. Huiyan Jing, David Fein, Renee Randazzo, and Joel Outten were extremely supportive and helpful in teaching me high throughput screening, cell culture, and molecular biology techniques required for this project. Sean Maloney and Tom Colace consulted on figure design and both served as microscope experts able to assist in troubleshooting when needed. The advice of Parag Shah and Hana Oh Chen helped me

to make the decision to pursue my research in this lab. I am also grateful to Manash Chatterjee, Dan Jaeger, Tianhua Wang, and Edinson Lucumi for their support.

I would like to thank many of my Penn CBE classmates for their kindness throughout the years, including Dalia Levine, Christine Carag Krieger, Olga Shebanova, Greg Robbins, and Pia Rodriguez. Your friendship and advice helped encourage my decision to pursue a PhD and to make the years of graduate school enjoyable.

An additional note of thanks goes to my family for their never-ending support of me and my many goals in life, as well as to my friends outside of Penn for their many years of support and friendship.

Finally, I thank David Michael Wasserman for his unconditional love and support, as well as for being a source of occasional scientific advice.

ABSTRACT

HIGH THROUGHPUT SCREENING FOR THE ENHANCEMENT OF ADENO-ASSOCIATED VIRUS TYPE 2 TRANSDUCTION

Alexis Jessica Wallen

Dr. Scott L. Diamond

Adeno-associated virus (AAV) is a promising vector for human gene therapy. Although more effective than non-viral vectors, AAV still requires improvement in efficacy in order to become a successful gene therapy vector. With this in mind, we have sought to identify and examine identified enhancers of adeno-associated virus type 2 (AAV2) transduction. Using a high throughput screening system with recombinant AAV2 carrying the luciferase reporter gene (AAV2-Luc), we found siRNA sequences and chemical compounds which increase AAV2 reporter gene expression. We specifically identified a hexamer seed region 5'-UGUUUC-3' which facilitated AAV2 transduction. Chemical compound enhancers included ellagic acid, 1,10-phenanthroline, EGFR tyrosine kinase inhibitors, nucleoside analogs, and DNA alkylating agents. Although several of these compounds, such as EGFR tyrosine kinase inhibitors and DNA alkylating agents, were known enhancers of AAV transduction, compounds such as ellagic acid and 1,10-phenanthroline were newly identified as facilitating AAV2 transduction. After identifying these enhancers, we have further sought to understand a mechanistic basis for them through studies which individually quantified enhancement at

stages including the virus-receptor interaction, the viral DNA introduction into the cell, reporter gene RNA transcription, and the production of protein from the transgene. The identification of siRNAs and chemical compounds which enhance transduction can lead to a better understanding of AAV2 biology and may provide a foundation for the engineering of novel AAV formulations, delivery systems, or vectors.

Contents

List of Tables

List of Figures

Chapter 1

Introduction

Modern medicine has led to major advances in the prevention and treatment of human diseases. Drugs and biotechnology products are available to treat a variety of ailments. Antibiotics serve as an effective cure for bacterial infections, many pills can treat disease by blocking or promoting a particular biological pathway, vaccines can prevent infection, and monoclonal antibodies can treat cancer as well as other diseases. However, many illnesses still cannot be adequately addressed with existing medications. Gene therapy, the use of nucleic acids to prevent or treat a disease, is a novel approach that holds promise for treating many of these conditions. Either ribonucleic acid (RNA) or deoxyribonucleic acid (DNA) are introduced using either a non-viral or viral delivery vehicle, called a vector. Although non-viral methods have many advantages, including a low risk of pathogenicity, non-viral methods have thus far failed to show adequate transgene expression for therapeutic benefit. Viral gene therapy methods hold great potential, however, further research is required to develop a safe and effective gene therapy vector. In this work, we will focus on high throughput screening for enhancers of adeno-associated virus type 2 (AAV2), a promising vector for viral-mediated gene delivery.

1.1. Non-viral Gene Therapy

Traditional non-viral methods of gene therapy include injection of "naked" plasmid DNA or of a formulation which packages the DNA. In the first case, plasmid DNA is injected directly. In the second case, plasmid DNA is formulated with either a lipid or polymer. In a cationic lipid system, the positively charged lipid associates with the negatively charged DNA. This both condenses the DNA and shields the negative charge from the cell's lipid bilayer membrane, facilitating transport of the DNA into the cell. A similar system can be formulated using polymers which mimic lipids, but which allow special engineering and targeting of the system[1, 2]. Variations on these systems include the use of electroporation, gold nanoparticles, or ultrasound to enhance delivery[3].

Although these systems are considered safer than viral methods, there is potential for the non-viral carrier to elicit an immune response to both the carrier as well as to the transgene. Care must be taken in the design of such as system in order to minimize an immune system response.

While non-viral gene delivery does have several characteristics making it desirable for gene therapy applications, it has thus far been limited by low transgene expression. The main application of plasmid DNA for gene therapy has been the development of vaccines, which require only a small amount of antigen to be expressed in order for the immune system to respond. However, even DNA vaccines have shown limited success[4, 5].

1.2. Viral Gene Therapy

Viral gene therapy has the advantage of being more efficient than non-viral gene therapy. Viruses have evolved over time to be highly capable of transducing human cells, and the wide variety of virus strains allows researchers a large toolbox of characteristics from which to choose. Some viruses are specific to certain types of tissue or to dividing or non-dividing cell types. Viruses can be selected that do or do not integrate into the genome.

While it is helpful to have so many different viruses from which to choose, most viral methods of gene delivery do present a safety concern, especially given the clinical history of treatments with retroviruses and adenovirus. In the case of retrovirus, the gene therapy succeeded in curing X-linked severe combined immunodeficiency (X-linked SCID), but several of the patients developed leukemia[6-9]. In the case of adenovirus, a 1999 clinical trial for the liver-directed gene therapy treatment of ornithine transcarbamylase deficiency led to the immune-response linked death of a patient[10, 11]. Although these trials showed promise for efficacy of human gene therapy, it was clear that the development of a safer vector was needed. Adeno-associated virus (AAV) is seen as a promising viral vector for gene delivery with a strong safety profile.

1.3. Adeno-associated Virus as a Gene Therapy Vector

AAV, although widespread in the population, has not been known to cause any human disease. This small virus, with a diameter of 20 nm packaging 4.7 kb of single-stranded

DNA, was originally discovered as a contaminant in an adenovirus preparation and is incapable of replicating in the absence of a helper virus[12]. The engineered virus additionally has all replication genes removed, so replication does not proceed even if a helper virus is present. The wild-type virus integrates into the human genome at a specific location on chromosome 19 which has not been implicated in oncogenesis [13, 14]. The engineered virus does not integrate into the genome due to the missing *Rep* gene which facilitates integration [15, 16]. In general, the low immune response and lack of associated human disease make it a strong candidate for viral gene therapy. The virus additionally exists in nature in a variety of serotypes, which show differences in tropism for various target organs within the human body.

Adeno-associated virus does, however, have some disadvantages as a vector. Because the engineered virus lacks the ability to insert into the chromosome, gene expression will be lost over time in dividing cell types. Additionally, thus far success in clinical trials has been elusive due to limited transgene expression. In laboratory experiments, previous researchers have found a range of anywhere from 1 in 100 to 1 in 10^6 viral particles will succeed in transducing cells, depending upon the cell line and conditions used [17-19]. However, strong advances are being made in increasing transduction efficiency through directed evolution of virus and targeted virus mutations.

1.4. Adeno-associated Virus type 2 biology

In this work, we have chosen to focus on adeno-associated virus type 2 (AAV2), as it is the most well-characterized serotype. The biological pathway for AAV viral entry and

gene expression contains numerous steps involving host proteins that control the level of transgene delivery and expression. First, AAV must bind to heparin sulfate proteoglycan cell surface receptors [20, 21]. Following binding, AAV must be endocytosed in the presence of $\alpha_V\beta_5$ integrin and with activation of Rac-1 [21]. Following endosome escape, the viral genome must gain entry to the nucleus, where viral DNA synthesis and transcription of the viral genome take place.

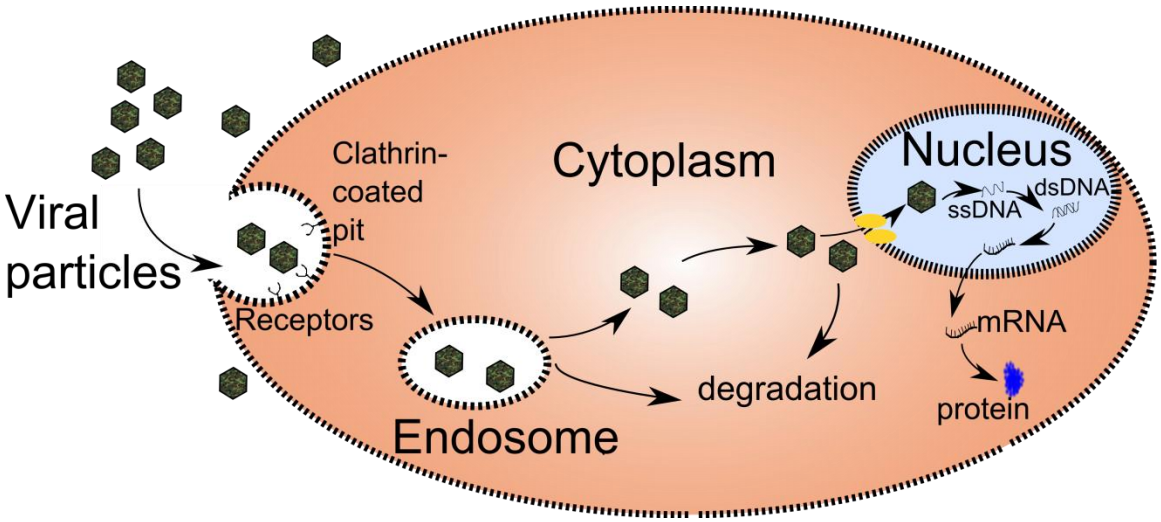

Figure 1.1: Adeno-associated viral transduction. Viral particles attach to cell surface receptors, are endocytosed via a clathrin-coated pit, escape from the endosome, are transported to the perinuclear space, cross the nuclear membrane, are uncoated, and the second strand of DNA is synthesized. Once double-stranded DNA is in place, normal cellular machinery is used to transcribe DNA to RNA, which is then transported out of the nucleus, where RNA is translated to protein.

In this work, we seek to add to the adeno-associated virus literature in an attempt to enhance adeno-associated virus transduction efficiency. Although this virus has been extensively studied, there are still many unknowns in the viral transduction pathway. Here, we use two high throughput screens to better understand the virus, with the dual

goals of providing insight into the biology of the virus and providing new information to benefit future efforts to design better formulations and/or engineer next generation AAV serotypes.

1.5. Pseudotyped AAV

AAV exists in nature in a variety of serotypes which have slight differences. For example, whereas type 2 binds to heparan sulfate proteoglycan, type 1 binds to sialic acid on the cell surface and type 9 binds to galactose on the cell surface [22, 23]. Coreceptors additionally facilitate the binding to these primary receptors. A pseudotyped vector contains the capsid from one serotype and the genome from a different serotype, allowing independent manipulation of the viral capsids and genome [24-26].

1.6. RNA Interference

RNA interference is a naturally occurring process in which antisense RNA is used to generate a host cell response which leads to the degradation of the complementary RNA[27]. siRNA, or short interfering RNA, is a short double-stranded RNA of 21-23 nucleotides which effectively uses this cellular machinery to generate a strong knock-down of RNA [28]. This knock-down of RNA leads to a decrease in corresponding protein, allowing loss-of-function experiments.

Despite optimization of siRNA sequence selection, both sequence-dependent and sequence-independent off-target effects may occur, causing unintended effects [29-36]. For

example, an individual siRNA targeting a particular gene can show a different mRNA expression profile from another siRNA that successfully targets the same gene [29]. An additional type of sequence-dependent off-target effect arises from the hexamer seed region, located at positions 2-7 of the siRNA sequence. This region can bind to the 3'UTR of various mRNA species and can lead to a complex pattern of mRNA cleavage and translational silencing [31, 33], thereby functioning in a similar manner as microRNA (miRNA).

In the first of two high throughput screens described in this work, we utilize this mechanism to identify siRNA enhancers of viral transduction.

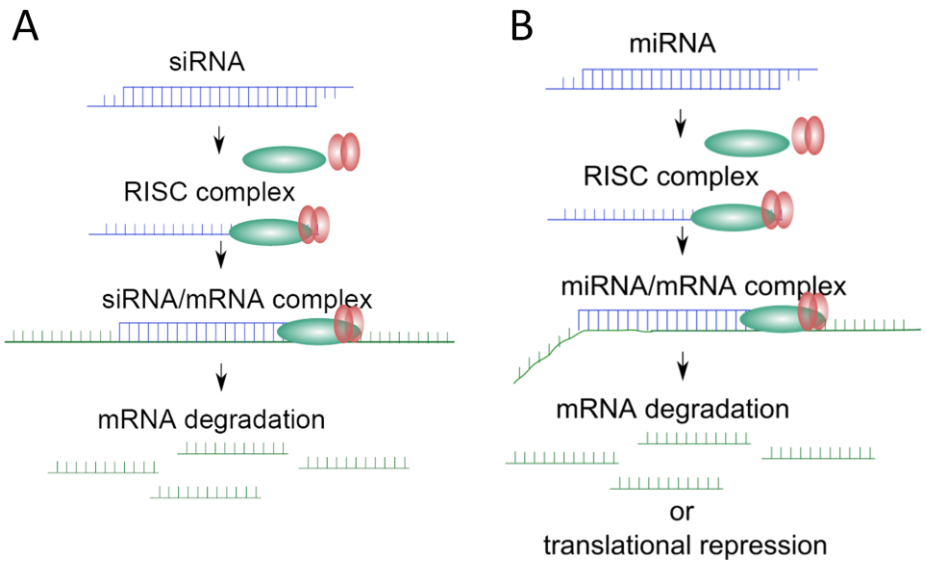

Figure 1.2: Mechanism of siRNA and miRNA pathway. A) In the siRNA pathway, double-stranded siRNA is introduced into the cell, where it is recognized by and loaded into the RNA-induced silencing complex (RISC). When complementary mRNA is found, the RNase is activated and cleaves the mRNA strand. B) in the miRNA pathway, similar events occur, however the miRNA can be either perfectly complementary to the mRNA or complementary to only the hexamer seed region. The result is either mRNA degradation or translational repression.

1.7. Chemical Modifiers of Viral Transduction

As described in section 1.4, the interaction between viruses and host cells is complex. Chemical modifiers have the potential to interact with the virus or its products at each step of the viral transduction pathway and to activate or inhibit these stages. In a second high throughput screen, we used small molecule chemical compounds known to be pharmacologically active in order to perturb this system and learn more about the cell-virus interaction and enhancements of this interaction.

1.8. Objectives

The overarching goal of this work was identification of enhancers of AAV2 transduction, with the desired outcome of learning more about the AAV2 pathway and providing information that can lead to the engineering or formulation of a more effective AAV2 vector. In order to do so, we have conducted two high throughput screens. In the first, we examined siRNA and were able to identify a consensus hexamer seed region. In the second, we identified several chemical compound enhancers of AAV2, some previously known to enhance AAV2 and some which were newly identified.

Chapter 2

siRNA High Throughput Screen

The majority of this work has been published in *Molecular Therapy*.[37]

Adeno-associated virus (AAV) is a promising vector for gene delivery. AAV vectors have several advantages including: low pathogenicity, low immune response, long term episomal expression in nondividing cell types, and specific organ targeting based on the serotype used [38-41]. However, insufficient transgene expression has limited the success of a number of human clinical trials that used AAV vectors [42-45]. Although AAV vectors result in higher transduction than nonviral methods, a major goal is to increase the efficiency of gene transfer. This cannot be simply overcome by continually increasing vector dosages, as higher doses are more likely to elicit an immune response and would present additional challenges to manufacturing capacity, cost of treatment, and/or treatment administration.

Although the early steps of binding and endocytosis are well studied, many virus-host interactions remain unknown which may enhance or reduce viral transgene expression. The ability of knocking down individual targets makes siRNA extremely useful for high throughput screening. A number of published studies have used this technique to examine virus/host cell interactions[46-52], usually in the context of reducing viral infection (as opposed to enhancing transgene expression).

To help identify intracellular barriers to AAV transgene expression, we conducted a high throughput screen using short interfering RNA (siRNA) to knock-down mRNA corresponding to 5,520 Applied Biosystems "druggable genome" targets. In the present study, off-target effects caused by a common seed region sequence were observed in 4 of the top 5 screening hits. Also, mRNA profiling was used to investigate additional off-target effects where a complex phenotype emerged involving downregulation of genes of the interferon pathway.

2.1. Materials and Methods

2.1.1. Cell culture

Human Aortic Endothelial Cells (HAEC; Lonza, Walkersville, MD) were cultured in supplemented Clonetics EGM-2 (Lonza, Walkersville, MD) at 37ºC and 5% CO_2. Prior to siRNA treatment, cells were rinsed with Dulbecco's phosphate-buffered saline and incubated with 0.05% Trypsin-EDTA (Invitrogen, Santa Clara, CA), then seeded onto 96 or 384 well flat bottom plates (BD Bioscience, Franklin Lakes, NJ). Human bronchial epithelial cells (Lonza, Walkersville, MD) were grown in cell culture flasks containing supplemented bronchial epithelial growth media (BEGM) for 4-5 days at 37ºC and 5% CO_2. Human bronchial epithelial cells were then seeded at a density of 10^5 per well onto 96 well flat bottom plates (BD Bioscience, Franklin Lakes, NJ) and cultured in an equal mixture of bronchial epithelial basal media and Dulbecco's modified Eagle's medium

(Invitrogen, Santa Clara, CA). Cells became confluent within 4 days and were allowed to grow for 2 weeks prior to forward transfection.

2.1.2. Druggable genome library

The Druggable Genome Library (Applied Biosystems, Foster City, CA) was used for screening. This library consists of 5,520 gene targets and 3 siRNAs per gene. The library was provided in 384 well plates, each well containing 0.25 nmol of lyophilized siRNA. The two columns on the right of the plate were left empty for controls. Sterile nuclease-free water (Applied Biosystems, Foster City, CA) was added to each well in order to resuspend the siRNA at a concentration of 3125 nM. Additional nuclease-free water was used to dilute the siRNA to a working concentration of 330 nM. For the primary screen, the three siRNAs targeting the same gene were pooled together in equal quantities to create a pooled master. The pooled master was then used to create assay plates containing 2 µL of siRNA, with each individual siRNA at a concentration of 110 nM, for a total pooled siRNA concentration of 330 nM. For the confirmatory screen, the desired individual siRNAs were aliquoted from the diluted master, and used to create assay plates containing 2 µL of siRNA, with each individual siRNA at a concentration of 330 nM. Seven columns on the right and left sides of each plate contained controls. Following the confirmatory screen, work was performed at larger scale (96 wells or less per plate), and in those cases the siRNA were ordered individually and resuspended using sterile nuclease-free water at a concentration of 3125 nM.

2.1.3. Mutated siRNAs

For examination of off-target effects resulting from the seed region of the siRNA sequences, three mutated siRNA sequences were designed in which individual point mutations were introduced into positions 1, 4, and 14, respectively, of the siRNA strand corresponding to Applied Biosystems siRNA 145736 (CLIC2 sequence C). In each case, the siRNA sense strand was complementary to its mutated antisense strand. The mutated siRNAs were chemically identical to the original Applied Biosystems Silencer siRNAs, with the exception of the point mutations, and sequences are given in **Table 2.1**.

Gene Name	siRNA ID#	Letter Code	Antisense Sequence	Primary Screen Fold Increase (pooled)	Secondary Screen Fold Increase (single siRNA)
SLC5A2	41847	B	5'-ACAGUGCCUCUGUUGGUUCtg-3'	13.9	6.0
ABCA8	117435	A	5'-U*UGUUUC*AUAACAAUGAGCtg-3'	17.7	4.6
CLIC2	145736	C	5'-A*UGUUUC*UAAGGAGCAGGGtg-3'	16.9	4.3
GPR124	34695	B	5'-A*UGUUU*AGUCGGAGAAGCCtg-3'	7.0	3.4
LCK	668	A	5'-A*UGUUUC*ACCACCUCUCCCtg-3'	22.1	3.4
CLIC2(C)-A1U mutant			5'-**U***UGUUUC*UAAGGAGCAGGGtg-3'		
CLIC2(C)-U4A mutant			5'-A*UG**A**UUC*UAAGGAGCAGGGtg-3'		
CLIC2(C)-G14C mutant			5'-A*UGUUUC*UAAGGA**C**CAGGGtg-3'		

Table 2.1. siRNA sequences providing the top hits in secondary screening of individual siRNAs, and point-mutated siRNA sequences based on CLIC2 sequence C. The bases shared in the seed region between four of the five sequences are italicized. The point mutations made to CLIC2 sequence C are in bold font and underlined.

2.1.4. Reverse transfection protocol

The protocol used for HAEC transfection was adapted from the method described by Barker and Diamond [53]. HAEC were cultured in Clonetics EGM-2 (Lonza, Walkersville, MD). siRNA (Applied Biosystems, Foster City, CA) was added to a well plate. The

well plate was either frozen overnight or held at room temperature for less than two hours. If the plate was frozen, it was thawed and allowed to equilibrate to room temperature prior to use. siPort NeoFX™ (Applied Biosystems, Foster City, CA) diluted in Opti-Mem™ (Lonza, Walkersville, MD) was added to the siRNA plate and allowed to incubate at room temperature for 10 minutes. HAEC grown in a cell culture flask were then added to the plate at a seeding density of 4.5×10^4 cells per cm^2. The siRNA were allowed to transfect the cells for 24 hours.

2.1.5. Forward transfection protocol

siRNA (Applied Biosystems, Foster City, CA) was thawed at room temperature and then added to siPort NeoFX™ (Applied Biosystems, Foster City, CA) diluted in Opti-Mem™ (Lonza, Walkersville, MD). The mixture was allowed to incubate at room temperature for 10 minutes prior to addition to 96 well plates. The siRNA were allowed to transfect the cells for 24 hours.

2.1.6. Interferon protocol

Frozen recombinant human αA-Interferon and β-Interferon (Calbiochem, San Diego, CA) were thawed on ice and diluted in Dulbecco's Phosphate Buffered Saline (Invitrogen, Santa Clara, CA) and serially diluted prior to addition to a 96 well plate. Virus addition followed within 20 minutes of addition of interferon to the well plate.

2.1.7. Luciferase transduction protocol

Adeno-associated virus, type 2, containing a CMV promoter and firefly luciferase sequence (AAV2-Luc) was added to the well plate. The virus was then allowed to transduce the cells for 24 hours. On the third day, cells were assayed for gene expression using the Bright-Glo assay kit (Promega, Madison, WI) following the vendor's protocol. A scrambled siRNA sequence was used as a negative control (Silencer Negative Control 1; Applied Biosystems, Foster City, CA).

2.1.8. Fluorescence transduction protocol

After 24 hours of exposure to siRNA, adeno-associated virus, type 2, containing a CMV promoter and enhanced green fluorescent protein sequence (AAV2-EGFP) was added to the plate. The virus was then allowed to transduce the cells for a minimum of 48 hours prior to imaging and flow cytometry analysis.

2.1.9. Flow Cytometry

An Accuri C6 Flow Cytometer (Accuri Cytometers, Ann Arbor, MI) was used for quantitative analysis of individual cell fluorescence. Cells were harvested into Dulbecco's Phosphate Buffered Saline (Invitrogen, Santa Clara, CA) and then held on ice until measurement. 20,000 counts per sample were recorded.

2.1.10. Cell viability assay

Cells were assayed for viability using the Cell Titer Glo assay kit (Promega, Madison, WI) following the vendor's protocol.

2.1.11. Quantitative real-time PCR

Cells were treated with siRNA and were then harvested a day later for total RNA content using the Absolutely RNA microprep kit (Stratagene, La Jolla, CA). Superscript III reverse trasnscriptase and oligo(dT) (Invitrogen, Carlsbad, CA) was used to reverse transcribe the RNA. The resulting cDNA was then purified using the Qiagen PCR purification kit (Qiagen, Valencia, CA). The CLIC2 forward primer used was CACTACAAGCTAGACGGT and the reverse primer used was CCAGGAACGGAGGATT. The MX1 forward and reverse primers, respectively, were CGCAGGGACCGCCTTGGACC and GGGTGGGATGCAGCAGCTGGA. The IFI44L forward primer and reverse primers used were, respectively, GGTGGGTCCAGTTGGGTCTGGA and GCACAGTCCTGCTCCTTCTGCC. The IFIT5 forward and reverse primers used were, respectively, AGGCTGTTACCCTGAACCCAGAT and GGTCTGTTGTGTGTGGCCTTCT. The GAPDH transcript was used to normalize between samples. The GAPDH forward primer and reverse primers were, respectively, TGCACCACCAACTGCTTAGC and the GGCATGGACTGTGGTCATGAG. A Roche LightCycler (Indianapolis, IN) was used to generate a standard curve and optimize PCR conditions for each primer. The

LightCycler FastStart DNA MasterPLUS SYBR Green I kit (Roche, Indianapolis, IN) and Light Cycler melting curve analysis was used to perform quantitative real-time PCR.

2.1.12. Transcription Profiling

Cells were grown in 24 well plates at a seeding density of 45,000 cells/cm^2. Cells were harvested using 0.05% Trypsin-EDTA (Invitrogen, Carlsbad, CA) 24 hours after siRNA transfection. Total RNA was purified from cell lysate using the Absolutely RNA kit (Agilent, Santa Clara, CA). For each sample, 0.2-0.3 ug of purified RNA was amplified, fragmented, and then hybridized to the Human Gene 1.0ST microarray (Affymetrix, Santa Clara, CA)according to the Affymetrix GeneChip Expression Analysis Technical Manual protocol. Following hybridization, washing, and staining, the microarray was imaged using a confocal scanner with fluorescence excitation at 570 nm. Two sequential scans were conducted and a mean fluorescence signal was calculated. The resulting signals were analyzed using the Affymetrix Microarray Suite 5.0 and default values provided by Affymetrix. Fold change, p-value, and Significance Analysis of Microarray[54] (SAM) q-value were calculated. Transcripts whose SAM q-value were less than 25 and having a fold-change difference greater than 1.25 (indicating up-regulation) or less than -1.25 (indicating down-regulation) were identified.

2.1.13. Identification of hexamer seed region in 3' untranslated region

The UTRdb[55, 56] contains the untranslated sequences of eukaryotic mRNAs. The 3' untranslated regions of each of the top 50 genes identified as a possible hit in siRNA primary screening as well as the 3' untranslated regions of genes identified in transcription profiling were searched for the presence of the hexamer seed region 5'-GAAACA-3'.

2.2. Results

2.2.1. Primary and secondary screening

An siRNA library targeting 5,520 gene sequences was screened as pools (3 siRNA pooled per targeted gene) to examine the effect of each targeted gene on AAV2 transduction of cultured human aortic endothelial cells (HAEC). Three siRNAs at a concentration of 10 nM per targeted gene were pooled (30 nM total) and reverse transfected into human aortic endothelial cells (HAEC) in three replicate wells. At 1 day post-siRNA delivery, the HAEC were transduced with AAV2 coding for the firefly luciferase gene (AAV2-Luc) at 8.60 x 10^6 genome copies per well and the luciferase was then assayed 24 hr post-transduction (**Figure 2.1a**). The Robust Z-factor [53, 57] provides a metric of the median absolute deviation by which an individual knockdown condition (averaged over 3 replicates) differs from the population median (median luminescence

signal of 3.9 x 10^3 RLU). A total of 50 hits (~1 % hit rate) were scored as those siRNA pools with Robust Z-factor > 4.75, corresponding to replicate wells having >8.4-fold enhancement of luciferase expression.

The top 50 hits from the pooled primary screening were confirmed in a secondary screen by testing individually each of the three siRNAs (*not shown*). In this confirmation test, each individual siRNA was added such that the siRNA concentration prior to virus addition was 30 nM (See **Appendix Table A1** for siRNA sequences). A total of 10 targeted genes were confirmed that had at least one siRNA sequence providing significant improvement in transduction efficiency (**Figure 2.1b**). Three of the top ten gene hits (SLC13A4, SLC5A2, SLC5A3) came from solute carrier families, with sequence B against SLC5A2 resulting in greater than 6-fold enhancement of luciferase transgene expression. Sequence C against CLIC2 resulted in greater than 4-fold enhancement of transgene expression.

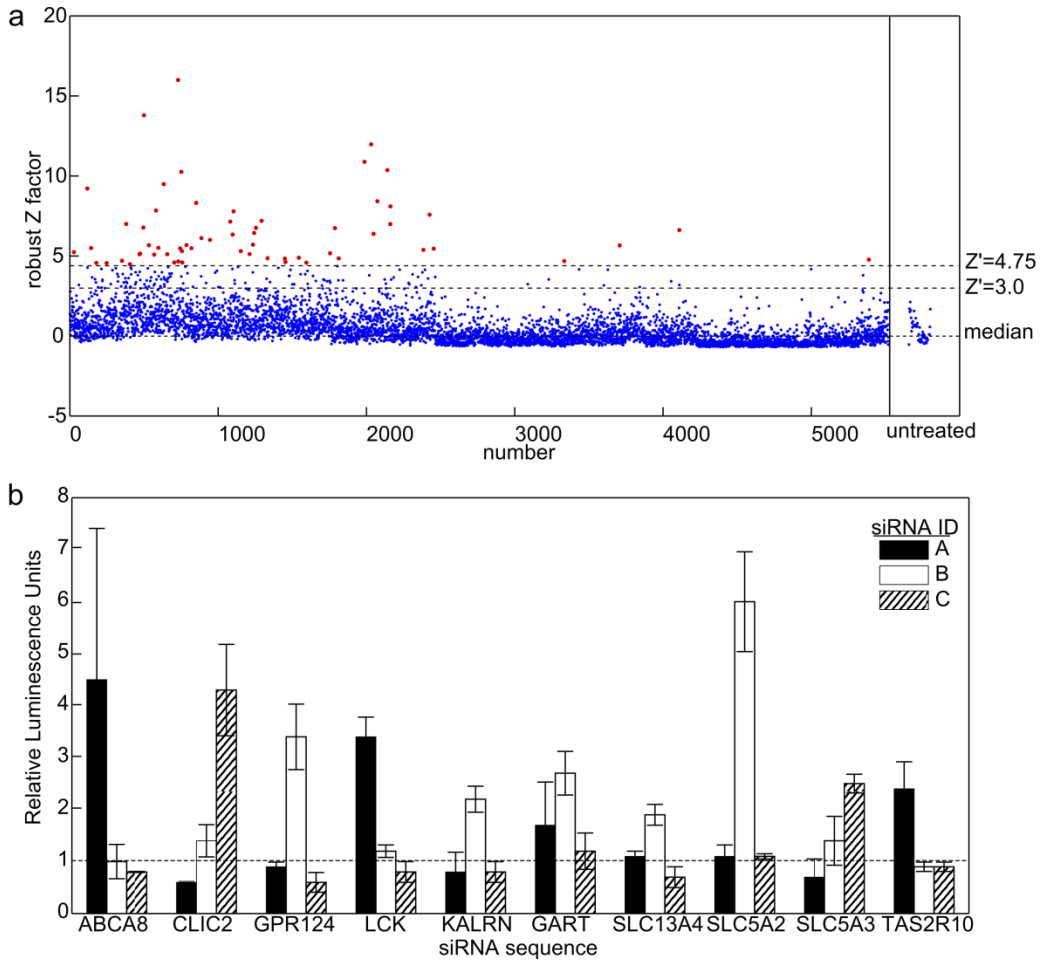

Figure 2.1. Primary and secondary screening for siRNA enhancers of AAV transduction. (a) Robust Z-factor for 5,520 siRNA pools (average of three replicates) examined in primary screen for enhancement of AAV transduction as detected by enhancement of the luciferase transgene. A cut-off of Robust Z-factor > 4.75 defined 50 hits (red). Data from untreated wells (average of eight replicates) is shown on the right. Z-factor = 0 (median) and Z = 3.0 are marked as a reference. (**b**) A total of 10 of the top 50 pooled screening hits were confirmed as enhancers of AAV transduction when each siRNA (sequences A, B, C) of each pool was tested individually. At least one of the three sequences tested in each pool resulted in a significant enhancement of luciferase expression.

Cell viability following knockdown with SLC5A2 sequence B and CLIC2 sequence C was unchanged (**Figure 2.2**), indicating that enhancements in transgene expression were not likely due to toxicity of a particular siRNA sequence.

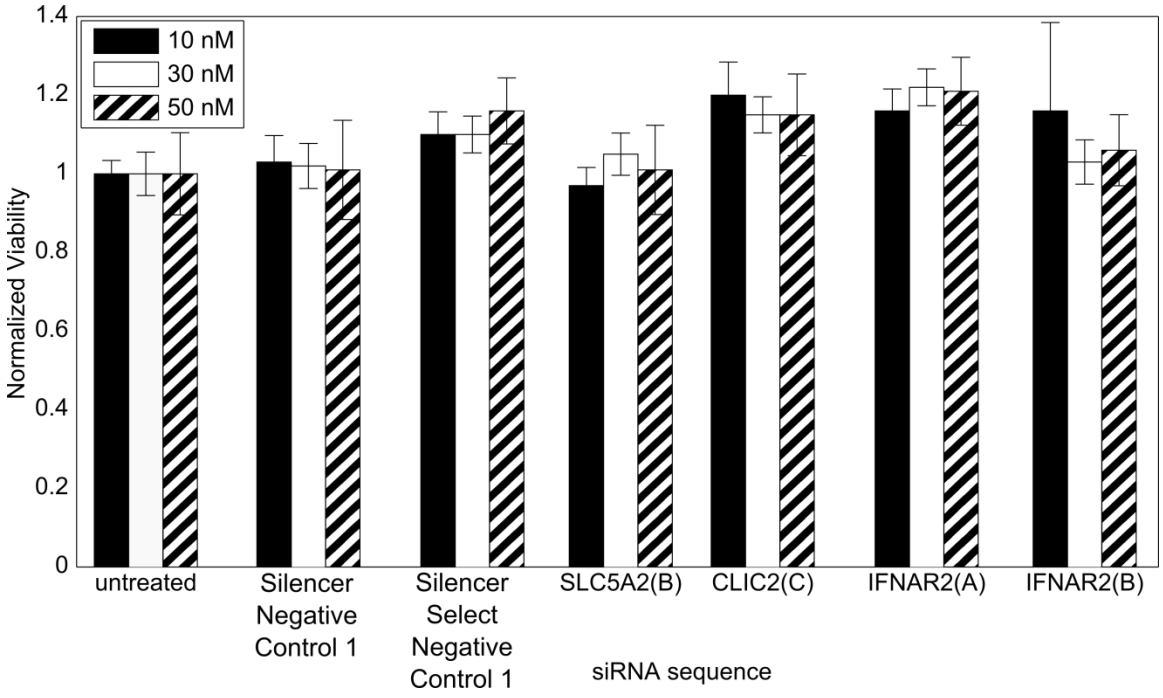

Figure 2.2. Viability of HAEC following siRNA knockdown with indicated sequences. HAEC were reverse transfected with indicated siRNA sequences and were assayed for viability 24 hours later.

2.2.2. Off-target effect of siRNA sequences against CLIC2

Since only sequence C against CLIC2 enhanced transgene expression, we used qRT-PCR to verify the extent of CLIC2 mRNA knockdown. As shown in **Figure 2.3**, the amount of CLIC2 mRNA knockdown was similar for each sequence at siRNA concentrations of 30 nM or 100 nM. We conclude that the mechanisms by which sequence C caused a

substantial, dose-dependent increase in AAV2 transduction was not due to the reduction in CLIC2 mRNA.

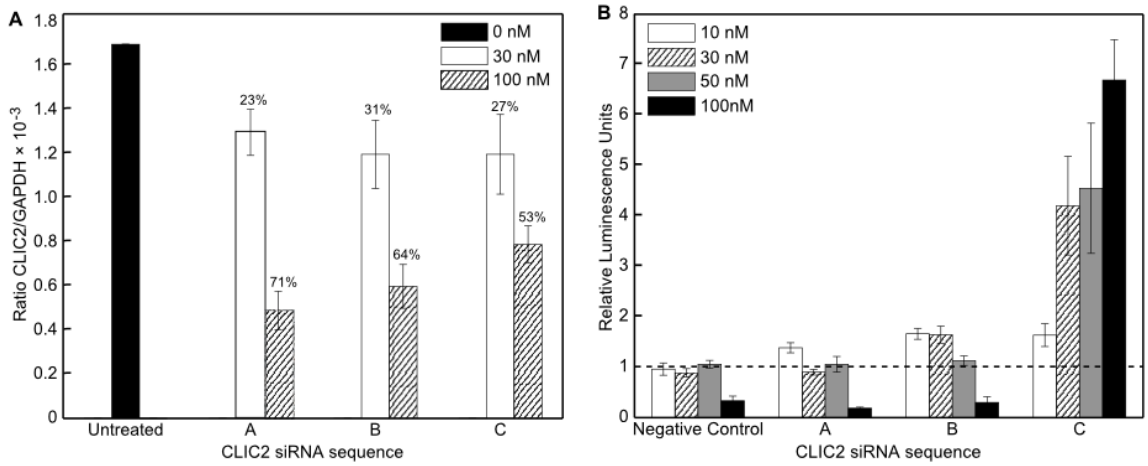

Figure 2.3. Demonstration of off-target mechanism of action of CLIC2 siRNA. (**a**) qRT-PCR measurement of CLIC2 mRNA knockdown in HAEC at 24 hr following transfection with 3 different siRNA sequences at concentrations of 30 nM and 100 nM, normalized against GAPDH mRNA signal. (**b**) Luciferase luminescence relative to scrambled siRNA negative control for CLIC2 siRNA sequences A, B, and C used at four concentrations of 10, 30, 50, and 100 nM. AAV transgene expression was uncorrelated with CLIC2 mRNA knockdown.

2.2.3. Seed region off-target effects

Analysis of the top siRNA sequence hits from single siRNA confirmation screening revealed that 3 of the top 5 shared an identical nucleotide sequence at positions 2-7 of the antisense strand and that a fourth siRNA shared positions 2-6 with those sequences (**Table 2.1**). To investigate if the observed off-target effect stemmed from this U_2GUUUC_7 seed region of the antisense strand, three siRNAs consisting of the CLIC2 sequence C containing point mutations were examined (**Table 2.1**). These siRNAs were then transfected into HAEC at a range of concentrations from 10 to 100 nM and AAV2-

Luc was added 24 hr later (**Figure 2.4**). Where the point mutation was introduced into position 1or position 14 of the sequence, increases in transduction were comparable to the original CLIC2 sequence C. However, when the U4A point mutation was introduced into the middle of the hexamer seed region, the siRNA sequence performance was similar to the negative control and did not display the increases in transduction efficiency observed with the other sequences. Comparison of knockdowns with the CLIC2 sequence C and the mutated CLIC2 sequence C in which the nucleotide at position four (U4A) indicates a microRNA-like mechanism for the off-target siRNA mediated enhancement of luciferase expression.

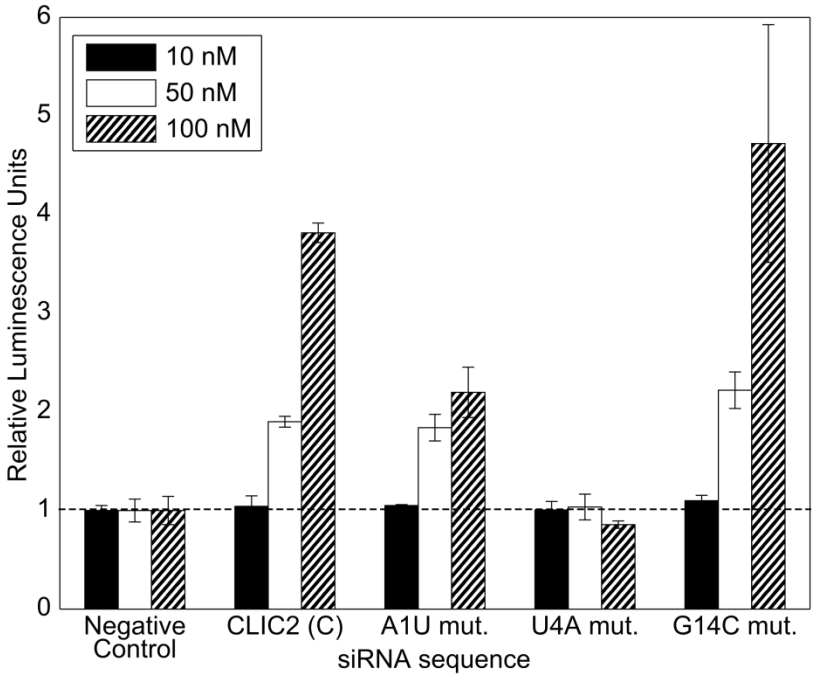

Figure 2.4. Hexamer region of CLIC(C) antisense strand mediates enhanced AAV2 transgene expression. Effect of CLIC2 siRNA sequence C and CLIC2(C) siRNA mutants on AAV2 transduction of HAEC, normalized to scrambled siRNA negative control.

2.2.4. Identification of hexamer seed region in 3' untranslated region

The 3' untranslated region of genes identified in primary screening were searched for complementarity to the hexamer seed region 5'-UGUUUC-3' (the sequence 5'-GAAACA-3' was searched for in the 3' untranslated region). The results are presented in **Appendix Table A1**. No trends were found with regards to the presence or absence of this sequence within the 3' untranslated region.

2.2.5. Transcription profiling following siRNA transfection implicate interferon pathways

Additional off-target effects of siRNA can arise through global phenotypic changes in the mRNA profile due to the siRNA. Differences in the mRNA expression profile between CLIC2(C) and CLIC2(C)-U4A mutant sequences due to off-target effects specific to the hexamer seed region were tested by mRNA profiling. In comparing the HAEC response to CLIC2 sequence C versus U4A mutant siRNA sequence (no AAV2 added), a total of 28 transcripts were enhanced, while 40 transcripts were decreased (**Appendix Table A2**) Several transcripts related to the interferon pathway were downregulated: interferon-induced protein 44-like (IFI44L), interferon-inducible myoxovirus resistance1 (MX1), and interferon-induced protein with tetratricopeptide repeats (IFIT5). The IFI44L and MX1 transcripts were specifically among the top 5 transcripts identified, and the top 2 for which a known function or pathway could be assigned. Transfection with CLIC2

sequence C siRNA resulted in a reduction of IFI44L, MX1, and IFIT5 mRNAs relative to transfection with CLIC2-U4A mutant siRNA as confirmed by qRT-PCR (**Figure 2.5**).

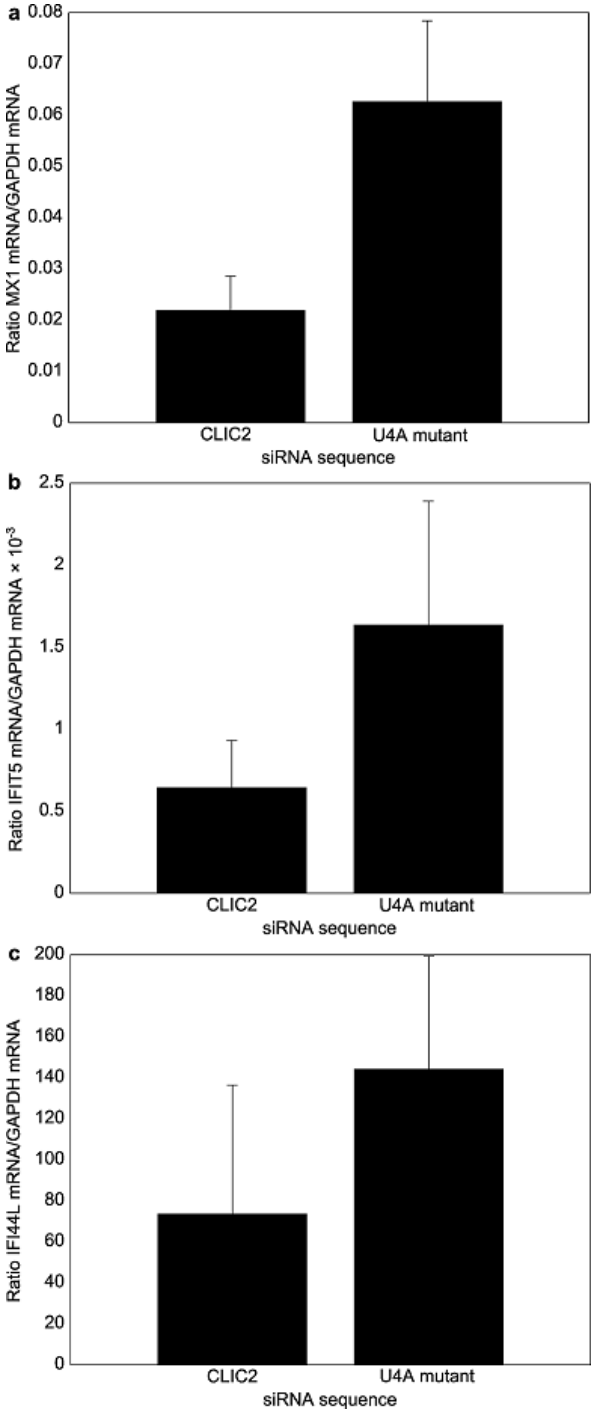

Figure 2.5. HAEC were transfected with CLIC2 sequence C and qRT-PCR was used to quantify relative levels of IFI44L, MX1, and IFIT5 mRNA. Results indicate that each of the three mRNAs was knocked down in the presence of CLIC2 sequence C, but not in the presence of the mutated siRNA sequence.

To further investigate the interferon pathway which is a known modulator of viral processes [58-60], several knockdowns were conducted. IFI44L, MX1, and IFIT5 knockdowns when tested individually did not result in an enhancement of AAV2-Luc transduction (*not shown*), indicating that CLIC2 sequence C siRNA creates a complex phenotype that results in enhanced transgene expression. In an additional test of interferon pathway processes, two unique siRNA sequences targeting the interferon (alpha, beta, and omega) receptor 2 (IFNAR2) led to an increase in virus transduction (**Figure 2.6a**). In contrast, the addition of recombinant alpha interferon and beta interferon directly into the cell culture at the time of transduction led to a decrease in transgene expression (**Figure 2.6b**) with no change in cell viability (*not shown*).

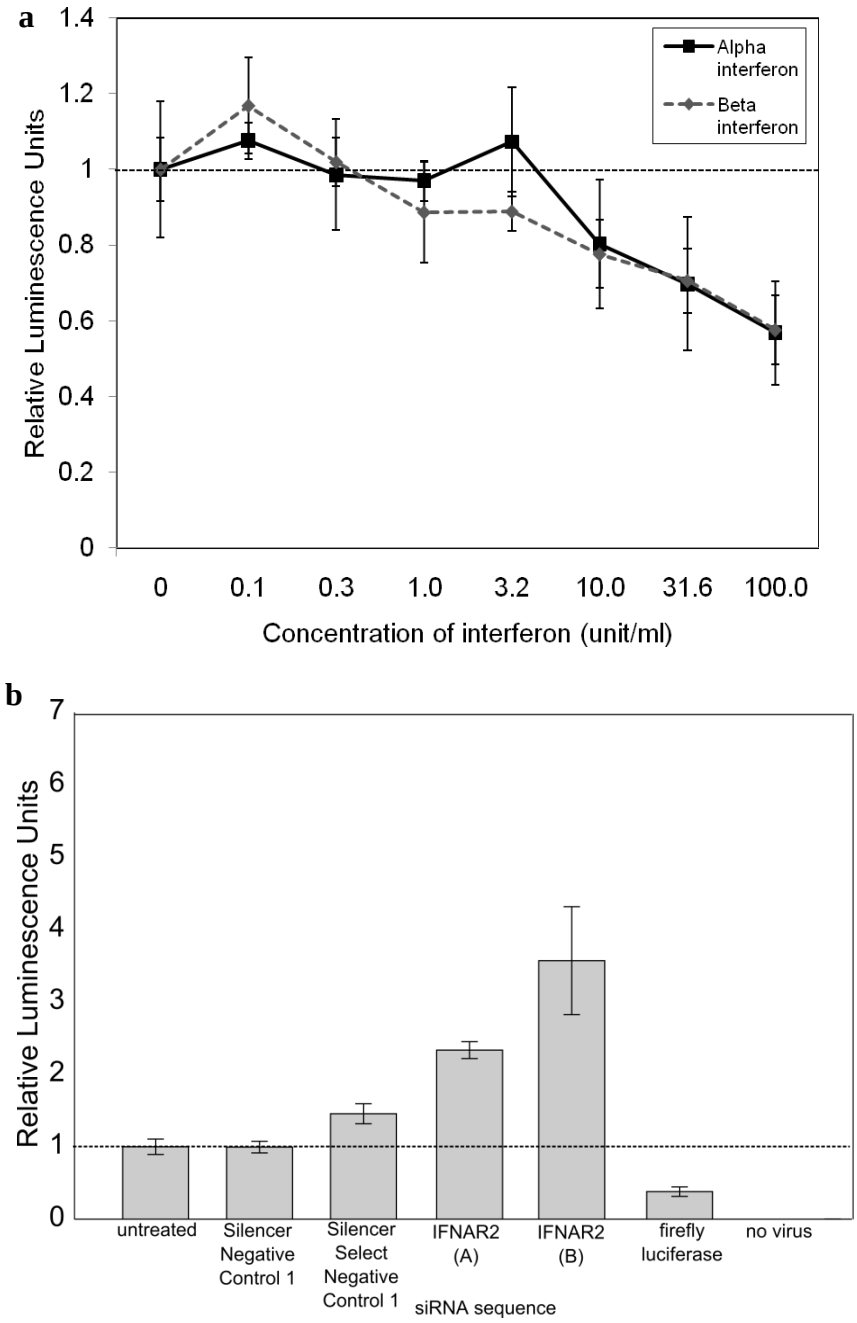

Figure 2.6. Effect of Type 1 interferons. (a) The addition of alpha interferon or beta interferon leads to a dose-dependent decrease in AAV2 transduction. (b) Knockdown of interferon (alpha, beta, omega) receptor 2 using two different siRNA sequences leads to an increase in viral transduction.

2.2.6. Human Airway Culture

We evaluated if the enhancing effect of CLIC sequence C siRNA was cell-specific by testing enhancement of AAV2 transduction of a human bronchial epithelium. In order to test the effectiveness of these siRNA sequences in a primary cell line, both the SLC5A2 sequence B and CLIC2 sequence C were evaluated in human bronchial epithelium using adeno-associated virus type 2 coding for enhanced green fluorescent protein (EGFP), followed by evaluation using fluorescence microscopy and flow cytometry. At the highest siRNA concentration tested, an increase in fluorescence of 27% was observed for SLC5A2 sequence B and an increase in fluorescence of 61% was observed for CLIC2 sequence C (**Figure 2.7**). Although the siRNA sequences were identified using HAEC cells, the results were not specific to the endothelium and may be useful for gene therapy applications in respiratory diseases such as cystic fibrosis. These results also confirm that the enhancing effects were not unique for the firefly luciferase reporter gene product since SLC5A2 sequence B and CLIC2 sequence C siRNAs increased in fluorescence from EGFP as measured using flow cytometry and were consistent with the luciferase enhancements.

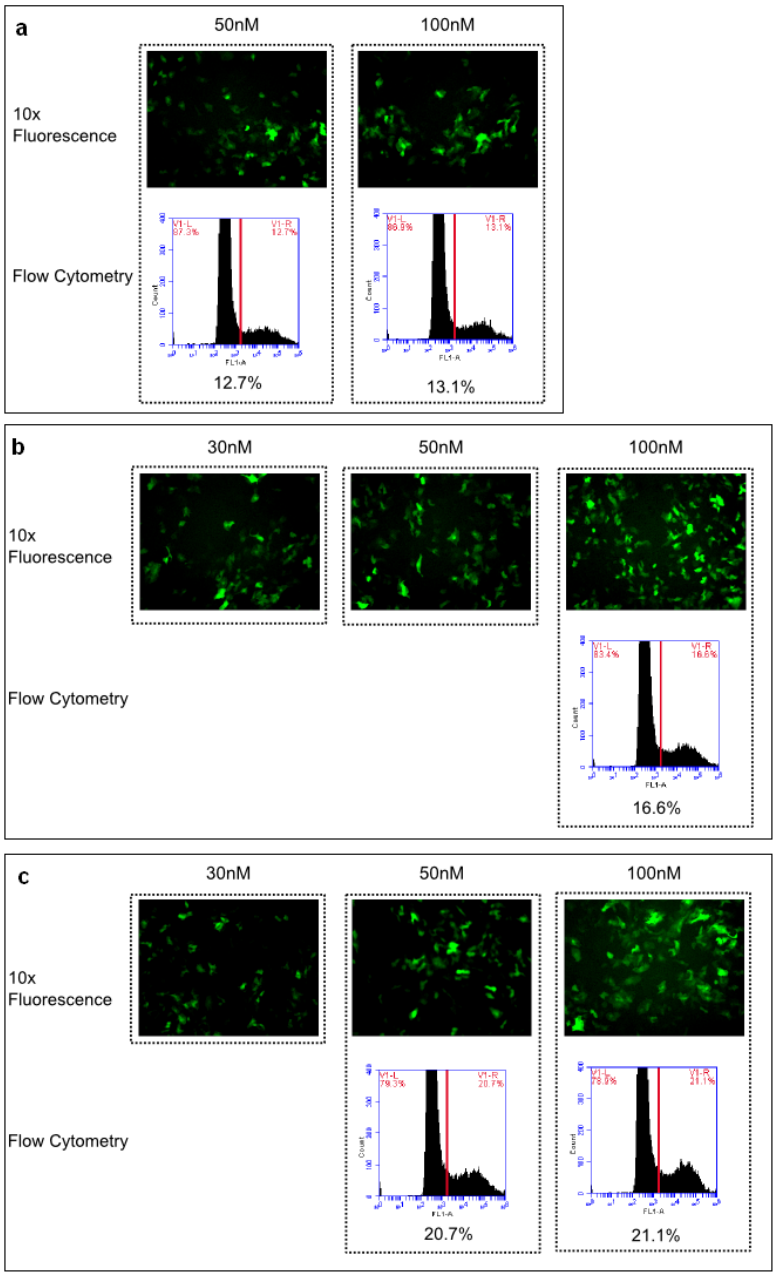

Figure 2.7. siRNA mediated enhancement of AAV2 transduction of human epithelial cells. Fluorescence microscopy images and flow cytometry data for human bronchial epithelium culture treated with **(a)** scrambled siRNA negative control, **(b)** SLC5A2 sequence B and **(c)** CLIC2 siRNA sequence C and then transduced with AAV2 containing EGFP.

2.2.7. Combination effects

Two experiments were carried out in which the effect of pair-wise combinations of siRNAs was examined. The total siRNA concentration used was constant at 50 nM. In the first of these experiments, pair-wise combinations of the top single siRNA sequence for each of the top ten genes were examined (**Figure 2.8a**). In the second, pair-wise combinations of the three siRNA sequences for the top three genes (CLIC2, GPR124, and SLC5A2) were examined (**Figure 2.8b**). As expected, SLC5A2 sequence B and CLIC2 sequence C both provided high results both alone and in combination with other sequences. GPR124 sequence B also provided a strong signal. In each of the two experiments, the highest signal came from a mixture of two siRNA sequences. For example, GPR124 sequence A provided 2-fold improvement when used on its own, and CLIC2 sequence C provided 4.3-fold improvement on its own, but the combination gave 5.6-fold improvement. The pairwise tests generally resulted in additive enhancement but not synergistic enhancements.

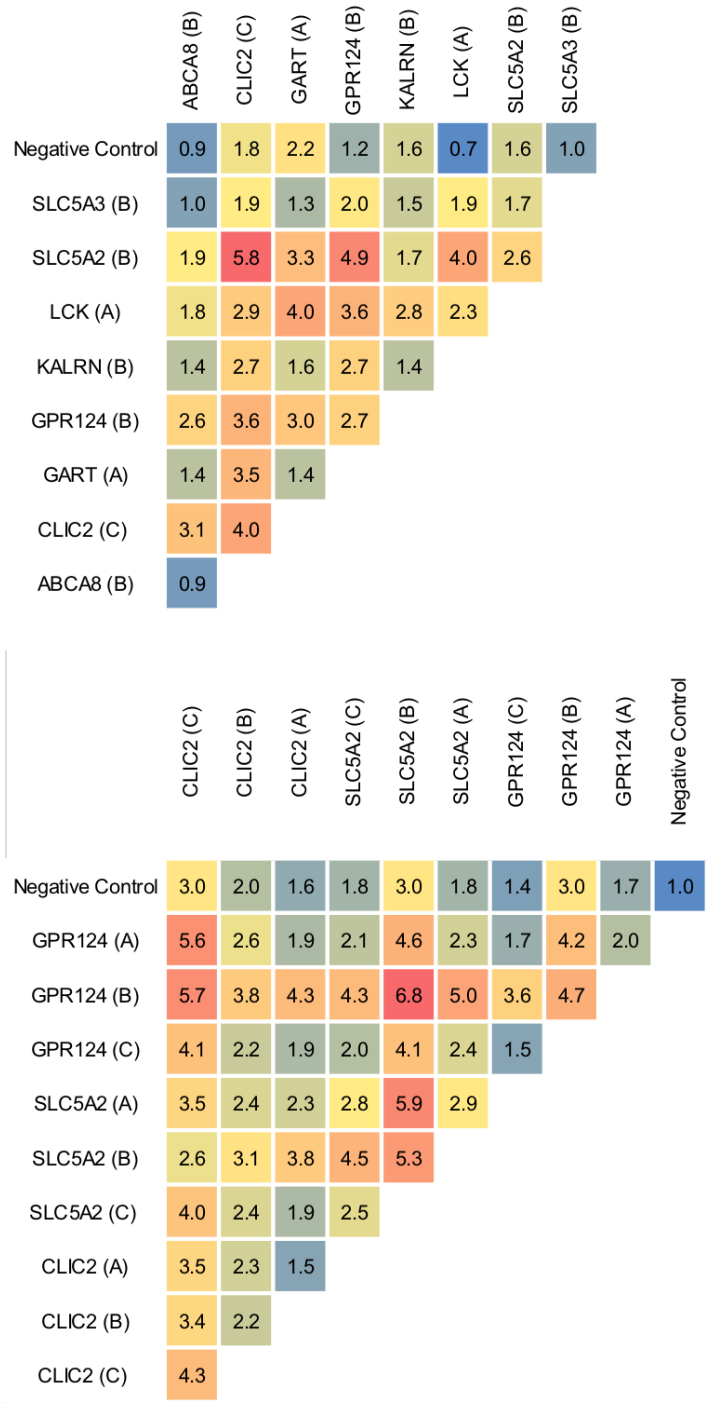

Figure 2.8. Pairwise interactions among confirmed siRNA hits. Heat map of pairwise interactions between siRNA sequences (total siRNA concentration/well = 50 nM) for the top 10 confirmed hits (**a**) or the 3 different sequences against the top 3 hits (**b**).

2.2.8. Co-administration of siRNA with AAV

In order to examine the use of siRNA in combination with adeno-associated viral gene delivery, two experiments were performed in which the siRNA was co-administered with the viral vector. In the first, the virus was pre-mixed with the siPort/siRNA mixture and then cells were added within thirty minutes (**Figure 2.9a**). In the second, the virus was added immediately following the addition of cells to the siPort/siRNA mixture (**Figure 2.9b**). The main difference between these two experiments was the exposure of virus to a higher concentration of siPort/siRNA for a short period of time in the pre-mixed experiment. The experiments showed similar results to each other, and additionally followed the same general trend of results observed for the standard transduction protocol in which 24 hours elapsed between addition of siRNA and addition of virus. For the SLC5A2 sequence B and CLIC2 sequence C sequences, increases in viral transduction in the range of 50 to 150% were observed for the 50 nM condition.

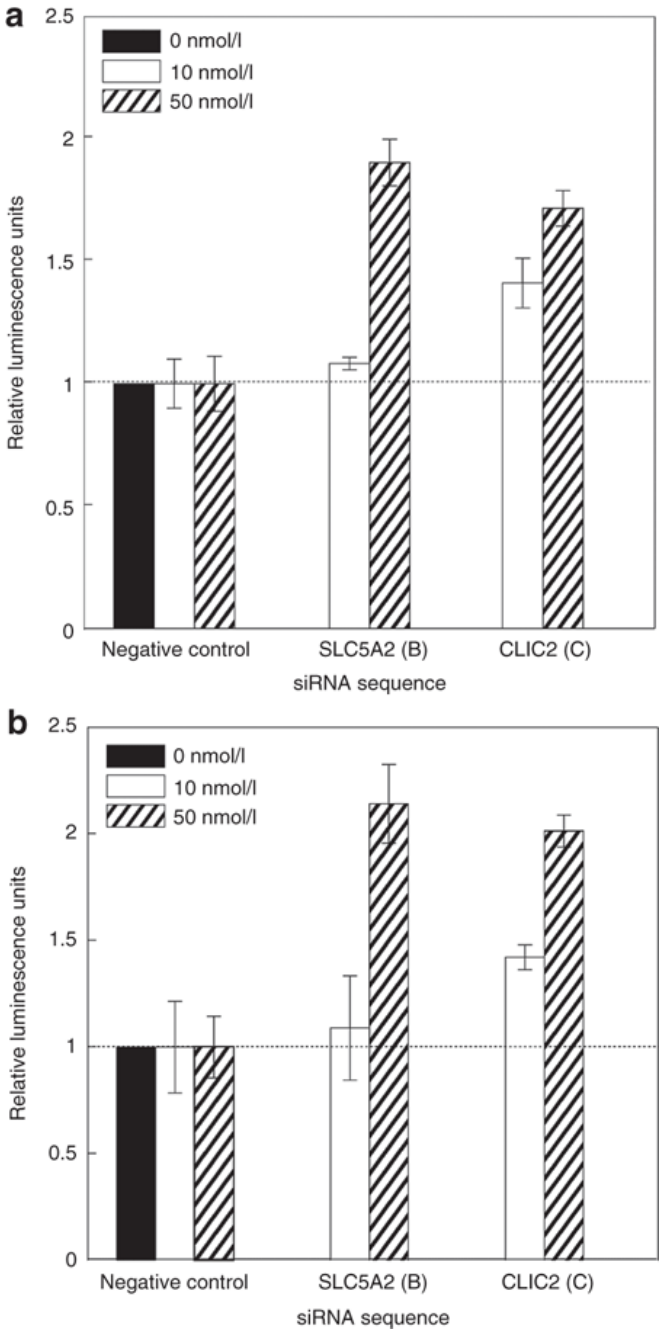

Figure 2.9. Coadministration of adeno-associated virus serotype 2 and short interfering RNA (siRNA) to human aortic endothelial cells enhances transgene expression. (a) Virus was premixed with siRNA lipoplexes and then added to cells. (b) Cells were reverse transfected and virus was immediately added after adding cells to siRNA formulation.

2.2.9. Common screening hits between Adenovirus and AAV2

Three primary screening hits were common to both an adenovirus screen and the AAV2 screen. These three hits were subject to a follow-up experiment. The top two out of these, ARF GTPase-acting protein (GIT2) and Olfactory Receptor 51E1 (OR51E1), were each screened using three novel siRNA sequences not present in the original screen. A third, phosphoribosylglycinamide formyltransferase, phosphoribosylglycinamide synthetase, phosphoribosylaminoimidazole synthetase (GART), had previously been in confirmatory studies using the original siRNA sequences from primary screening. This third enhancer was retested using those original siRNA sequences. As demonstrated in **Figure 2.11**, siRNA enhancement from these three genes was minimal.

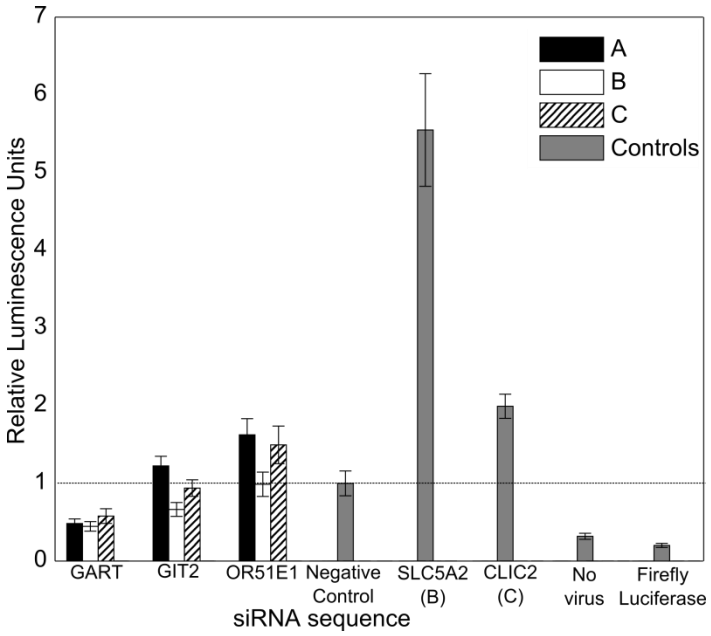

Figure 2.10. siRNA primary screening hits common to adenovirus and adeno-associated virus screens. Effect of GART, GIT, OR51E1 on AAV2 transduction of HAEC, normalized to scrambled siRNA negative control.

2.2.10. Serotype-Independence of Enhancement

In order to better understand the mechanism for enhancement of the top siRNA screening hits, HAEC transfected with SLC5A2 sequence B or CLIC2 sequence C were then transduced with either AAV2 or pseudotyped AAV2/1, which contains the AAV2 genome packaged into an AAV type 1 capsid. As demonstrated in **Figure 2.11**, the siRNA enhancement was independent of the capsid selected.

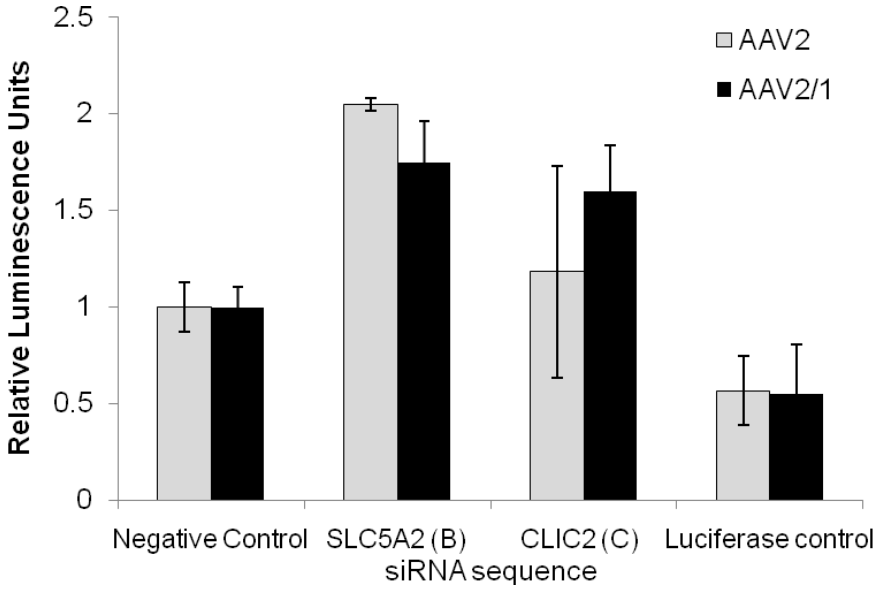

Figure 2.11. Pseudotyped AAV2/1 vector shows similar transduction trends to AAV2 vector. Cells treated with 50 nM siRNA were transduced with either AAV2 or AAV2/1 at a multiplicity of infection of 10,000, followed by Bright-Glo Assay.

2.3. Discussion

The use of siRNA high throughput screening targeting 5,520 genes allowed the identification of enhancers of adeno-associated viral gene delivery. By screening pools of 3 siRNAs per targeted gene in triplicate, a stringent Robust Z-score > 4.75 provided for a ~ 1 % hit rate. When individual siRNA sequences were retested, only 10 of the 50 targeted genes (20 % confirmation rate) resulted in AAV-Luc enhancements when the siRNA sequences were tested individually (**Figure 2.1**). One of the strongest inducers was the CLIC(C) sequence which had a beneficial action on transduction that was not correlated to CLIC mRNA knockdown (**Figure 2.3**), indicating an off-target effect. Inspection of a number of the confirmed siRNA sequences that enhanced transgene expression led to the identification of a common hexamer seed region [5'-U_2GUUUC_7-3'] (**Table 1**). The U4A mutation in this hexamer seed region of the antisense strand destroyed the enhancing activity of the CLIC(C) siRNA (**Figure 2.4**), indicating an important role for off-target microRNA-like silencing as a mechanism enhancing AAV2 transduction. At present, no off-target silenced mRNAs have been identified that result in the enhanced transduction. The off-target effects of siRNAs were beneficial to AAV2 transduction of both human endothelium and human bronchial epithelium (**Figure 2.7**). Interestingly, siRNA sequences when used together provided additive benefits to AAV2 transduction (**Figure 2.8)** and never resulted in cross-antagonism (< 1-fold enhancement).

Several of the top mRNA levels that are down-regulated specifically by the CLIC(C) siRNA sequence but not the CLIC(C)-U4A mutant siRNA were interferon-inducible

genes (IFI44L, MX1, and IFIT5). Due to this result, the interferon pathway was further explored and knockdown of the interferon (alpha, beta, omega) receptor 2 was shown to improve transduction (**Figure 2.6a**). This receptor is activated by type I interferons. The type I interferons serve as an early warning system in anti-viral defense. In response to a stimulus from a pathogen, type I interferons are synthesized and secreted [60]. The type I interferons then bind to receptors IFNAR1 or IFNAR2, and the janus kinase (JAK), tyrosine kinases (Tyk2), and signal transducers and activators of transcription (STAT1 and STAT2) comprise the downstream pathways leading to production of interferon-induced proteins [58, 59, 61, 62]. Many proteins are induced by the interferons, although a main pathway consists of the expression of protein kinase R (PKR). PKR then inhibits protein synthesis by inducing RNAse L to destroy RNA and by activating eukaryotic initiation factor 2 (eIF2) to lessen protein translation [63, 64]. Other mechanisms additionally recruit the adaptive immune response [58]. Notably, a current literature search shows several studies in which AAV has been used to deliver interferon-β for cancer gene therapy [65-67]. These studies show promising results; however the results presented in this paper suggest that caution should be used when combining the AAV vector with interferon, due to the potential that the interferon could inhibit future re-administration of the vector.

With respect to therapeutic strategies to enhance transduction, we report that co-administration of siRNA lipoplexes with AAV2 results in enhanced transgene expression (**Figure 2.9**), suggesting that the enhancement is due to siRNA-modulated pathways distal of changes in receptor engagement, endocytosis, or endosome escape. We

conclude that siRNA sequences containing the hexamer seed region [5'-U_2GUUUC_7-3'] result in a complex alteration of phenotype involving both translational silencing and multiple off-target mRNA knockdowns that together modulate the interferon pathway response to viral infection. However in regard to gene therapy, this alteration of phenotype can lead to enhancements in AAV transgene expression in human endothelium and epithelial cells.

Although the GART, GIT, and OR51E1 genes appeared promising based on their common appearance in hits from adenovirus and AAV2 screens, further study showed limited enhancement from these genes (**Figure 2.10**).

Enhancement of the pseudotyped vector AAV2/1 by the top screening hits SLC5A2 sequence B and CLIC2 sequence C was comparable to enhancement by the AAV2 vector (**Figure 2.11**). The only difference between these two vectors is the capsid and its associated cellular receptors. The primary receptor for AAV2 is heparan sulfate proteoglycan, whereas the main receptor for AAV2/1 is sialic acid. This suggests that the enhancement activity of these sequences is unrelated to virus/cell surface receptor interaction.

Chapter 3

Chemical Compound Screen

3.1. Abstract

A total of 2,320 molecules from two different chemical compound libraries were screened for their ability to enhance adeno associated virus type 2 transduction of cultured human endothelium. Of these compounds, 20 provided two-fold or greater enhancement at a concentration of 10 μM in primary screening.

3.2. Introduction

The interaction of adeno-associated virus with a cell consists of a pathway which includes surface receptor binding, endocytosis, endosomal escape, accumulation in the perinuclear space, transport into the nucleus, capsids uncoating, the synthesis of the second strand of DNA, transcription of the viral DNA to RNA, transport of the RNA out of the nucleus, and translation of the RNA. In chapter 2, we discussed a high throughput screen for the identification of siRNA enhancers of this process. In this chapter, we adopted a high throughput screening approach to identify chemical compounds which enhance the AAV2 transduction process. We then explore mechanistic details of selected compounds.

Cells were treated with compounds from the Sigma Library of Pharmacologically Active Compounds (LOPAC) and National Institute of Neurological Disorders and Stroke (NINDS) followed by addition of adeno-associated virus type 2 in order to identify compounds which may enhance viral transduction. A total of 2,230 compounds were screened.

20 compounds were identified as primary screening hits which enhanced viral transduction greater than two-fold in primary screening. These hits included several families of compounds. Of those compound families, antioxidants, nucleoside analogs, cell cycle arrestors, and alkylating agents were examined in more detail. Additionally, metal chelation as a mechanism was investigated based on one of the top primary screening hits.

3.3. Materials and Methods

3.3.1. Cell culture

Human Aortic Endothelial Cells (HAEC; Lonza, Walkersville, MD) were cultured in supplemented Clonetics EGM-2 (Lonza, Walkersville, MD) at 37ºC and 5% CO_2. Prior to screening, cells were rinsed with Dulbecco's phosphate-buffered saline and incubated with 0.05% Trypsin-EDTA (Invitrogen, Santa Clara, CA), then seeded onto 384 well flat bottom plates at a concentration of 860 cells per well in 15 ul of media (BD Bioscience, Franklin Lakes, NJ).

3.3.2. Compound libraries

The LOPAC (Sigma-Aldrich, Milwaukee, WI) and NINDS (Microsource Discovery Systems, Gaylord, CT) libraries were used for screening. LOPAC contains 1,280 chemicals at a concentration of 10 mM of compound suspended in 100% DMSO. The NINDS library contains 1,040 chemicals at a concentration of 10 mM of compound suspended in 100% DMSO.

A pin tool was used to transfer 0.1 microliters from the plates into a dilution plate containing 25 ul of media, resulting in a final concentration of 40 μM of compound in media. From these dilution plates, 5 ul of diluted compound was added to the cells in 15 ul of media, resulting in 20 ul of cells containing a concentration of 10 μM of compound. The final DMSO concentration per well after compound was mixed with cells was 0.1%. The cells were incubated in the presence of chemical compounds for 24 hours prior to the addition of virus.

For further confirmation of screening results, chemicals were individually purchased from Sigma (Milwaukee, WI) and dissolved in phosphate buffered saline if soluble in aqueous solvents. Compounds that were not soluble in aqueous solvents were dissolved in DMSO and subsequently added to cells in media such that the final DMSO concentration was 1%. A list of specific compounds and catalog numbers investigated is provided in the Appendix.

3.3.3. Luciferase transduction protocol

Adeno-associated virus, type 2, containing a CMV promoter and firefly luciferase sequence was added to the well plate at a multiplicity of infection of 10,000 viral genome copies per cell. The virus was then allowed to transduce the cells for 24 hours. On the fourth day following initial cell seeding, cells were assayed for gene expression using the Bright-Glo assay kit (Promega, Madison, WI) following the vendor's protocol.

3.3.4. Fluorescence transduction protocol

After 24 hours of exposure to chemicals, adeno-associated virus, type 2, containing a CMV promoter and enhanced green fluorescent protein sequence was added to the plate. The virus was allowed to transduce the cells for 24 hours and then the media containing virus and chemicals was replaced with fresh media. Microscopy images and flow cytometry took place 24 hours after the media was replaced.

3.3.5. Flow Cytometry

An Accuri C6 Flow Cytometer (Accuri Cytometers, Ann Arbor, MI) was used for quantitative analysis of individual cell fluorescence. Cells were harvested into Dulbecco's Phosphate Buffered Saline (Invitrogen, Santa Clara, CA) and then held on ice until measurement. 20,000 counts per sample were recorded.

3.3.6. Cell viability assay

Cells were assayed for viability using the Cell Titer Glo assay kit (Promega, Madison, WI) following the vendor's protocol.

3.3.7. Total Protein Quantification

The total amount of protein present in the sample was measured by BCA assay. Cells were released from the well plate using 0.25% Trypsin followed by the addition of media. They were then centrifuged to create a pellet which was washed with saline followed by the addition of lysis buffer containing 100 mM potassium phosphate, pH 7.8 and 2% Triton-X 100. Cells were incubated in lysis buffer for 40 minutes prior to BCA assay. The assay was conducted according to manufacturer's instructions using the Pierce BCA Assay Kit (Thermo Scientific, Rockford, IL).

3.3.8. DNA Purification

Cells treated with compound followed by AAV2-EGFP were then harvested two days later for total DNA content using the DNeasy Blood & Tissue Kit kit (Qiagen, Valencia, CA).

3.3.9. cDNA Synthesis

Cells treated with compound followed by AAV2-EGFP were then harvested two days later for total RNA content using the Absolutely RNA microprep kit (Stratagene, La Jolla, CA). Superscript III reverse trasnscriptase and oligo(dT) (Invitrogen, Carlsbad, CA) were used to reverse transcribe the RNA, resulting in cDNA.

3.3.10. Quantitative Real Time PCR

Purified DNA and synthesized cDNA were then amplified using the Roche LightCycler (Roche, Indianapolis, IN). LightCycler FastStart DNA MasterPLUS SYBR Green I kit (Roche, Indianapolis, IN) and Light Cycler melting curve analysis was used to perform quantitative real-time PCR. The EGFP DNA was measured using forward primer CGACAACCACTACCTGAGCA and the reverse primer GAACTCCAGCAGGACCATGT. GAPDH DNA or cDNA was used to normalize between samples according to the sample type used. The GAPDH forward primer and reverse primers were, respectively, TGCACCACCAACTGCTTAGC and the GGCATGGACTGTGGTCATGAG.

3.4. Results

3.4.1. Primary screening

2,320 compounds from the two screening libraries were examined for the effect of each chemical compound on AAV2 transduction of cultured human aortic endothelial cells. Cells were transferred into 384 well culture plates, and one day later chemicals dissolved in DMSO were transferred into each well such that the final concentration of DMSO in each well was 0.1%. On the next day, the HAEC were transduced with AAV2 coding for the firefly luciferase gene (AAV2-Luc) at 8.60 x 10^6 genome copies per well and the luciferase was then assayed 24 hours post-transduction (**Figure 3.1a**). These compounds are listed in Appendix 1. The Robust Z-factor [53, 57] provides a metric of the median absolute deviation by which an individual chemical (averaged over 2 replicates) differs from the population median. **Figure 3.1b** below shows representative data for a single plate as well as the Z-score plot of the two replicates. Compounds with Z-score greater than 3 for both replicates are included in the box at the top right of the figure. Compounds with Z-score less than -3 were not found.

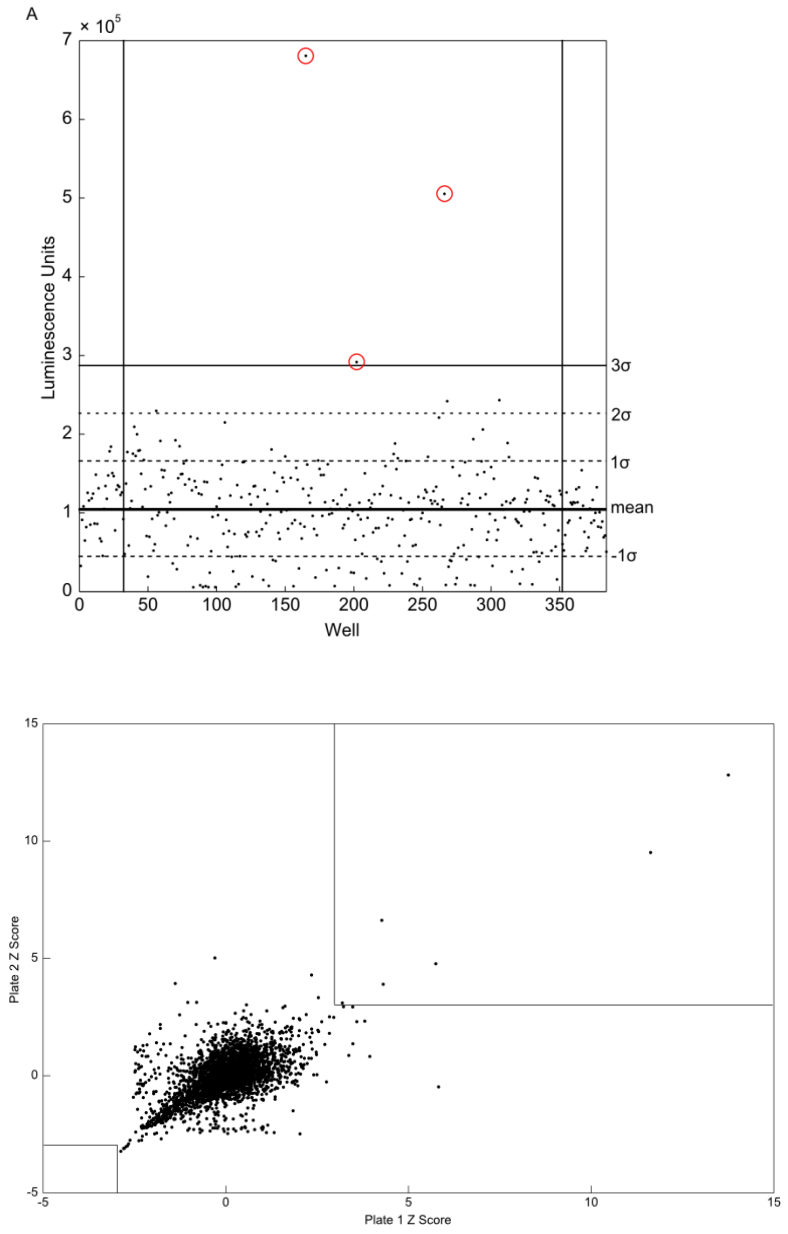

Figure 3.1. Chemical compound primary screening results. a: Results for a representative 384 well plate. Hits of three standard deviations above the mean for the plate are circled in red. b: Overall primary screening results.

The top hits from primary screening were further examined through the individual addition of these compounds to cells in 96 well plates. The most promising compounds from that work, as well as related compounds, were examined in more detail, including dose-response testing and viability testing.

From the primary screening results, it appeared that several families of related compounds emerged as hits. Ellagic acid, caffeic acid phenethyl ester, 7,4-dihydroxyflavone, daidzein, resveratrol, and 7,2-dihydroxyflavone are all antioxidant compounds.[68] Tyrphostin AG 698, Tyrphostin AG 490, and Tyrphostin AG 537 are all EGFR protein tyrosine kinase inhibitors. 4,5-dianiliophthalamide is additionally a protein tyrosine kinase inhibitor. Cell cycle arrestors were also examined due to the cell cycle regulatory effects of daidzein and 1,10-phenanthroline. 5-bromo-2-deoxyuridine, vidarabine, and 3-azido-3-deoxythymidine are all nucleoside analogs. Carboplatin and melphalan are both alkylating agents. As previous reports had investigated EGFR protein tyrosine kinase inhibitors in detail,[69, 70] we chose to focus on antioxidants, nucleoside analogs, and alkylating agents. Additionally, as the metal chelator 1,10-phenanthroline provided a very strong signal in primary screening, we also included metal chelators in our investigation.

3.4.2. Mechanistic Studies

In order to probe the mechanism for several of the top hits, cells were treated with 10 μM of compound and transduced with AAV-EGFP 24 hours later. After 48 hours, cells were examined by fluorescence microscopy, flow cytometry, PCR for quantification of EGFP

DNA, qRT-PCR for quantification of EGFP RNA, and BCA assay for quantification of total cellular protein. Results are given in Table 3.1 below.

	Normalized Virus DNA (EGFP)	Normalized Virus RNA (EGFP)	Normalized Average Fluorescence	Normalized Total Protein
1% DMSO*	1.0	1.0	1.0	1.0
Ellagic acid*	1.0	61.1	33.4	2.0
Tyrphostin 698*	0.2	0.5	2.0	1.0
Melphalan*	0.6	2.7	2.6	1.7
Vidarabine	0.7	2.8	1.4	0.6
5-bromo-2'-deoxyuridine	0.8	5.1	2.3	0.8
1,10-phenanthroline	1.9	4.6	2.3	0.9
Carboplatin	1.0	1.7	1.2	0.7
MOI 0 (no virus)	0.0	0.0	0.1	1.0
MOI 1,000	0.1	0.2	0.2	1.0
MOI 10,000	1.0	1.0	1.0	1.0
MOI 100,000	10.0	2.0	1.5	0.8

Table 3.1. Normalized viral DNA, viral RNA, average fluorescence per cell, and total protein per well for selected compounds. For RNA and DNA measurements, the ratio of EGFP signal to GAPDH signal is calculated for each sample, and then that ratio is normalized to control. Conditions with an asterisk (*) contained 1% DMSO in the well and were normalized to the DMSO control. All other conditions are normalized to the MOI 10,000 sample.

3.4.3. Tyrosine kinase inhibitors

Three of the compounds found (Tyrpohstin AG 490, Tyrphostin AG 537, and Tyrphostin AG 698) are epidermal growth factor receptor (EGFR) protein tyrosine kinase inhibitors. EGFR is a cell surface receptor which when activated by ligand homodimerizes, forming a kinase on the internal surface of the cell membrane. It autophosphorylates and serves as a kinase for several other pathways.[71] Consistent with these results, previous work by Zhong and colleagues has shown that the addition of the EGFR protein tyrosine kinase

inhibitor Tyrphostin 23 increased AAV2 transduction. They found two specific mechanisms by which EGFR inhibition enhanced transduction; through decreased ubiquination of AAV2 capsids and through decreased FK506-binding protein inhibition of AAV2 second-strand DNA synthesis.[70] The existence of many EGFR protein tyrosine kinase inhibitors on the list of primary screening hits supports the finding that EGFR inhibition enhances transduction, and as shown in **Table 3.1**, reporter gene expression is increased when Tyrphostin 698 was exposed to cells. However, because previous reports investigated the effect of EGFR protein tyrosine kinase inhibitors in great detail, the current work did not study these compounds in depth.

3.4.4. Antioxidants

Several antioxidant compounds were identified in primary screening, including ellagic acid, caffeic acid phenethyl ester, 7,4-dihydroxyflavone, and 7,2-dihydroxyflavone. Ellagic acid was of particular interest as it was the strongest hit in primary screening and it continued to perform well in follow-up studies (**Figure 3.2 and Figure 3.3**). In order to follow-up on the success of ellagic acid as an enhancer, other compounds with similar functionality were examined. Caffeic acid, an antioxidant which demonstrated some enhancement during primary screening, showed poor performance in a dose-response curve (**Figure 3.4a**). Ascorbic acid (vitamin C) was added to growth media, but no enhancement of viral transduction was observed (**Figure 3.5**). N-acetyl cysteine was also added with no enhancement of viral transduction (**Figure 3.6**). Other anti-oxidants

including beta-carotene and bilirubin were also examined, but poor solubility in DMSO or aqueous solution prevented their experimental use (*data not shown).*

Although ellagic acid is primarily considered as an antioxidant compound, it also serves as a tyrosine protein kinase inhibitor, can induce cell cycle arrest, and has intercalating properties.[72-75] Due to the inability of other antioxidant compounds to facilitate adeno-associated virus transduction, it appears that the enhancement effect of ellagic acid is likely due to other effects.

3.4.4.1. Ellagic Acid

Ellagic acid was the top hit in primary screening and continued to perform well in dose-response studies (**Figure 3.2a**). Ellagic acid showed an impressive level of enhancement in high throughput screening, and it continued to show dose-dependent enhancement during follow-up studies. However, ellagic acid also demonstrated limitations, primarily in solubility and toxicity. Dissolution of ellagic acid at concentrations up to 10 mM in either DMSO or aqueous solution was extremely challenging, and most studies were performed by dissolving ellagic acid directly in media and replacing the growth media in the well with filtered growth media containing ellagic acid at the required concentration. Differences in enhancement and toxicity between experimental runs may have been due to variability caused by the difficulty in dissolving ellagic acid at the required concentration.

a)

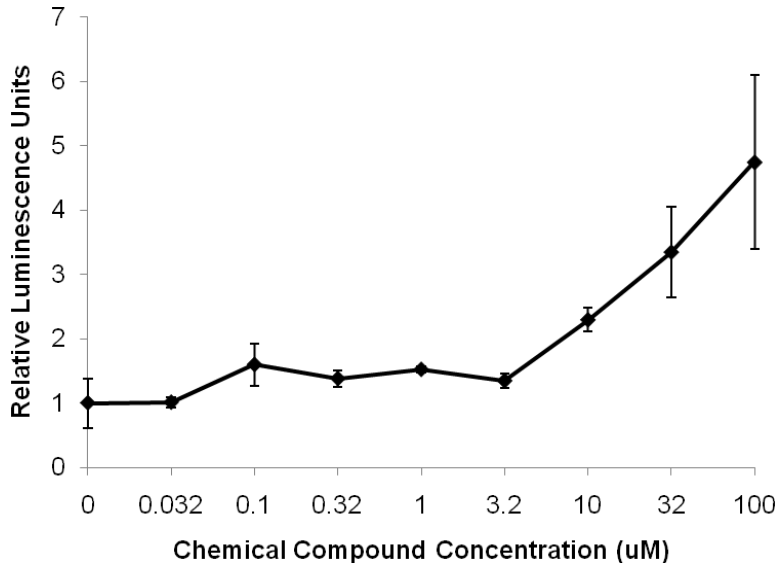
Relative Luminescence Units
0
1
2
3
4
5
6
7
0
0.032
0.1
0.32
1
3.2
10
32
100
Chemical Compound Concentration (uM)

b)

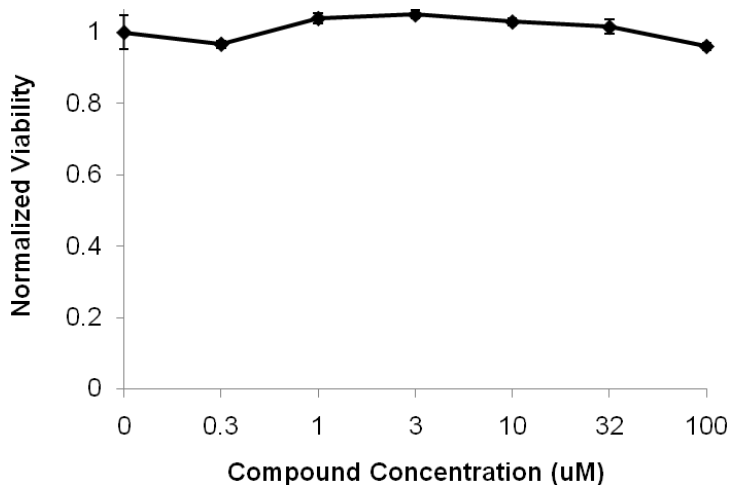
Normalized Viability
0
0.2
0.4
0.6
0.8
1
0
0.3
1
3
10
32
100
Compound Concentration (uM)

c)

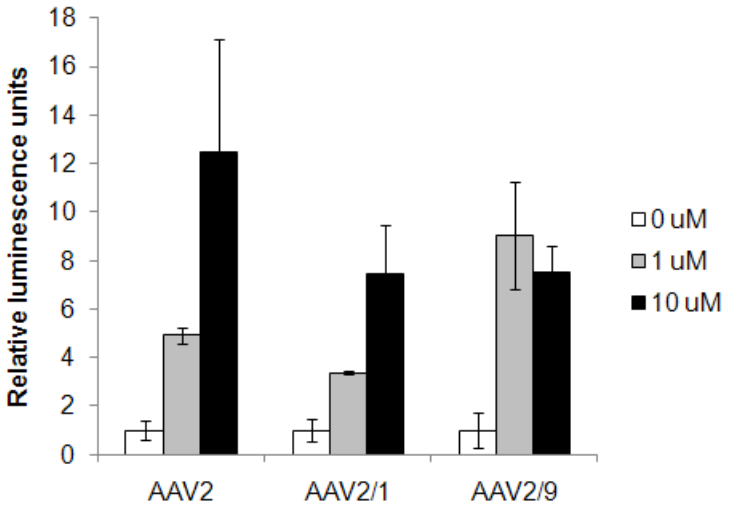

Figure 3.2 Ellagic acid luciferase assay and viability results. a) Ellagic acid was dissolved at a concentration of 100 µM in media, serially diluted in media, and added to HAEC. 24 hours later, adeno-associated virus was added, followed by luciferase assay after another 24 hours. b) Normalized cell viability following 48 hours of cell exposure to ellagic acid dissolved in media. c) AAV serotype 2, 2/1, and 2/9 were added to HAEC following treatment with ellagic acid.

HAEC treated with 10 µM ellagic acid were additionally subject to transduction with AAV2-EGFP and examined using fluorescence microscopy, PCR, qRT-PCR, flow cytometry, and BCA assay. As shown in **Table 3.1**, the amount of viral DNA measured in the cell was the same as the 1% DMSO control, whereas viral RNA and fluorescence was greatly increased (61 fold change and 33 fold change, respectively). The total protein per well as measured by BCA assay increased two-fold.

Because the viral RNA and fluorescence levels changed so dramatically, the PCR data was examined more closely for insight into mechanism to determine whether this result

was a global increase in protein level or restricted to the increase in viral RNA and reporter gene signal (**Table 3.2**). The increase in GAPDH RNA and the large normalized GAPDH RNA/GAPDH DNA value, in combination with the two-fold increase in protein quantity by BCA assay, suggests that the results may be related to a global increase in overall protein. A previous report also described an increase in GAPDH mRNA and total protein levels as a result of ellagic acid exposure.[75]

	GAPDH DNA	GAPDH RNA (from cDNA)	GAPDH RNA/ GAPDH DNA
1% DMSO*	1.0	1.0	1.0
Ellagic acid*	0.8	8.3	9.7
Tyrphostin 698*	3.3	0.4	0.1
Melphalan*	0.9	0.01	0.02
Vidarabine	4.3	0.1	0.03
5-bromo-2'-deoxyuridine	2.2	0.3	0.1
1,10-phenanthroline	0.7	0.1	0.1
Carboplatin	1.1	0.8	0.7
MOI 0 (no virus)	4.3	0.7	0.2
MOI 1,000	1.9	1.1	0.6
MOI 10,000	1.0	1.0	1.0
MOI 100,000	1.3	0.1	0.1

Table 3.2 Normalized values for quantitative real time PCR measurement of GAPDH DNA, GAPDH RNA (by measurement of cDNA), and the ratio of RNA/DNA. Compounds indicated with an asterisk have been normalized by the 1% DMSO measurement, whereas others were normalized by the MOI 10,000 condition.

Figure 3.3 provides corresponding information for fluorescence microscopy and flow cytometry. As compared with the 1% DMSO control, the cells treated with ellagic acid are elongated and much more fluorescent (**Figure 3.3a,b**). Flow cytometry showed more granularity in ellagic acid treated cells, as indicated by an increased side scatter measurement (**Figure 3.3c,d**). An overlay of the fluorescence clearly shows that the

ellagic acid treated cells have much higher levels of fluorescence following transduction with AAV2-EGFP (**Figure 3.3e**).

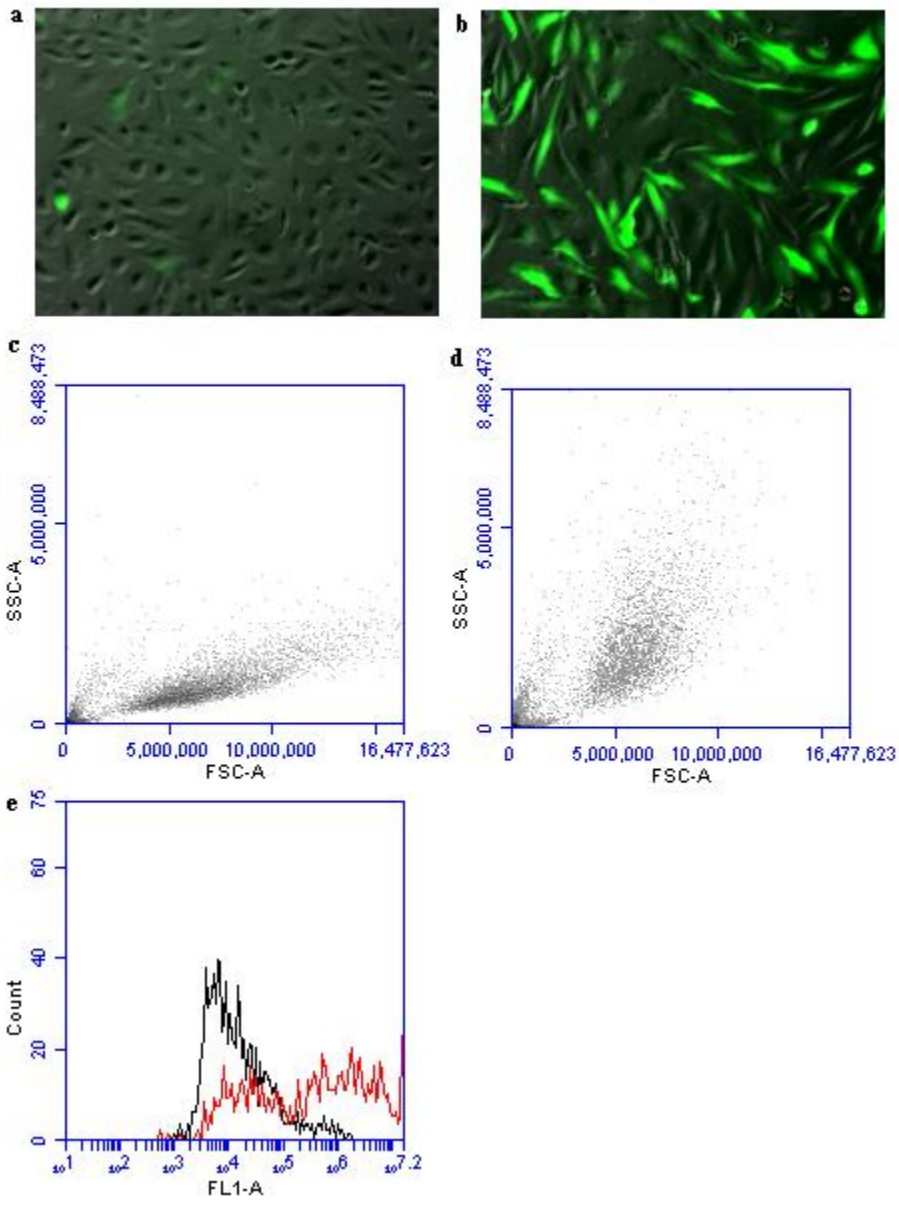

Figure 3.3. Fluorescence microscopy images and flow cytometry data for HAEC treated with ellagic acid followed by AAV2-EGFP transduction. a. Image of HAEC treated with 1% DMSO followed by AAV2-EGFP. b. Image of HAEC treated with ellagic acid in 1% DMSO followed by AAV2-EGFP. c. Forward and side scatter results for HAEC treated with 1% DMSO followed by AAV2-EGFP from flow cytometry. d.

Forward and side scatter results for HAEC treated with ellagic acid in 1% DMSO followed by AAV2-EGFP from flow cytometry. e. Histogram overlay of fluorescence area for HAEC treated with 1% DMSO (black) and ellagic acid in 1% DMSO followed by HAEC treated with AAV2-EGFP (red).

3.4.4.2. Caffeic Acid Phenethyl Ester

Caffeic acid demonstrated a 2.5 fold enhancement in primary screening (**Appendix Table A4**) and was therefore examined more closely for a dose response. Additionally, caffeic acid phenethyl ester is an antioxidant compound, which allowed further probing of the potential for antioxidants to serve as a class of enhancing molecules.[76] **Figure 3.4a** below shows that the compound only moderately benefited viral transduction, while **Figure 3.4b** demonstrates that cell viability was unaffected by the virus.

a)

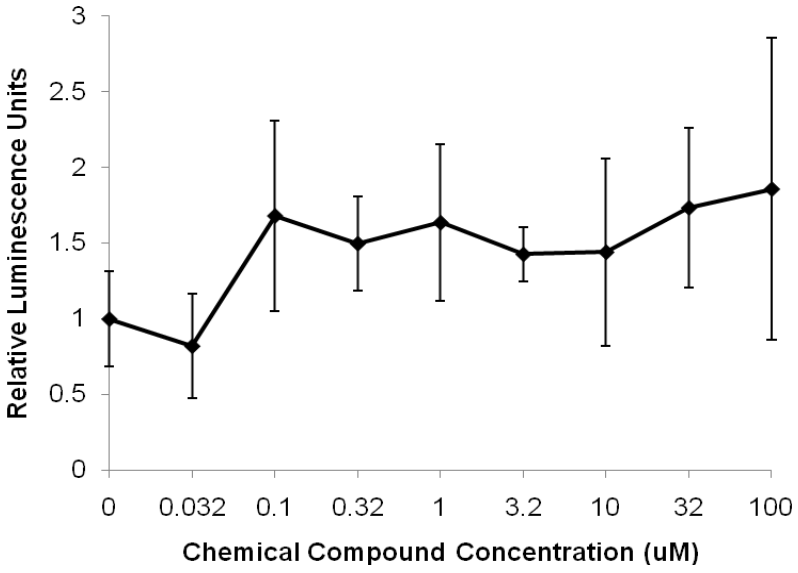

b)

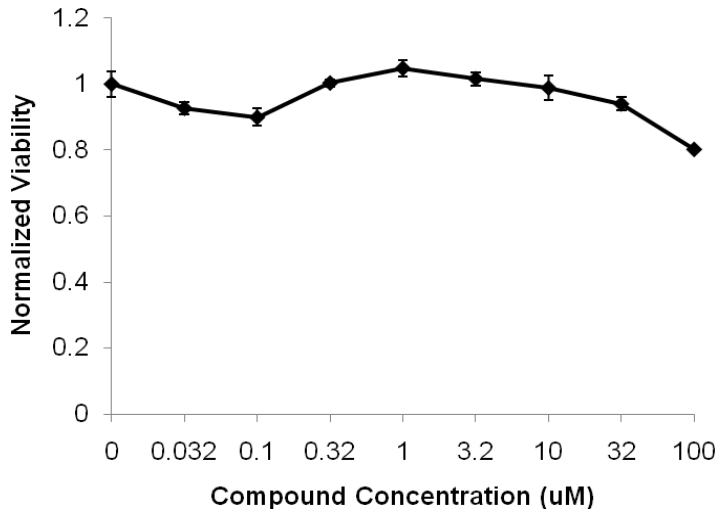

Figure 3.4. Caffeic acid phenethyl ester results. a) Caffeic acid phenethyl ester was dissolved at a concentration of 10 mM in DMSO, serially diluted in DMSO, and added to HAEC cells in media such that the final DMSO concentration in each well was 1%. 24 hours later, adeno-associated virus was added, followed by luciferase assay after another 24 hours. **b)** Viability of HAEC following 48 hours of exposure to caffeic acid dissolved in DMSO.

3.4.4.3. Ascorbic acid

In order to further examine antioxidant functions, ascorbic acid (vitamin C) was added to cells followed by treatment with virus containing the luciferase reporter gene. As shown in **Figure 3.5** below, the addition of ascorbic acid had no effect on viral transduction.

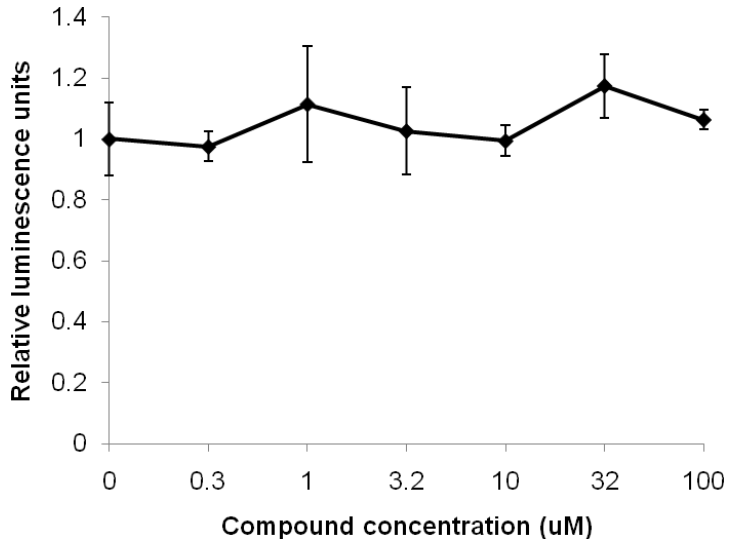

Figure 3.5. Ascorbic acid luciferase assay dose response results. Ascorbic acid was dissolved at a concentration of 100 µM in media, serially diluted in media, and added to HAEC. 24 hours later, adeno-associated virus was added, followed by luciferase assay after another 24 hours.

3.4.4.4. N-acetyl cysteine

N-acetyl cysteine is another antioxidant compound.[77] It was additionally tested in order to probe possible antioxidant enhancement of AAV2 transduction. The compound appears to have a moderate effect at best, most likely explained by an artifact of the experimental procedure (edge effects), as shown in **Figure 3.6**.

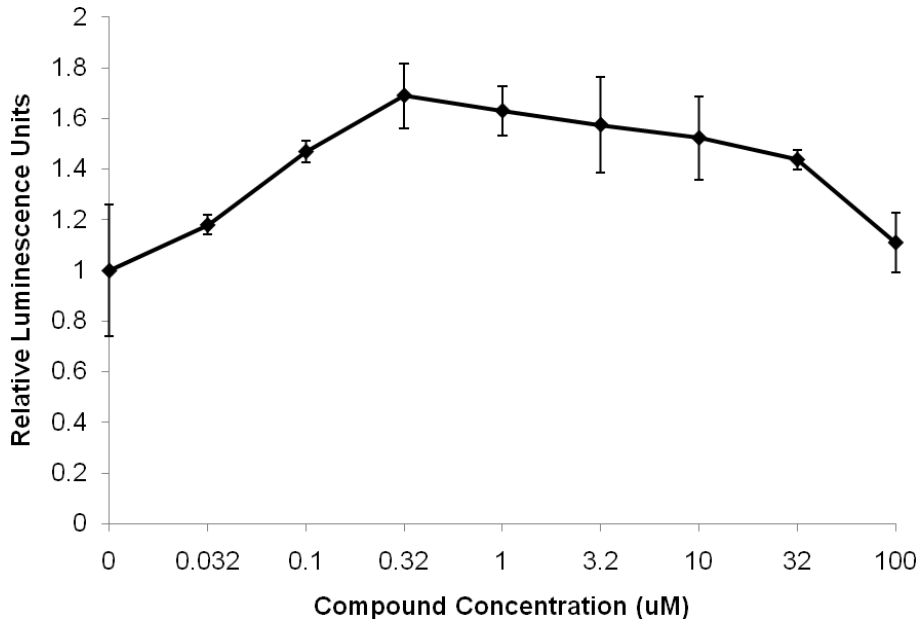

Figure 3.6. N-acetyl cysteine luciferase assay dose-response results. N-acetyl cysteine was dissolved at a concentration of 100 µM in media, serially diluted in media, and added to HAEC. 24 hours later, adeno-associated virus was added, followed by luciferase assay after another 24 hours.

3.4.5. Metal Chelators

1,10-phenanthroline is a metal chelator which was one of the top hits identified in the primary screen. 1,10-phenanthroline was examined in more detail. Additionally, ethylenediaminetetraacetic acid (EDTA), a commonly used metal chelator, was examined to see if enhancement would be observed in other metal chelators.

3.4.5.1. 1,10-phenanthroline

1,10 phenanthroline is a metal chelator which inhibits metalloproteases and additionally activates p53 transcriptional activity.[78] 1,10-phenanthroline was the second strongest hit

identified in primary screening, with a normalized luminescence value of 6.4 (**Appendix table A4**). Although this compound was capable of providing significant enhancement, it was also demonstrated to be toxic to HAEC at values above 3 uM, which explains the sharp drop in reported enhancement at high compound doses (**Figure 3.7b**). 1,10-phenanthroline enhanced adeno-associated viral transduction for pseudotyped viruses AAV2/1 and AAV2/9, suggesting that the response to compound is independent of cell surface receptor binding (**Figure 3.7c**).

a)

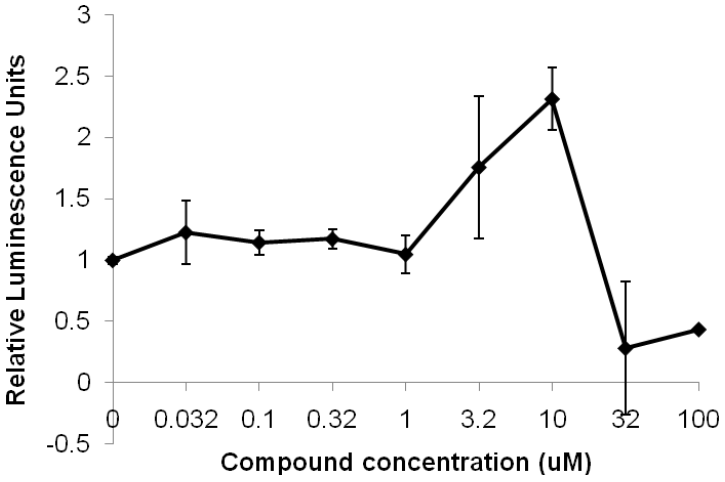

b)

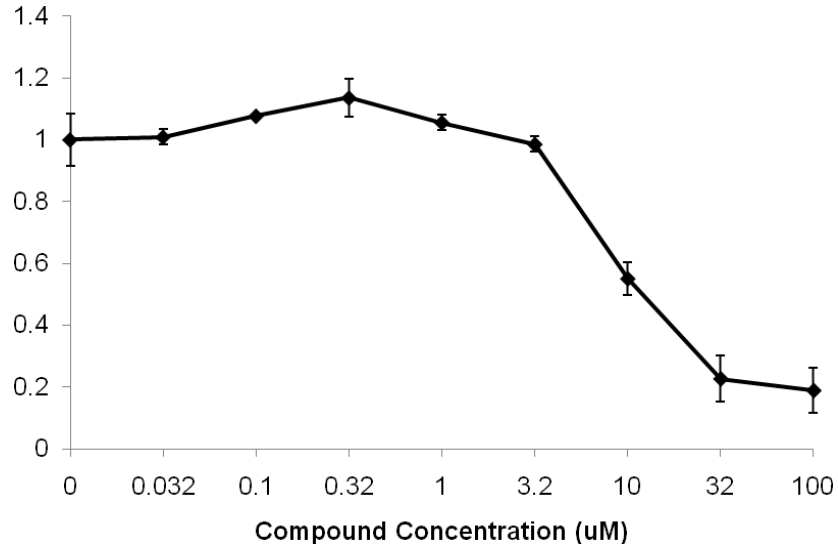

c)

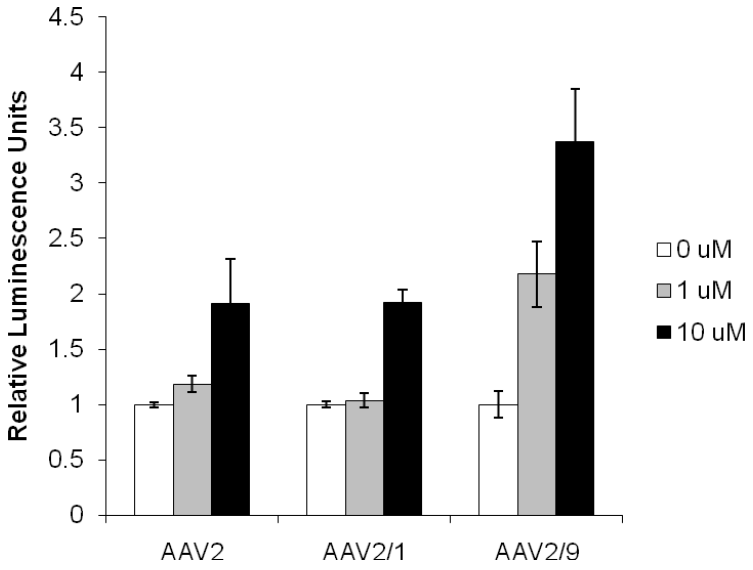

Figure 3.7. Luciferase assay and viability results for HAEC treated with 1,10-phenanthroline. a) 1,10 phenanthroline luciferase assay results. 1,10 phenanthroline was dissolved at a concentration of 10 mM in DMSO, serially diluted in DMSO, and added to HAEC cells in media such that the final DMSO concentration in each well was 1%. 24 hours later, adeno-associated virus was added, followed by luciferase assay after

another 24 hours. b) HAEC viability following 48 hours exposure to 1,10 phenanthroline dissolved in DMSO. c) Luciferase assay results for HAEC exposed to 1,10-phenanthroline followed by AAV2, AAV2/1, or AAV2/9. Two 1,10-phenanthroline concentrations were measured.

HAEC treated with 10 μM 1,10-phenanthroline were additionally subject to transduction with AAV2-EGFP and examined using fluorescence microscopy, PCR, qRT-PCR, flow cytometry, and BCA assay. As shown in **Table 3.1**, the amount of viral DNA measured was two-fold higher than in the control sample. Viral RNA present was additionally increased to 4.6 times greater than control, and the average fluorescence was 2.3 times higher than in the control. The total protein in the well was about the same as the control. **Figure 3.8** provides corresponding information for fluorescence microscopy and flow cytometry. Cells treated with the 1,10-phenanthroline do not show a large morphological change as determined by microscopy or by flow cytometry (**Figure 3.8a,b,c,d**). An overlay of the fluorescence data shows the overall fluorescence profile shifting to the right in addition to the appearance of a small group of very highly fluorescent cells. (**Figure 3.8e**).

Overall, the data suggest that 1,10-phenanthroline does not affect the virus/receptor interaction due to the non-serotype specificity, however DNA levels are increased. Therefore, it is possible that 1,10 phenanthroline may be protecting the virus from degradation during endosome processing, perhaps by interfering with metalloproteases.

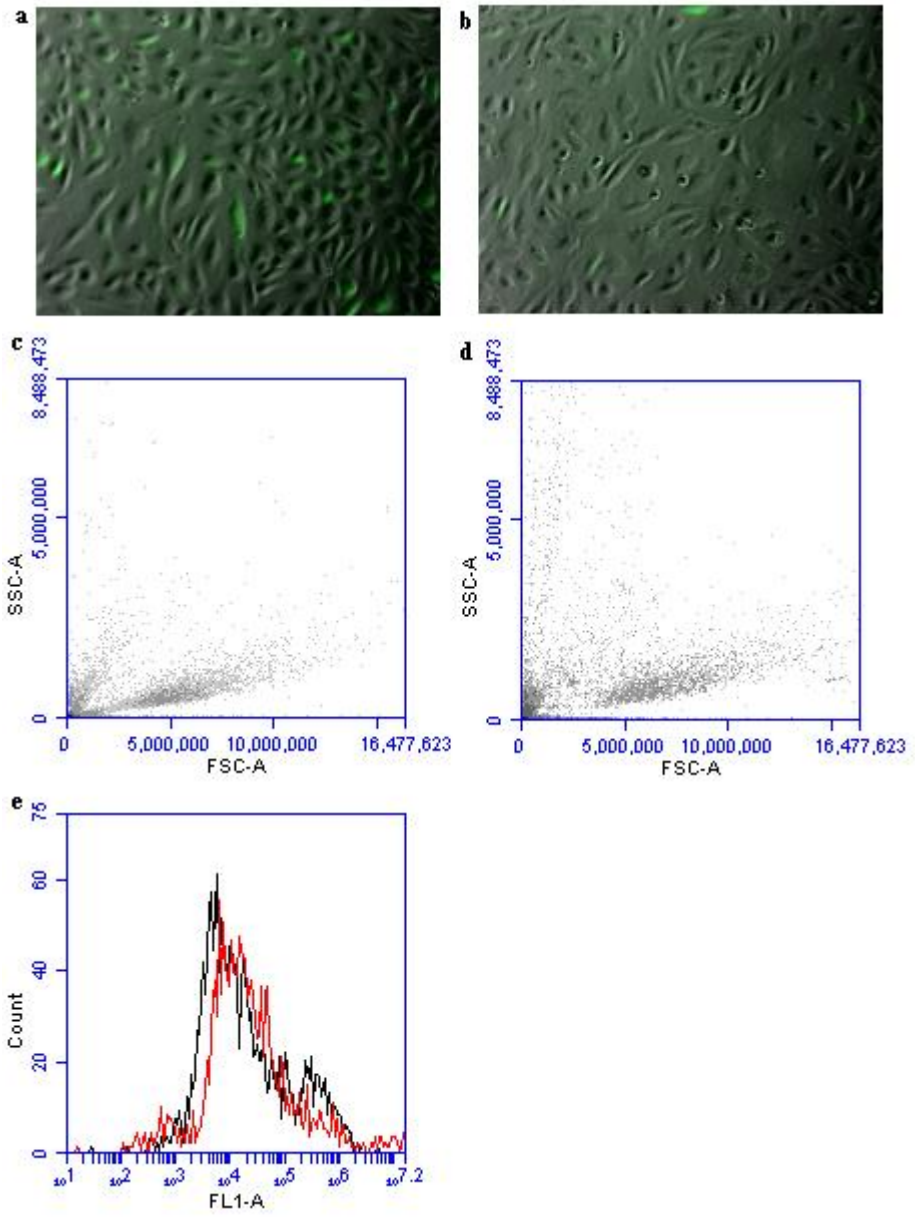

Figure 3.8. Fluorescence microscopy images and flow cytometry data for HAEC treated with 1,10 phenanthroline followed by AAV2-EGFP transduction. a. Image of HAEC transduced with AAV2-EGFP. b. Image of HAEC treated with 1,10-phenanthroline followed by AAV2-EGFP transduction. c. Forward and side scatter results for HAEC transduced with AAV2-EGFP from flow cytometry. d. Forward and side scatter results for HAEC treated with 1,10-phenanthroline followed by AAV2-EGFP from flow cytometry. e. Histogram overlay of fluorescence area for HAEC treated with AAV2-EGFP (black) and HAEC treated with 1,10-phenanthroline followed by AAV2-EGFP (red).

3.4.5.2. Ethylenediaminetetraacetic acid (EDTA)

An alternative metal chelator, ethylenediaminetetraacetic acid (EDTA), was examined and found to have no effect on viral transduction, leading to the conclusion that 1,10-phenanthroline's effect on viral enhancement is not general to all metal chelators, although it is possible that it may be specific to a subclass of metal chelators such as zinc chelators.

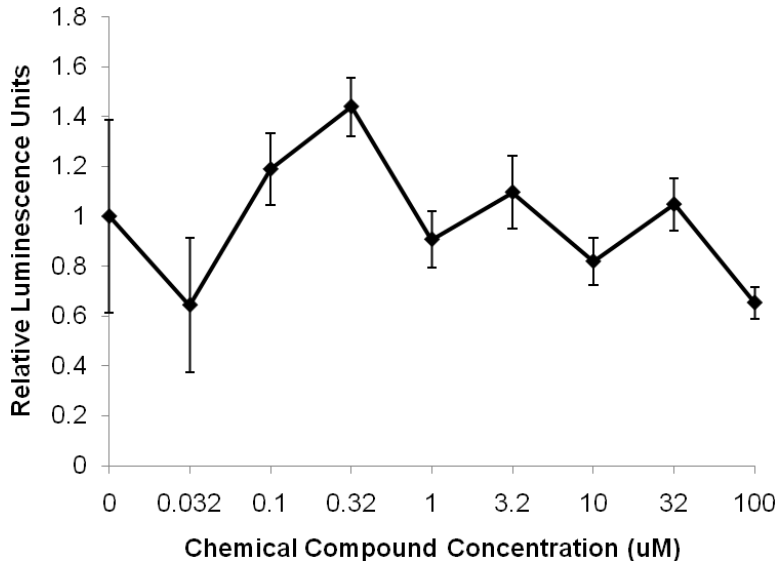

Figure 3.9. EDTA luciferase assay dose response results. EDTA was dissolved at a concentration of 100 µM in media, serially diluted in media, and added to HAEC. 24 hours later, adeno-associated virus was added, followed by luciferase assay after another 24 hours.

3.4.6. Alkylating Agents

Carboplatin, cisplatin, and melphalan all provided dose-dependent enhancement of adeno-associated virus transduction of HAEC. At high concentrations, both cisplatin and melphalan showed a decrease in luminescence signal which was explained by the toxicity of these compounds at high concentrations. Based on these results, it appears that DNA alkylation is a mechanism for increased adeno-associated virus transduction. Russel, Alexander, and Miller demonstrated that treating cells with radiation or DNA-damaging chemicals enhanced adeno-associated virus transduction, and our results corroborate those findings.[18, 79, 80]

3.4.6.1. Carboplatin

Carboplatin, an alkylating agent, was found to have a dose-dependent enhancement of adeno-associated virus activity. Carboplatin demonstrated a 2.5 fold increase in transduction efficiency in primary screening (**Appendix Table A4**). Carboplatin dissolved in DMSO led to an enhancement of up to 7 fold at high concentrations with an EC50 based on all available data of about 50 μM (**Figure 3.10a**). When dissolved in media and filtered, carboplatin's enhancement activity was more limited, with a maximum enhancement of about 2 fold. (**Figure 3.10b**). This discrepancy may be due to an effect of DMSO or due to limitations of compound solubility in aqueous solution. Although the compound is commonly known to be toxic due to its DNA alkylation

activity, no viability changes were observed in a dose-response assay over this range (**Figure 3.10c, d**).

a)

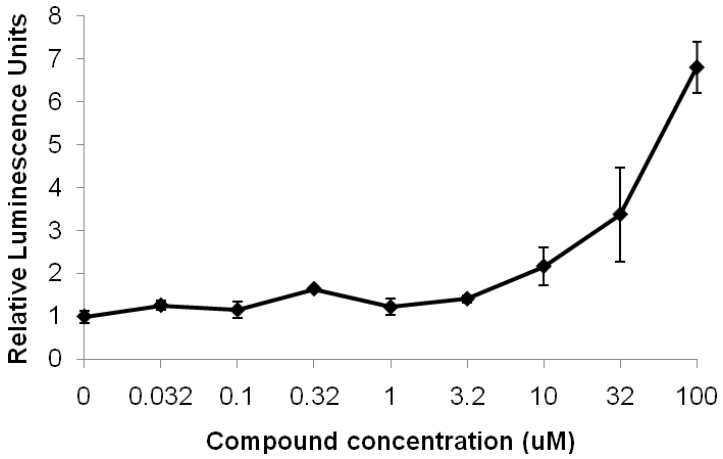

b)

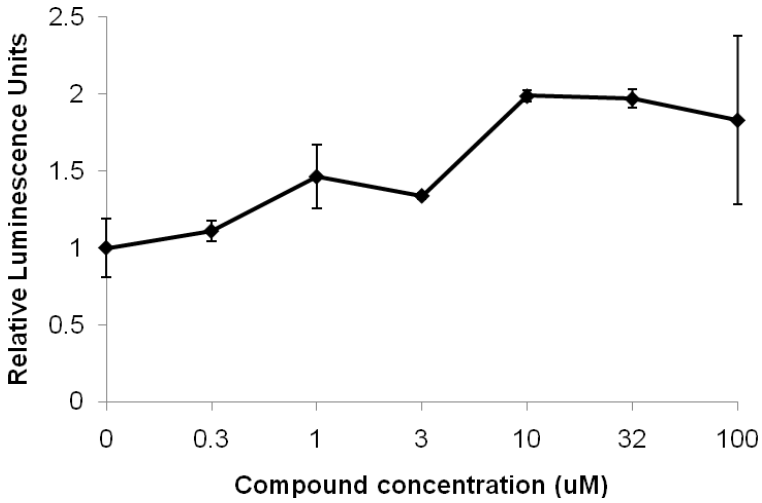

c)

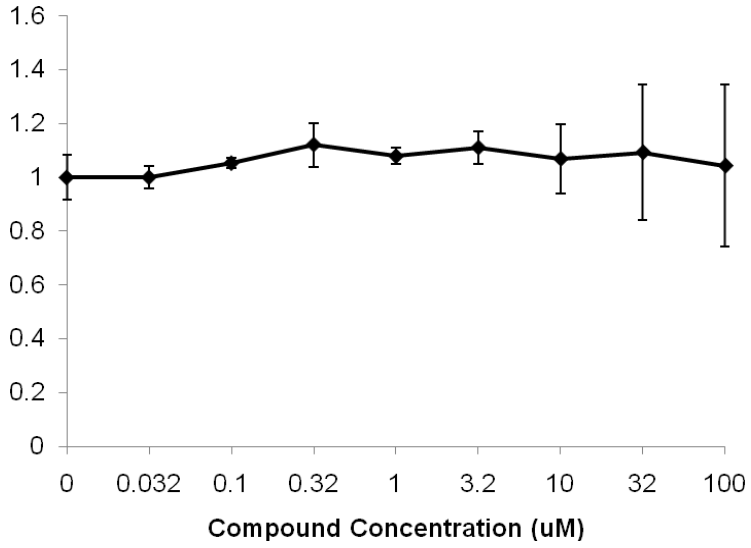
1.6
1.4
1.2
1
0.8
0.6
0.4
0.2
0
0
0.032
0.1
0.32
1
3.2
10
32
100
Compound Concentration (uM)

d)

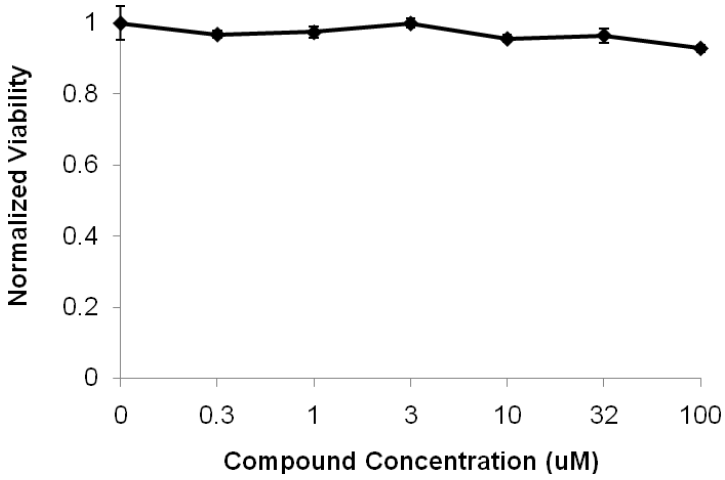
Normalized Viability
1
0.8
0.6
0.4
0.2
0
0
0.3
1
3
10
32
100
Compound Concentration (uM)

e)

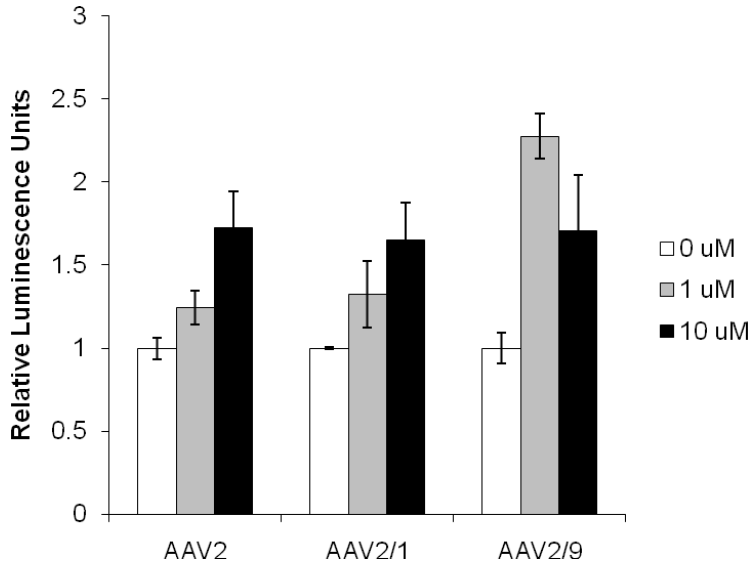

Figure 3.10. Carboplatin results. a) Carboplatin was dissolved at a concentration of 10 mM in DMSO, serially diluted in DMSO, and added to HAEC cells in media such that the final DMSO concentration in each well was 1%. 24 hours later, adeno-associated virus was added, followed by luciferase assay after another 24 hours. b) Carboplatin was dissolved at a concentration of 10 mM in media, serially diluted in media, and added to HAEC cells in media. 24 hours later, adeno-associated virus was added, followed by luciferase assay after another 24 hours. c) HAEC viability after 48 hours of exposure to carboplatin dissolved in DMSO, normalized to DMSO control. d) HAEC viability after 48 hours of exposure to carboplatin dissolved in media. e) Luciferase assay results for HAEC exposed to carboplatin followed by treatment with AAV2, AAV2/1, or AAV2/9.

HAEC treated with 10 µM carobplatin were additionally subject to transduction with AAV2-EGFP and examined using fluorescence microscopy, PCR, qRT-PCR, flow cytometry, and BCA assay. As shown in **Table 3.1**, the amount of viral DNA was the same as the control sample, although viral RNA present was increased by a factor of 1.7. The average fluorescence was 20% higher than in the control. The total protein in the well was less than the control. **Figure 3.11** provides corresponding information for

fluorescence microscopy and flow cytometry. Cells treated with the carboplatin do not show a large morphological change as determined by microscopy or by flow cytometry (**Figure 3.11a,b,c,d**). An overlay of the fluorescence data shows the overall fluorescence profile shifting slightly to the right. (**Figure 3.11e**).

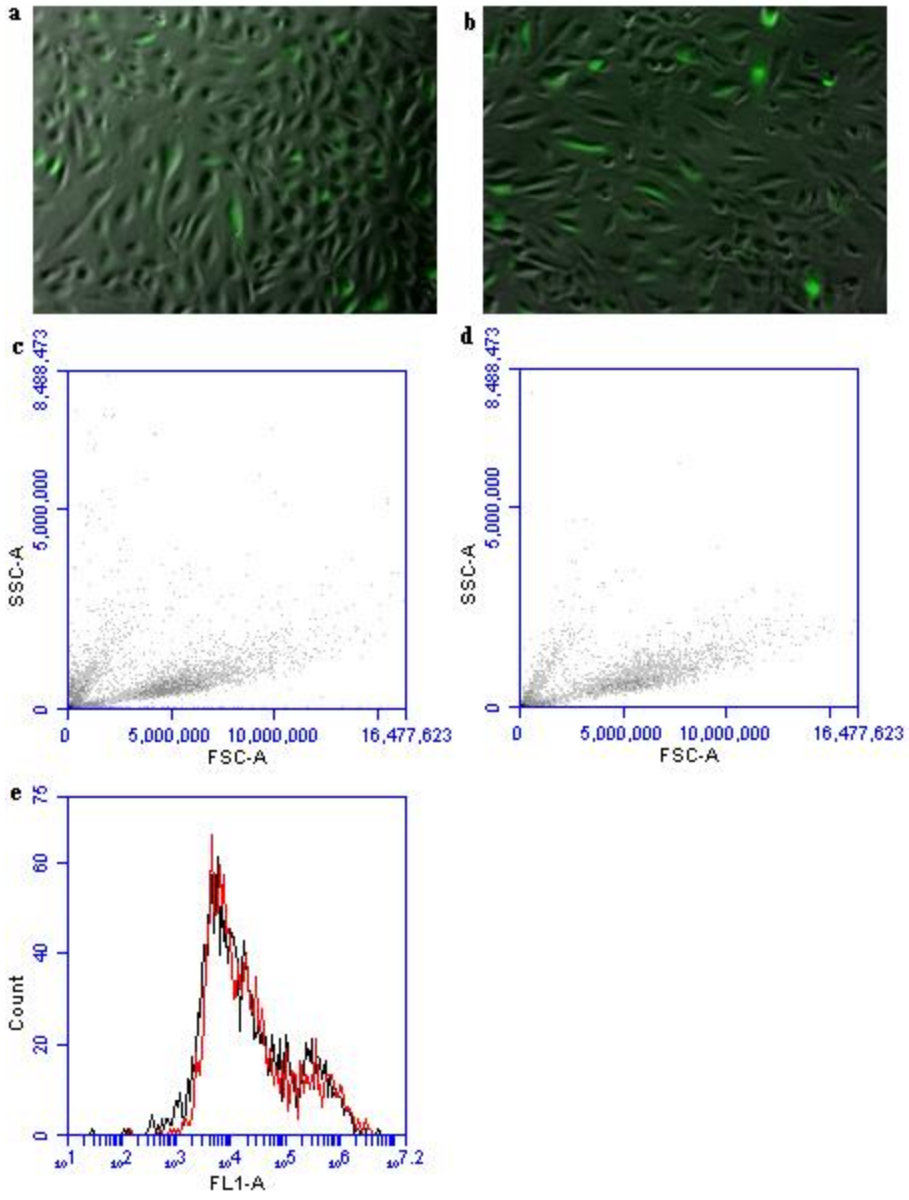

Figure 3.11. Fluorescence microscopy images and flow cytometry data for HAEC treated with carboplatin followed by AAV2-EGFP transduction. a. Image of HAEC transduced with AAV2-EGFP. b. Image of HAEC treated with carboplatin followed by AAV2-EGFP transduction. c. Forward and side scatter results for HAEC transduced with AAV2-EGFP from flow cytometry. d. Forward and side scatter results for HAEC treated with carboplatin followed by AAV2-EGFP from flow cytometry. e. Histogram overlay of fluorescence area for HAEC treated with AAV2-EGFP (black) and HAEC treated with carboplatin followed by AAV2-EGFP (red).

3.4.6.2. Cisplatin

Cisplatin, a compound highly related to carboplatin, was also tested and found to be beneficial for viral transduction. Alexander and colleagues previously reported that cisplatin facilitates adeno-associated virus transduction.[79] Cisplatin is a very similar compound to carboplatin. It was evaluated in order to determine if enhancement due to carboplatin was due to the bidentate carboxylate group of the carboplatin or due to the *cis*-diammine platinum portion of the molecule which it has in common with cisplatin. As shown in **Figure 3.12a**, cisplatin is also capable of enhancing viral transduction, with enhancement of nearly 4-fold at its peak. However, as shown in **Figure 3.12b**, toxic effects begin to be seen between 10 and 100 uM, limiting cisplatin's effectiveness.

a)

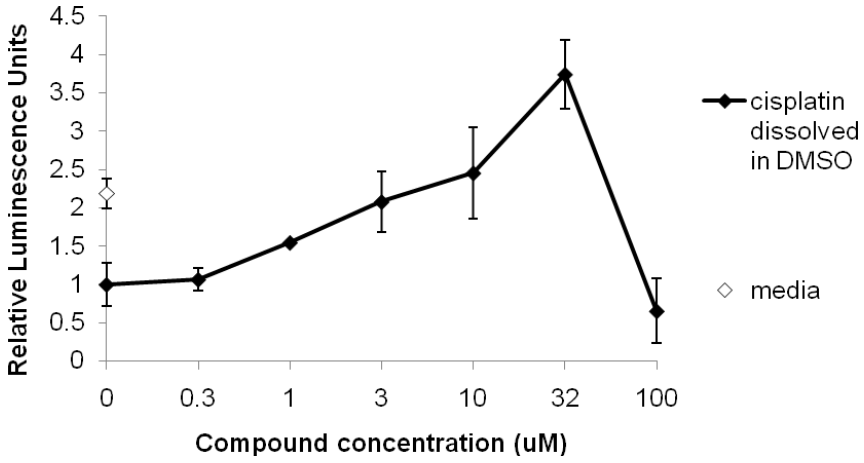

b)

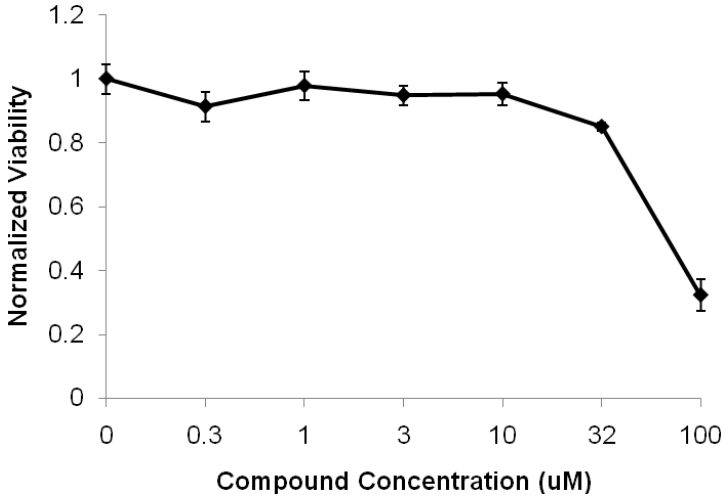

Figure 3.12. Cisplatin results. a) Cisplatin was dissolved at a concentration of 10 mM in media, serially diluted in media, and added to HAEC cells in media. 24 hours later, adeno-associated virus was added, followed by luciferase assay after another 24 hours. **b)** Cell viability after 48 hours of exposure to cisplatin.

3.4.6.3. Melphalan

Melphalan is another DNA alkylating agent which caused enhancement in primary screening, with the observed enhancement of 2.1 fold. In subsequent dose-response experiments, melphalan was capable of enhancement of up to 5-fold, although at high concentrations toxicity was observed (**Figure 3.13a,b**).

a)

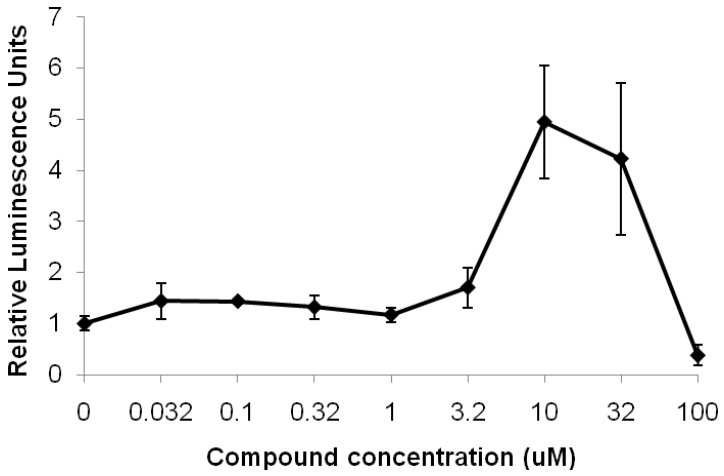

b)

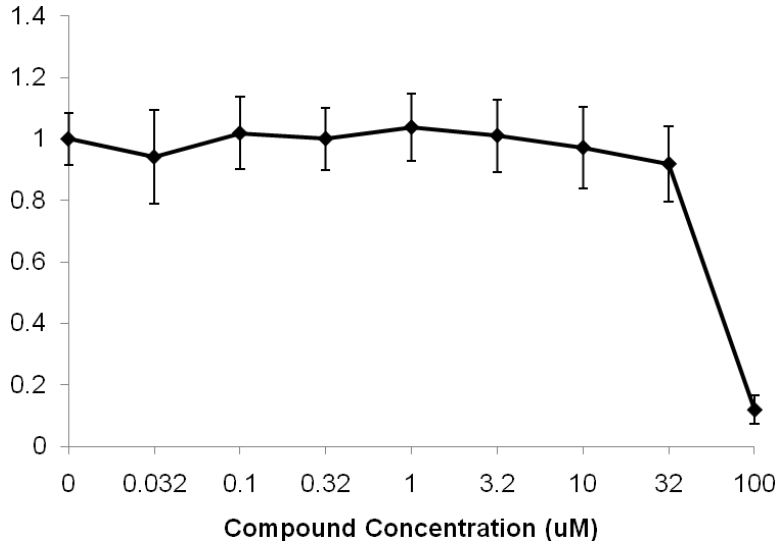

c)

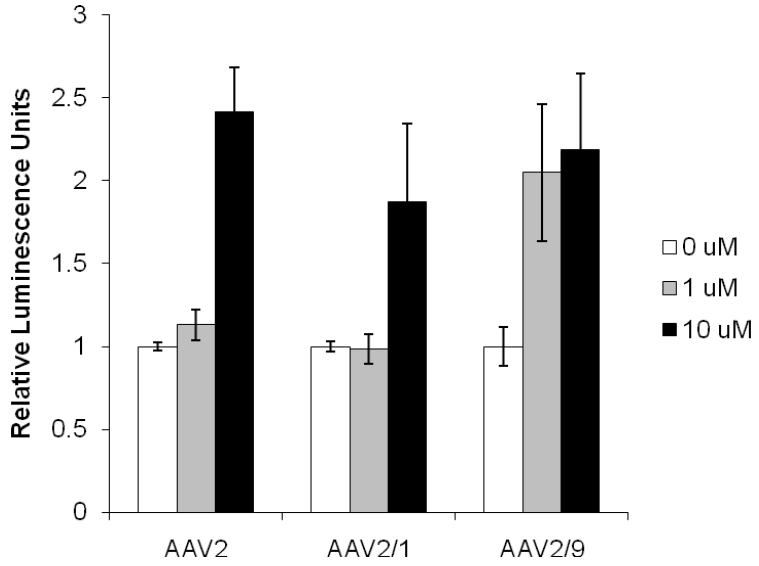

Figure 3.13. Melphalan luciferase assay and viability results. a) Melphalan was dissolved at a concentration of 10 mM in DMSO, serially diluted in DMSO, and added to HAEC cells in media such that the final DMSO concentration in each well was 1%. 24 hours later, adeno-associated virus was added, followed by luciferase assay after another 24 hours. b) Cell viability after 48 hours of exposure to melphalan dissolved in DMSO. c) Luciferase assay results for HAEC exposed to melphalan followed by exposure to AAV2, AAV2/1, or AAV2/9.

HAEC treated with 10 μM melphalan were additionally subject to transduction with AAV2-EGFP and examined using fluorescence microscopy, PCR, qRT-PCR, flow cytometry, and BCA assay. As shown in **Table 3.1**, the amount of viral DNA measured in the cell was less than in the 1% DMSO control, whereas viral RNA and fluorescence were each increased greater than two-fold (2.7 and 2.6 fold, respectively). The total protein per well as measured by BCA assay increased by 70%. **Figure 3.14** provides corresponding information for fluorescence microscopy and flow cytometry. As compared with the 1% DMSO control, the cells treated with melphalan appear to have a small highly fluorescent population (**Figure 3.14a,b**). Flow cytometry showed no morphological changes between cells treated with melphalan and those treated with DMSO only (**Figure 3.14c,d**). An overlay of the fluorescence data shows that the fluorescence profile of the melphalan treated cells is shifted to the right slightly in comparison with the 1% DMSO only treated cells (**Figure 3.14e**).

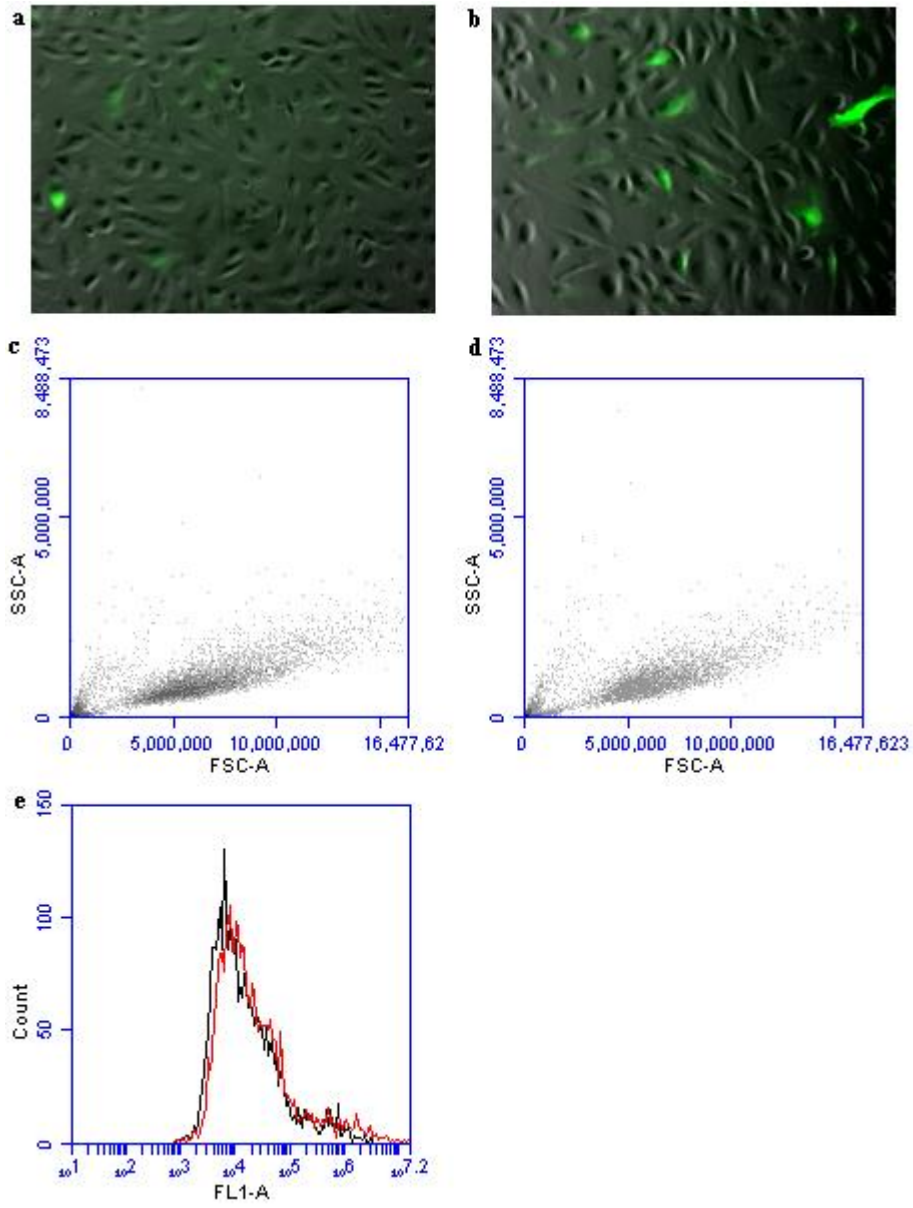

Figure 3.14. Fluorescence microscopy images and flow cytometry data for HAEC treated with melphalan followed by AAV2-EGFP transduction. a. Image of HAEC treated with 1% DMSO followed by AAV2-EGFP. b. Image of HAEC treated with melphalan in 1% DMSO followed by AAV2-EGFP. c. Forward and side scatter results for HAEC treated with 1% DMSO followed by AAV2-EGFP from flow cytometry. d. Forward and side scatter results for HAEC treated with melphalan in 1% DMSO followed by AAV2-EGFP from flow cytometry. e. Histogram overlay of fluorescence area for HAEC treated with 1% DMSO (black) and melphalan in 1% DMSO followed by HAEC treated with AAV2-EGFP (red).

3.4.7. Nucleoside Analogs

Three of the compounds (5-bromo-2-deoxyuridine, vidarabine, and AZT) identified in primary screening are nucleoside analogs which are incorporated during DNA synthesis. Two of the three are often used as anti-viral drugs. AZT is well-known as a reverse transcriptase inhibitor for HIV treatment, and vidarabine is used for several different virus types. The third compound, 5-bromo-2-deoxyuridine, is most often used for molecular biology experiments as a way to study DNA synthesis. It is important to note that the engineered AAV2 is a single-stranded DNA virus that is not replication competent, and therefore some mechanisms that interfere with viral replication (for example, reverse transcriptase inhibition) should not affect this virus. However, the evidence here that these nucleoside analogs enhance AAV2 transduction was initially surprising. However, these results do fit with the findings of previous researchers that DNA damage enhances AAV2 transduction.[18, 79, 80]

Four nucleoside analogs were examined in this study. Three of the four were reproducibly found to be beneficial for viral transduction and were well-tolerated in viability assays. Overall, it appears that the addition of nucleoside analogs assists in the viral transduction of adeno-associated virus.

3.4.7.1. Azidothymine (AZT)

Azidothymine (AZT) is a nucleoside analog commonly used as an HIV reverse transcriptase inhibitor which demonstrated viral enhancement of 2.2 fold in primary screening (**Appendix Table A4**). As shown in **Figure 3.15**, AZT demonstrated at most a moderate enhancement in dose-response testing, which may be due to experimental artifact (well plate edge effects). Although AZT did not demonstrate enhancement in dose-response studies presented here, in preliminary work it demonstrated enhancement of up to 2.5-fold (*data not shown*), suggesting that limitations of the compound's stability may have led it to be less effective during later experiments.

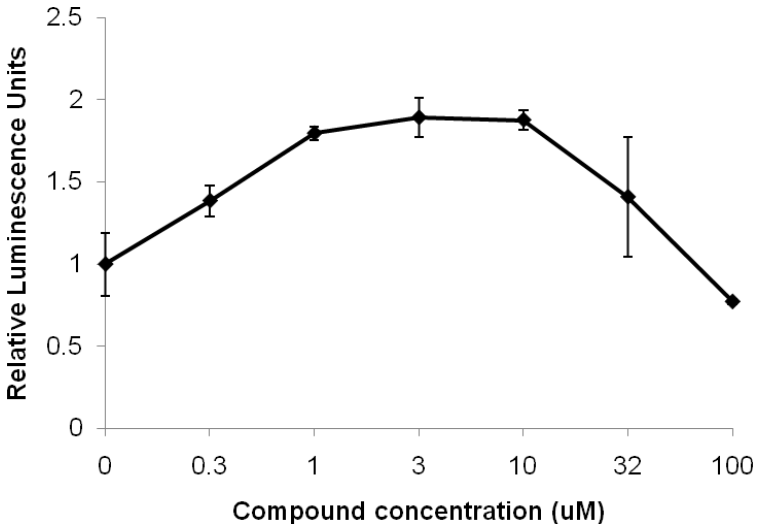

Figure 3.15. Azidothymine (AZT) luciferase results. AZT was dissolved at a concentration of 10 mM in media, serially diluted in media, and added to HAEC cells in media. 24 hours later, adeno-associated virus was added, followed by luciferase assay after another 24 hours.

3.4.7.2. Adenine 9-beta-d-arabinofuranoside (Vidarabine)

Adenine 9-beta-d-arabinofuranoside (vidarabine) is a nuceloside analog which demonstrated a 2.4 fold increase in viral transduction in primary screening (Supplementary Table S3). In dose-response testing, vidarabine showed enhancement of up to three-fold at high concentrations, with an EC50 of about 16 µM (**Figure 3.16**).

a)

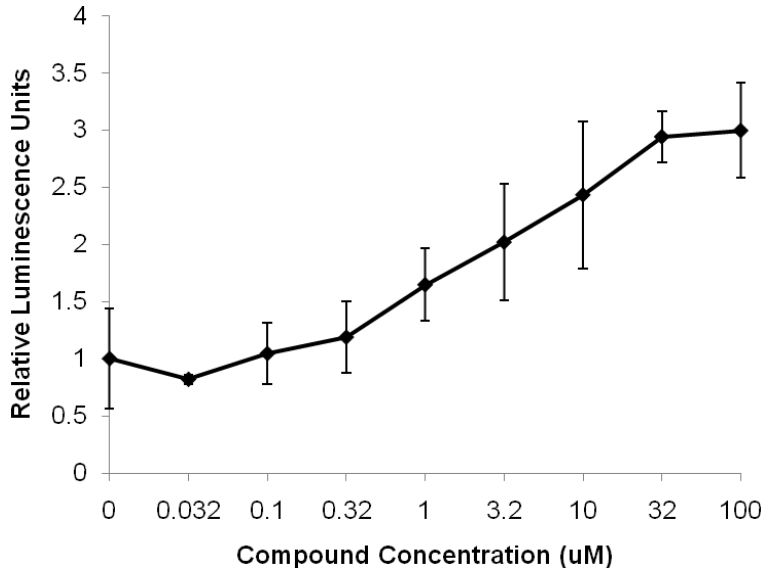

b)

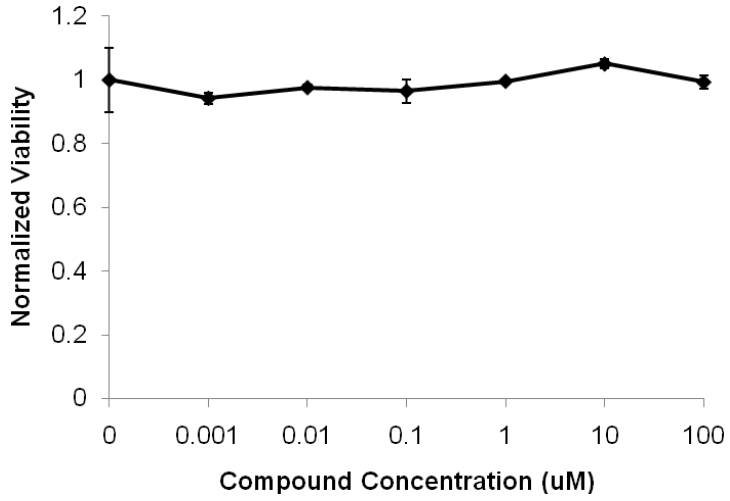

c)

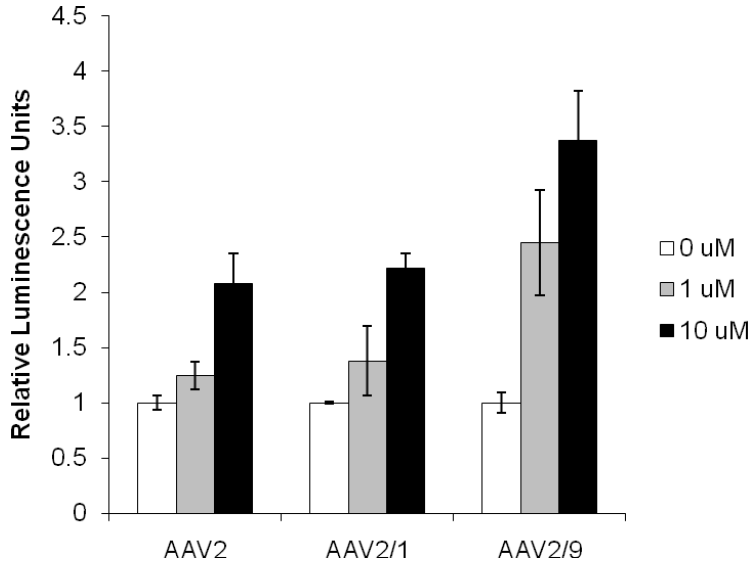

Figure 3.16. Vidarabine luciferase and viability results. a) Vidarabine was dissolved at a concentration of 10 mM in media, serially diluted in media, and added to HAEC cells in media. 24 hours later, adeno-associated virus was added, followed by luciferase assay after another 24 hours. b) HAEC viability following 48 hours of exposure to vidarabine. c) Luciferase assay results for HAEC exposed to vidarabine followed by addition of AAV2, AAV2/1, or AAV2/9.

HAEC treated with 10 μM vidarabine were additionally subject to transduction with AAV2-EGFP and examined using fluorescence microscopy, PCR, qRT-PCR, flow cytometry, and BCA assay. As shown in **Table 3.1**, the amount of viral DNA was less than in the control sample, although viral RNA present was increased by a factor of 2.8. The average fluorescence was 40% higher than in the control. The total protein in the well was less than the control. **Figure 3.17** provides corresponding information for fluorescence microscopy and flow cytometry. Cells treated with the vidarabine do not show a large morphological change as determined by microscopy or by flow cytometry (**Figure 3.17a,b,c,d**). An overlay of the fluorescence data shows the overall fluorescence profile shifting slightly to the right. (**Figure 3.17e**).

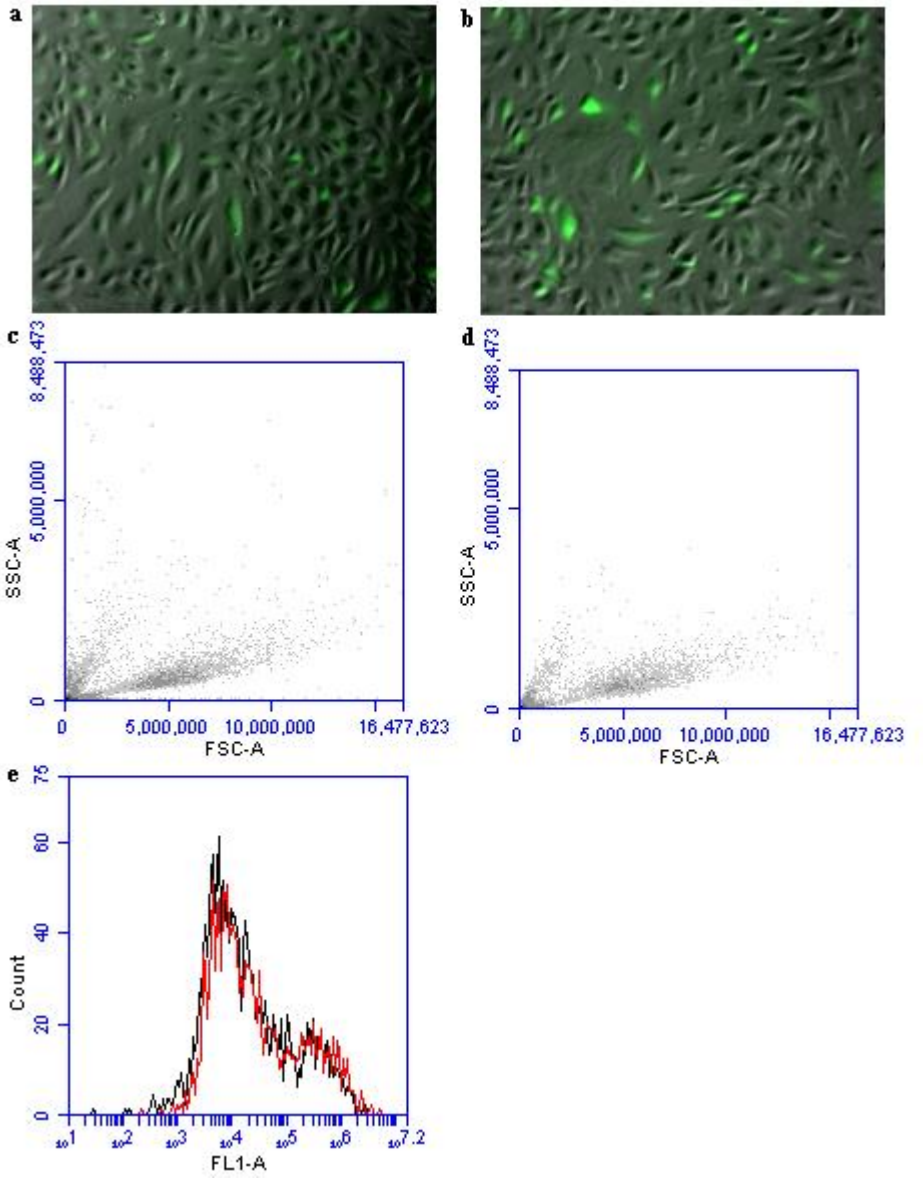

Figure 3.17. Fluorescence microscopy images and flow cytometry data for HAEC treated with vidarabine followed by AAV2-EGFP transduction. a. Image of HAEC transduced with AAV2-EGFP. b. Image of HAEC treated with 10 µM vidarabine followed by transduction with AAV2-EGFP. c. Forward and side scatter results for HAEC transduced with AAV2-EGFP from flow cytometry. d. Forward and side scatter results for HAEC treated with 10 µM vidarabine followed by transduction with AAV2-EGFP from flow cytometry. e. Histogram overlay of fluorescence area for HAEC transduced with AAV2-EGFP (black) and 10 µM vidarabine followed by HAEC treated with AAV2-EGFP (red).

3.4.7.3. Cytosine arabinofuranoside (Cytarabine)

Based on the high representation of nucleoside analogs as primary screening hits, a related compound, cytarabine (cytosine beta-d-arabinofuranoside), was additionally examined. This compound is a cysteine analog. Cytarabine was examined as a nucleoside analog not identified in primary screening to validate the ability of this class of chemicals to provide enhancement. Cytarabine showed an increase of nearly 4-fold enhancement at higher doses, with an EC50 of about 16 µM (**Figure 3.18a**).

a)

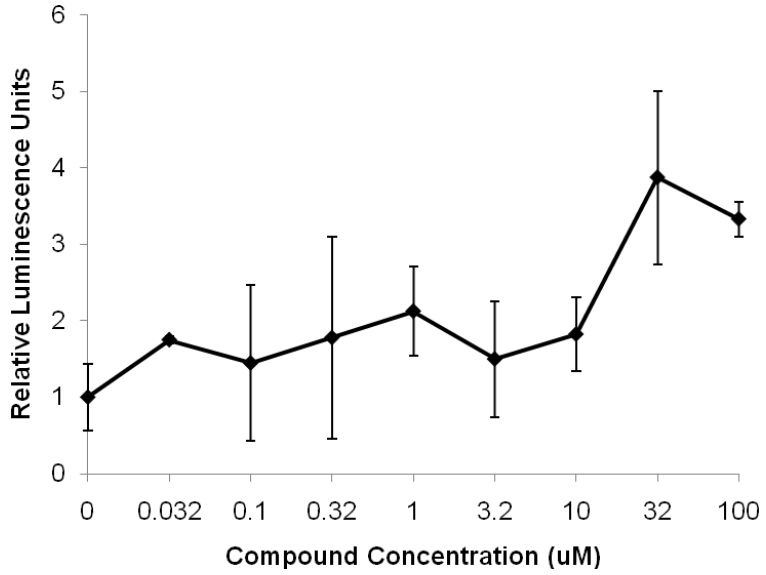

b)

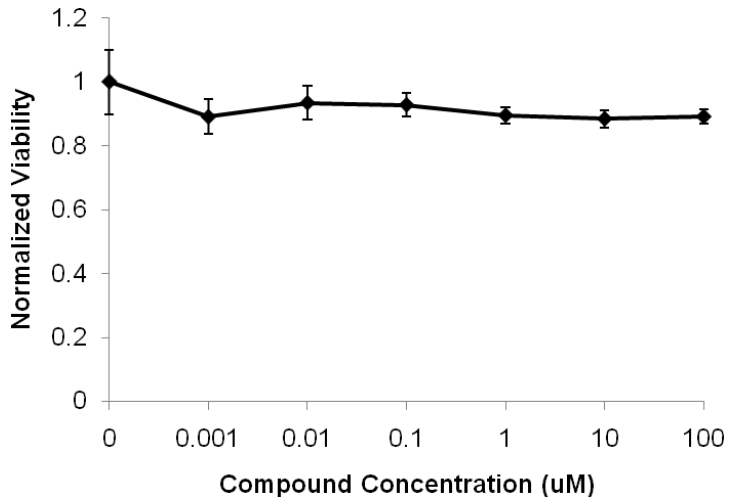

Figure 3.18. Cytarabine luciferase and viability results. a) Cytarabine was dissolved at a concentration of 10 mM in media, serially diluted in media, and added to HAEC cells in media. 24 hours later, adeno-associated virus was added, followed by luciferase assay after another 24 hours. **b)** HAEC viability following 48 hours of exposure to cytosine arabinofuranoside.

3.4.7.4. 5-bromo-2'-deoxyuridine

5-bromo-2'-deoxyuridine is a nucleoside analog which was identified as an enhancer at the level of 2.6 fold enhancement in primary screening (**Appendix Table A4**). In dose-response testing, 5-bromo-2'-deoxyuridine showed continuous increase in enhancement activity of over 4-fold enhancement at the maximum concentration tested of 100 µM (**Figure 3.19a**). The EC50 for this compound is above 50 µM.

a)

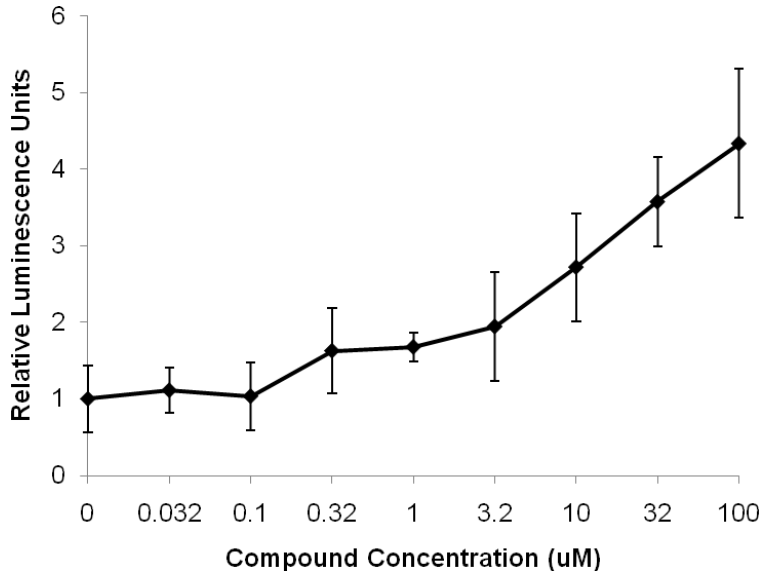
Relative Luminescence Units
0
1
2
3
4
5
6
0
0.032
0.1
0.32
1
3.2
10
32
100
Compound Concentration (uM)

b)

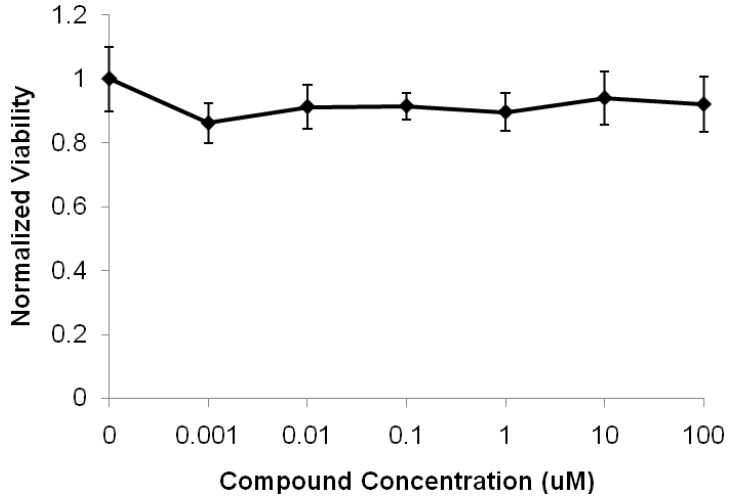
Normalized Viability
0
0.2
0.4
0.6
0.8
1
1.2
0
0.001
0.01
0.1
1
10
100
Compound Concentration (uM)

c)

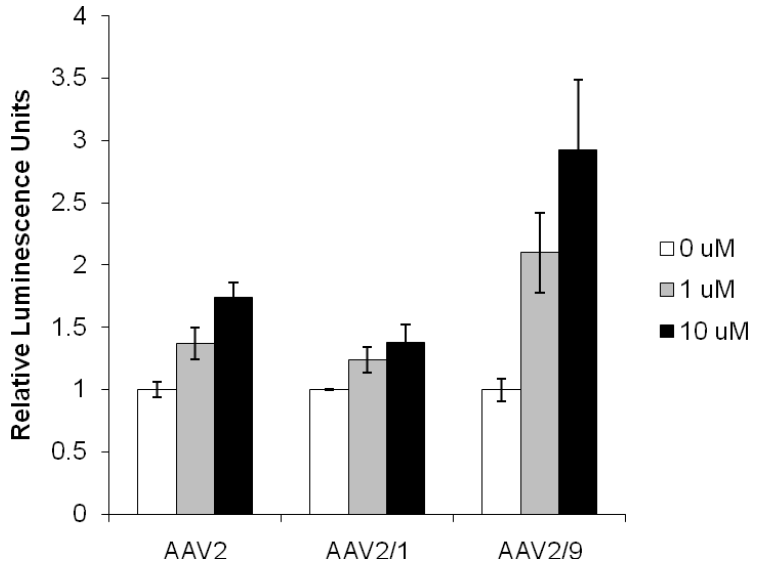

Figure 3.19. 5-bromo-2'-deoxyuridine luciferase and viability results. a) 5-bromo-2'-deoxyuridine was dissolved at a concentration of 10 mM in media, serially diluted in media, and added to HAEC cells in media. 24 hours later, adeno-associated virus was added, followed by luciferase assay after another 24 hours. b) HAEC viability following 48 hours of exposure to 5-bromo-2'-deoxyuridine. c) Luciferase assay results for HAEC treated with 5-bromo-2'-deoxyuridine followed by addition of AAV2, AAV2/1, or AAV2/9.

HAEC treated with 10 μM 5-bromo-2'-deoxyuridine were additionally subject to transduction with AAV2-EGFP and examined using fluorescence microscopy, PCR, qRT-PCR, flow cytometry, and BCA assay. As shown in **Table 3.1**, the amount of viral DNA was the less than in the control sample, although viral RNA present was increased by over five-fold. The average fluorescence was more increased more than 2 fold compared to control. The total protein in the well was less than the control. **Figure 3.20** provides corresponding information for fluorescence microscopy and flow cytometry. Cells treated with the 5-bromo-2'-deoxyuridine do not show a large morphological

change as determined by microscopy or by flow cytometry (**Figure 3.20a,b,c,d**). An overlay of the fluorescence data shows more cells exhibiting fluorescence at the very high end of the spectrum. (**Figure 3.20e**).

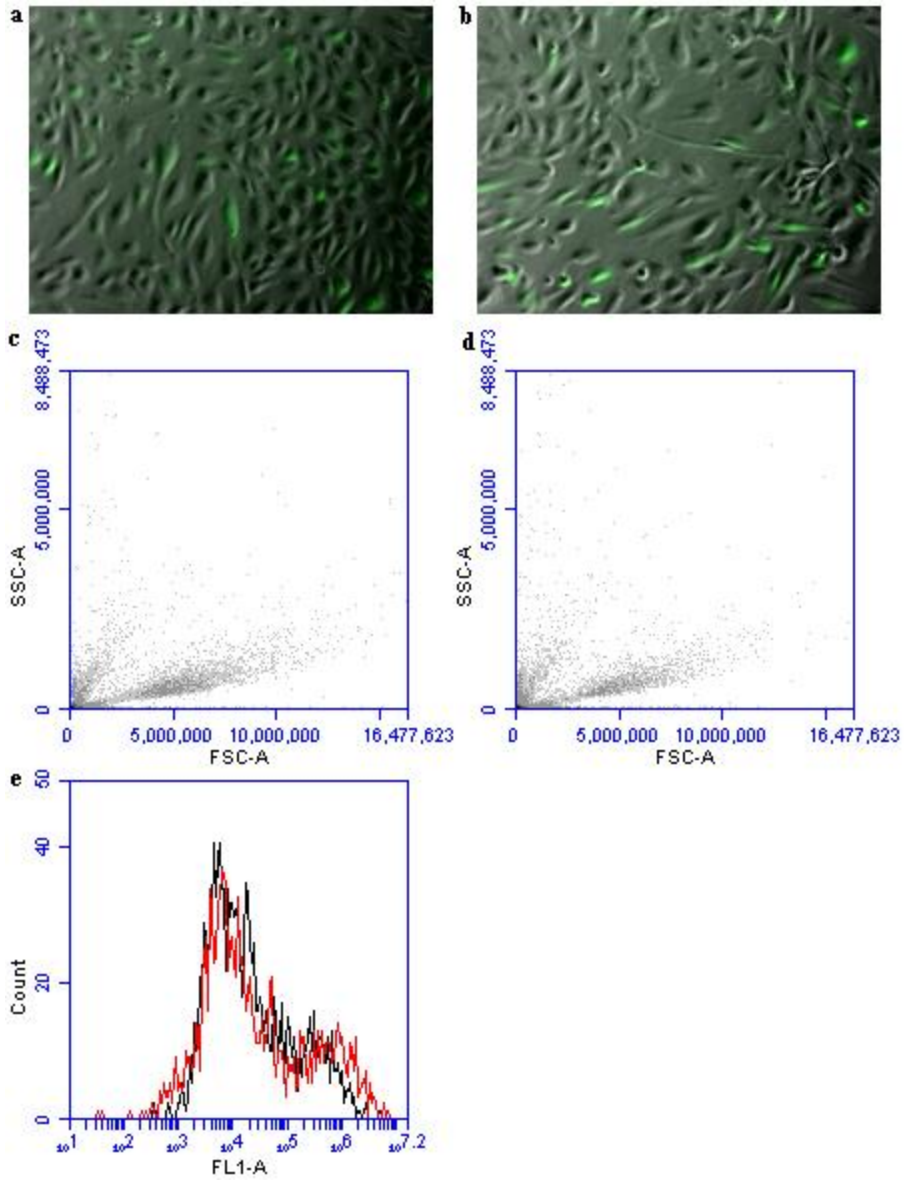

Figure 3.20. Fluorescence microscopy images and flow cytometry data for HAEC treated with 5-bromo-2'-deoxyuridine followed by AAV2-EGFP transduction. a. Image of HAEC transduced with AAV2-EGFP. b. Image of HAEC treated with 10 µM 5-bromo-2'-deoxyuridine followed by transduction with AAV2-EGFP. c. Forward and

side scatter results for HAEC transduced with AAV2-EGFP from flow cytometry. d. Forward and side scatter results for HAEC treated with 10 μM 5-bromo-2'-deoxyuridine followed by transduction with AAV2-EGFP from flow cytometry. e. Histogram overlay of fluorescence area for HAEC transduced with AAV2-EGFP (black) and 10 μM 5-bromo-2'-deoxyuridine followed by HAEC treated with AAV2-EGFP (red).

3.4.8. Cell Cycle Arrestors

1,10-phenanthroline, although cytotoxic, has been shown to increase transcription and activity of p53.[78] p53 serves many antitumorigenic roles within the cell, one of which is to temporarily arrest the cell cycle in the G1 phase.[81] Daidzein, which also halts progression of the cell cycle past G1, is another chemical which enhanced transduction in the compound screen. Previous reports have shown that the S-phase of the cell cycle is more permissive to viral transduction, so it is interesting that these compounds arrest the cell cycle in G1 rather than in S-phase.

The mechanism of action of these compounds for enhancement of viral transduction may therefore be unrelated to their cell cycle arresting activity, especially in light of the minimal enhancement activity demonstrated by NU 2058.

3.4.8.1. NU 2058

NU 2058 inhibits cyclin-dependent kinase 1 and cyclin-dependent kinase 2.[82] It was examined in order to evaluate the ability of cell cycle arrestors to enhance viral transduction, as inhibition of these kinases restricts the cell's ability to move from G1

into S phase. NU 2058 showed limited enhancement in dose-response testing. (**Figure 3.21**).

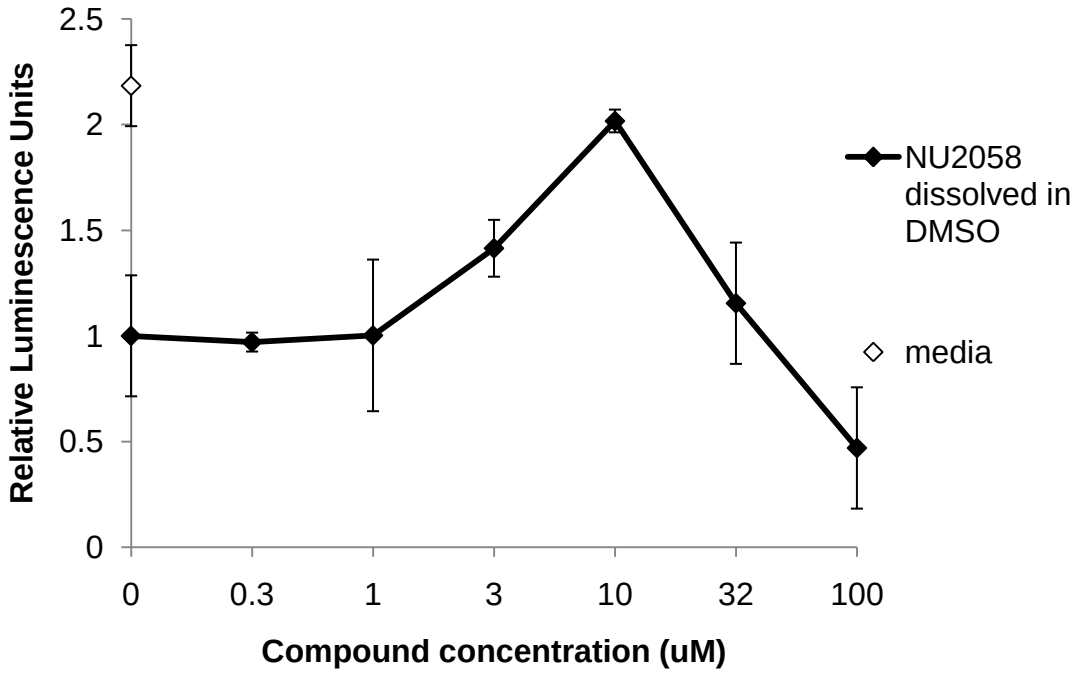

Figure 3.21: NU 2058 luciferase assay results. NU2058 was dissolved at a concentration of 10 mM in 100% DMSO, serially diluted in media, and added to HAEC cells in media. 24 hours later, adeno-associated virus was added, followed by luciferase assay after another 24 hours.

3.5. Discussion

Over two thousand compounds were tested for enhancement of adeno-associated viral transduction, and 20 (0.9%) were identified as hits with enhancement of two-fold or greater. These compounds represented many different types of pharmacologically active agents. Although a variety of families of compounds were tested, several classes of

molecules stood out as being overrepresented in the list of primary screening hits, including EGFR tyrosine kinase inhibitors, antioxidants, nucleoside analogs, and alkylating agents.

EGFR tyrosine kinase inhibitors were not studied in detail, although the presence of several Tyrphostin compounds in screening results did agree with previous data that these compounds enhance AAV2 transduction.

Several primary screening hits have antioxidant activity, including the top enhancer, ellagic acid. However, dose-response studies with other compounds including caffeic acid phenethyl ester, ascorbic acid, and N-acetyl cysteine, failed to show a smilar level of benefit. A detailed investigation of ellagic acid effects on the cell-virus interaction found that while viral DNA levels were unchanged, mRNA levels and reporter gene expression levels were very high. However, levels of cellular mRNA and total protein also appeared to increase.

1,10-phenanthroline, the second highest hit in primary screening, demonstrated enhancement of viral transduction that was not replicated with a second metal chelator tested, EDTA. This compound was the only chemical tested which resulted in an increase in viral DNA as measured by quantitative real time PCR, indicating that its mechanism is unique amongst the compounds investigated. However, as multiple viral pseudotypes which bind to different cell surface receptors all were enhanced by the addition of 1,10-phenanthroline, the mechanism is not related to increased binding of the virus to the cell surface.

DNA damaging agents including nucleoside analogs and alkylating agents facilitated AAV2 transduction, and specifically led to an increase in mRNA levels. This is consistent with previous research indicating that damaging cellular DNA enhances AAV transduction. .[18, 79, 80]

Cell cycle arrestors may be beneficial for adeno-associated viral transduction, but the one compound tested that was not identified in primary screening (NU 2058) did not enhance transduction.

The results from this study demonstrated the feasibility of the high throughput screening approach to identifying small molecule enhancers of AAV2. Furthermore, a small set of strong enhancers of AAV2 has been identified and some mechanistic insight was gained. These enhancers and their respective mechanisms can serve as a basis for further study.

Chapter 4

Conclusions and Future Work

4.1. Conclusions

Gene therapy holds the potential to allow a new set of diseases to be prevented, treated, or cured. Following successful delivery and expression of the target gene, cells produce the therapy themselves, allowing targeted, novel treatments that were impossible in the past.

While gene therapy holds such promise, there is a lot of research required to make this dream a reality. A major challenge for all gene therapy treatments is to identify a vector that will be safe and effective.

In many ways, adeno-associated virus is an ideal vector for gene delivery. This vector is safe, causing no known human disease and evoking little to no immune response. The ability to select from a variety of natural serotypes and/or engineer new serotypes allows it to be targeted to specific organs and disease types. The most pressing drawback to the use of this virus is limited efficacy.

In an effort to address this issue, we have used high throughput screening to identify enhancers of AAV2 transduction of human endothelium. In the first screen, we used siRNA knockdown of 5,520 human gene targets to identify siRNA enhancers. In the

second screen, we treated HAEC with 2,320 chemical compounds to identify small molecule enhancers.

The siRNA high throughput screen identified 10 siRNA sequence hits. One of the top hits, the CLIC2(C) siRNA sequence, enhanced transduction due to an off-target effect unrelated to a decrease in CLIC2 mRNA. The action of this siRNA was found to be related to a hexamer seed region [5'-U_2GUUUC_7-3'] which was shared with several other top siRNA sequence hits.

Although the specific mechanism by which the CLIC2(C) sequence acts remains unknown, transcription profiling implicated the interferon pathway. Knockdown of the interferon (alpha, beta, omega) receptor 2 was additionally shown to benefit transduction, and addition of interferon alpha or beta was shown to hamper transduction. These results have potential implications for cancer gene therapy, as one clinical strategy being studied uses AAV2 to deliver interferon-β to cancer cells. Although these studies have shown positive results, there is a possibility that repeat administration of the vector could be inhibited by the interferon transgene.

The chemical compound screen identified individual chemical hits as well as several categories of enhancing compounds. Specifically, ellagic acid, 1,10-phenanthroline, alkylating agents, nucleoside analogs, and EGFR protein tyrosine kinase inhibitors stood out. Although antioxidants initially appeared to benefit viral transduction, additional compounds which were tested such as ascorbic acid, n-acetyl cysteine, and curcumin all failed to demonstrate a gene delivery benefit. Additional chemical functions such as cell

cycle arrest and metal chelation did not appear to have strong enhancement effects. EGFR protein tyrosine kinase inhibitors were not examined in great detail since their mechanism of enhancing AAV has already been explored by other researchers.[70]

In primary screening, ellagic acid provided the strongest enhancement to AAV2 transduction, with nearly 8-fold stronger luminescence signal than control. Within the dose range studied, ellagic acid showed a dose-dependent increase in transduction efficiency with increasing dose. Detailed studies showed that the ellagic acid benefit can be measured beginning with strongly increased mRNA levels, although viral DNA levels are unchanged. However, there is some evidence that this may be due to a global mechanism of increased mRNA transcription, and must be studied further to determine whether this increase is specific to the AAV2 vector.

1,10-phenanthroline was the second-strongest hit identified in primary screening, with over 6-fold enhancement of signal. This enhancement comes downstream of viral attachment to cell surface receptors, but increased viral DNA signal is observed. This suggests that the effect of 1,10-phenanthroline comes at either the endosomal processing/transport stage or the viral second-strand DNA synthesis stage of the viral transduction process. Given the metalloprotease inhibitor characteristics of this compound, one possibility is that it protects the virus from degradation by metalloproteases during endosomal processing.

Both alkylating agents and nucleoside analogs were successful in enhancing AAV2 transduction. Both of these categories of chemicals damage DNA, and the cellular DNA repair mechanisms may be implicated in assisting viral transduction.[18, 79, 80]

4.2. Future Work

4.2.1. siRNA Mechanism

Future work is needed to determine the significance of the hexamer seed region identified in siRNA screening. A variety of different techniques can be used in an effort to tackle this problem.

First, as the field of miRNA research develops and more information is added to bioinformatic databases, the importance of this specific hexamer sequence may become clearer. Specifically, monitoring of the microRNA databse at www.mirdb.org would be beneficial.[83, 84]

Further transcriptional profiling with more controls added would allow finer tuning of microarray results. Specifically, a comparison could include active CLIC sequence A or B, active CLIC2 sequence C, and a mutated sequence with the mutation outside the hexamer seed region. Transcripts which are similar for the active CLIC2 sequence but not the mutant are then known to be related to CLIC2 knockdown rather than to the hexamer seed region. Transcripts which are similar for the two sequences containing the

hexamer seed region but that are lacking in CLIC2 sequence A or B would be the most critical to investigate.

Additionally, mechanistic studies similar to what was performed for the chemical compounds, including quantification of viral RNA and DNA, could be carried out for top siRNA hits in order to provide a better understanding of where the siRNA enhances the viral transduction pathway.

4.2.2. Examination of Additional Compound Hits

For this work, we selected a subset of screening hits to focus on. Of the screening hits, there remain several compounds which were not prioritized in this work, but which could yield interesting results. Specifically, SB 202190 (4-(4-Fluorophenyl)-2-(4-hydroxyphenyl)-5-(4-pyridyl)-1H-imidazole) and DAPH (4,5-Dianilinophthalimide) are ripe candidates for investigation. SB 202190 is a p38 MAP kinase inhibitor and had 3.5 fold enhancement in primary screening, which was the fourth highest hit. DAPH is a protein tyrosine kinase inhibitor and had three-fold enhancement in primary screening, making it the fifth highest hit. The p38 MAP kinase inhibition mechanism may prevent the cell from producing immune-related cell signals. The protein tyrosine kinase inhibition of DAPH may or may not affect adeno-associated virus via the same mechanism as the EGFR protein tyrosine kinase inhibition of the Tyrphostin compounds.

4.2.3. Detailed Mechanism for Chemical Enhancement

Although the DNA damaging agents and EGFR protein tyrosine kinase inhibitors have been previously investigated by other researchers, we have also identified a few chemicals whose enhancement is via an unknown function. A closer examination of these mechanisms may lead to a better understanding of AAV2 biology, ultimately resulting in optimized formulations for viral delivery vectors or improved engineering of the vector itself.

Although antioxidant effects were initially suspected to be the cause of ellagic acid enhancement, these results were not confirmed by studies involving other antioxidants. Ellagic acid appears to enhance viral transduction at a stage prior to or beginning with transcription of mRNA. Also, ellagic acid increases mRNA transcription and protein production non-specifically, although the extent to which viral mRNA and protein production took place appears to be much higher than the level of increase that we have measured. Initial studies can examine cellular mRNA and protein production to quantify how much of the ellagic acid benefit is due to non-specific mechanisms. Additional potential mechanisms for the enhancement of ellagic acid may be related to effects on the cell cycle or activation of DNA repair mechanisms in response to DNA intercalation.

1,10-phenanthroline also enhanced AAV2 transduction via an unknown mechanism, although in this case levels of viral DNA were increased as well as transgene mRNA and protein levels. In order to study this in more depth, it will be useful to determine whether the increase in DNA is due to an increased ability of the virus to survive the endosome

and enter the nucleus, or if it is due to an increase in the second strand synthesis of DNA. Known lyosome inhibitors could be added to the cells in order to determine if an increase in viral transduction is possible as a result of decreased viral degradation in the endosome. If so, then a combination of 1,10-phenanthroline and the lyosome inhibitor could be added to cells. The combination of the two chemicals would be expected to result in little to no additive effect. In order to determine if the increase is related to second strand synthesis of DNA, a DNA synthesis inhibitor with and without the 1,10-phenanthroline could be added to cells in order to block the second strand synthesis of DNA. Then viral DNA quantities could be measured. If the viral DNA is the same in both cases, then enhancement is likely due to an increase in DNA synthesis. If the viral DNA quantity is different between the two, then enhancement occurs prior to DNA synthesis.

4.2.4. Screening of Additional Compound Libraries

This study identified several chemical enhancers of adeno-associated virus transduction out of a total of 2,320 compounds studied. However, much larger chemical libraries are available for screening. A much larger data set of chemical enhancers could be generated using these libraries, in order to identify a more complete understanding of adeno-associated virus biology and methods of enhancement.

Additionally, the primary screen presented here looked at chemicals at a single concentration (10 μM in 0.1% DMSO). A more complete set of chemical enhancers could be generated by examining more than one concentration, as the selected

concentration could be toxic for some compounds or not high enough to be effective for others.

Appendix

Table A1. Presence of hexamer seed region within the 3'-untranslated region.

Gene Symbol	5'-GAAACA-3'
IFIT5	no match
IFI44L	hexamer in three locations within 3' UTR
MX1	no match
TRIM48	no match
SLC5A2	no match
CLIC2	hexamer in three locations within 3' UTR
OR51E1	no match
LCK	no match
SLC7A2	hexamer in one location within 3' UTR
ABCA8	no match
DRD1	hexamer in one location within 3' UTR
ZMYND8	hexamer in two locations within 3'UTR
KALRN	no match
GPR77	no match
MLL	hexamer in one location within 3' UTR
PIP5K1A	no match
TAS2R13	no match
ALPI	no match
BACE1	no match
TAS2R10	not found in database
CAMKK1	no match
C8G	no match
ITPKA	no match
GDPD1	hexamer in two locations within 3' UTR
RYR3	no match
FLAD1	no match
PDE5A	hexamer in one location within 3' UTR
RAD50	hexamer in one location within 3' UTR
VIPR2	no match
GRPR	no match
LPHN2	no match
NCOA6	no match
FZD2	no match
HGS	no match
GART	no match
PIK3C2A	hexamer in one location within 3' UTR

Gene Symbol	5'-GAAACA-3'
CDK16	no match
GPR126	hexamer in one location within 3' UTR
FMNL1	no match
DUSP4	hexamer in two locations within 3' UTR
PTPRD	no match
GIT2	hexamer in three locations within 3' UTR
NR4A3	hexamer in two locations within 3' UTR
ADRBK2	hexamer in one location within 3' UTR
SENP6	hexamer in two locations within 3' UTR
DGKD	hexamer in two locations within 3' UTR
NCOA1	hexamer in five locations within 3' UTR
ADRA2B	hexamer in three locations within 3' UTR
CNKSR1	no match
CDK18	hexamer in one location within 3' UTR
TPSAB1	no match
USP10	no match
KCNH5	hexamer in one location within 3' UTR
KREMEN2	hexamer in one location within 3' UTR

Table A2. HAEC mRNA transcripts that were up-regulated or down-regulated following delivery of CLIC(C) siRNA relative to CLIC(C)-U4A mutant.

Transcript ID	Gene Symbol	Name	RefSeq	p-value	SAM q-value (%)	Fold Change (Negative Indicates CLIC2 down-regulated vs mutant)
8165692		---	---	0.031631	17.9637	-2.73748
7902541	IFI44L	interferon-induced protein 44-like	NM_006820	0.022691	17.9637	-2.00103
8068713	MX1	myxovirus (influenza virus) resistance 1, interferon-inducible	NM_002462	0.015001	17.9637	-1.86237
7964640		---	---	0.017268	17.9637	-1.62343
7951091		---	---	0.009011	17.9637	-1.61372
7959482		---	---	0.019299	17.9637	-1.57954
8127987	SNORD50A	small nucleolar RNA, C/D box 50A	NR_002743	0.015405	17.9637	-1.56698
7969091		---	---	0.00999	17.9637	-1.55793
8140907		---	---	0.020332	17.9637	-1.53483
7952339	SNORD14C	small nucleolar RNA, C/D box 14C	NR_001453	0.018541	17.9637	-1.50519
7951341		---	---	0.014682	17.9637	-1.43389
7911331		---	---	0.014317	17.9637	-1.40324
7924463		---	---	0.014317	17.9637	-1.40324
7927089		---	---	0.014317	17.9637	-1.40324
7945347		---	---	0.014317	17.9637	-1.40324
7998115		---	---	0.014317	17.9637	-1.40324
8031997		---	---	0.014317	17.9637	-1.40324
8102530		---	---	0.014317	17.9637	-1.40324
8137668		---	---	0.014317	17.9637	-1.40324
7939912	TRIM48	tripartite motif-containing 48	NM_024114	0.005948	17.9637	-1.4031
8073332		---	---	0.010579	17.9637	-1.40015
8173627		---	---	0.002809	17.9637	-1.3619

Transcript ID	Gene Symbol	Name	RefSeq	p-value	SAM q-value (%)	Fold Change (Negative Indicates CLIC2 down-regulated vs mutant)
8081233		---	---	0.004376	17.9637	-1.36033
7982751		---	---	0.011742	17.9637	-1.35719
8173156		---	---	0.012164	17.9637	-1.35029
8069508	CCDC29	coiled-coil domain containing 29	ENST00000333394	0.004879	17.9637	-1.34807
8055486		---	---	0.008705	17.9637	-1.3451
8168412	LOC554203	alanyl-tRNA synthetase domain containing 1 pseudogene	BC029480	0.011567	17.9637	-1.33906
8165656		---	---	0.001565	17.9637	-1.33826
8065853		---	---	0.007025	17.9637	-1.33543
8022761		---	---	0.010789	17.9637	-1.31968
7929072	IFIT5	interferon-induced protein with tetratricopeptide repeats	NM_012420	0.012384	17.9637	-1.31614
7900214		---	---	0.000955	17.9637	-1.3111
8081107		---	---	0.008624	17.9637	-1.31104
7928821		---	---	0.010724	17.9637	-1.28762
8084605		---	---	0.005136	17.9637	-1.28731
7896746		---	---	0.010914	17.9637	-1.28075
8092594		---	---	0.011726	20.4893	-1.27162
8072139		---	---	0.004583	17.9637	-1.26927
7942379		---	---	0.006148	17.9637	-1.25061
7950003	MRGPRD	MAS-related GPR, member D	NM_198923	0.023057	24.8533	1.25216
7992756		---	---	0.007131	19.0368	1.25487
7934731	C1D	C1D nuclear receptor co-repressor	NM_006333	0.020163	24.8533	1.25554
7976806		---	---	0.014037	22.0738	1.25831
8131705	RPL23P8	ribosomal protein L23 pseudogene 8	NR_026673	0.004311	18.6434	1.25898
7913801		---	---	0.003384	18.6434	1.25992
7959144		---	---	0.015752	22.0738	1.27117
7941863		---	---	0.003355	18.6434	1.27129

Transcript ID	Gene Symbol	Name	RefSeq	p-value	SAM q-value (%)	Fold Change (Negative Indicates CLIC2 down-regulated vs mutant)
8122277		---	---	0.007724	19.0368	1.27417
8137131		---	---	0.009623	20.4893	1.27739
8060080	OR6B2	olfactory receptor, family 6, subfamily B, member 2	NM_001005853	0.028654	24.8533	1.28917
8120059		---	---	0.01944	22.8629	1.29556
7925031	FLJ30430	hypothetical protein FLJ30430	AK054992	0.000801	17.9637	1.29809
7932964	C1D	C1D nuclear receptor co-repressor	NM_006333	0.006937	18.6434	1.302
8175098	GPR119	G protein-coupled receptor 119	NM_178471	0.000619	17.9637	1.30264
8150034		---	---	0.007808	18.6434	1.30586
7972977		---	---	0.018187	22.0738	1.32413
8124510	HIST1H2BL	histone cluster 1, H2bl	NM_003519	0.035442	24.8533	1.34068
8019804	ROCK1	Rho-associated, coiled-coil containing protein kinase 1	BC041849	0.027604	24.8533	1.34177
7980906		---	---	0.01478	20.4893	1.34784
8052698	C1D	C1D nuclear receptor co-repressor	NM_006333	0.005958	18.6434	1.34983
7921358		---	---	0.003357	17.9637	1.3693
8026339	SNRPG	small nuclear ribonucleoprotein polypeptide G	NM_003096	0.016268	20.4893	1.42612
8164006		---	---	0.041601	24.8533	1.46167
8062490	SNORA60	small nucleolar RNA, H/ACA box 60	NR_002986	0.00077	17.9637	1.46669
8115679		---	---	0.045774	24.8533	1.59728
8129309		---	---	0.010283	17.9637	1.70123
7914216	SNORA16A	small nucleolar RNA, H/ACA box 16A	NR_003035	0.018496	18.6434	1.72586

Table A3. Chemicals purchased from Sigma for screening hit confirmation and follow-up experiments.

Catalog Number	Compound Description
E2250	Ellagic Acid
320056	1,10-Phenanthroline monohydrate
S7067	SB 202190
D3943	DAPH
B5002	5-Bromo-2′-deoxyuridine
T3434	Tyrphostin AG 490
T4693	Tyrphostin AG 537
T5193	Tyrphostin AG 698
C2538	Carboplatin
C8221	Caffeic acid phenethyl ester
A5762	Adenine 9-β-D-arabinofuranoside
W104	WIN 62,577
A2169	3′-Azido-3′-deoxythymidine
D7802	Daidzein
S0693	SB 204741
M2011	Melphalan
C1386	Curcumin
A8199	N-Acetyl-L-cysteine
C1768	Cytosine β-D-arabinofuranoside
T7165	Tyrphostin 23
22040	β-Carotene purum
N4286	NU20580

Table A4. Compound screening enhancer hits.

Compound Name	Function	Normalized Luminescence
Ellagic acid	Antioxidant, pp60^{src} tyrosine kinase inhibitor	7.9
1,10-Phenanthroline monohydrate	Metalloprotease inhibitor, metal chelator	6.4
Tyrphostin AG 698	EGFR protein tyrosine kinase inhibitor	3.7
4-(4-Fluorophenyl)-2-(4-hydroxyphenyl)-5-(4-pyridyl)-1H-imidazole	p38 MAP kinase inhibitor	3.5
4,5-Dianilinophthalimide	Protein tyrosine kinase inhibitor	3.0
5-Bromo-2 -deoxyuridine	Nucleoside analog, mutagen	2.6
Tyrphostin AG 490	JAK-2 protein tyrosine kinase inhibitor, EGFR protein tyrosine kinase inhibitor	2.5
Carboplatin	Alkylating agent, platinum analog	2.5
Caffeic acid phenethyl ester	Antioxidant	2.5
Vidarabine	Nucleoside analog, inhibits viral replication	2.4
WIN 62,577	Tachykinin receptor NK1 antagonist	2.4
7,4 -Dihydroxyflavone	Antioxidant	2.3
3-Azido-3-deoxythymidine (AZT)	Nucleoside analog, reverse transcriptase inhibitor	2.2
Daidzein	Antioxidant, isoflavone	2.2
Resveratrol	Antioxidant, flavanoid	2.1
N-(1-Methyl-1H-5-indolyl)-N′-(3-methyl-5-isothiazolyl)urea	Serotonin receptor 5-HT2B antagonist	2.1

Compound Name	Function	Normalized Luminescence
7,2 -Dihydroxyflavone	Antioxidant, flavanoid	2.1
Melphalan	Alkylating agent	2.1
Tyrphostin AG 537	EGFR protein tyrosine kinase inhibitor	2.1
8-Bromo-cAMP sodium	Protein kinase A activator	2.0

References

1. Roth CM, Sundaram S. Engineering synthetic vectors for improved DNA delivery: Insights from intracellular pathways. *Annu Rev Biomed Eng* 2004; **6:** 397-426.

2. Elouahabi A, Ruysschaert J-M. Formation and Intracellular Trafficking of Lipoplexes and Polyplexes. *Mol Ther* 2005; **11**(3)**:** 336-347.

3. Widera G, Austin M, Rabussay D, Goldbeck C, Barnett SW, Chen M *et al.* Increased DNA Vaccine Delivery and Immunogenicity by Electroporation In Vivo. *The Journal of Immunology* 2000; **164**(9)**:** 4635-4640.

4. Wang R, Doolan DL, Le TP, Hedstrom RC, Coonan KM, Charoenvit Y *et al.* Induction of Antigen-Specific Cytotoxic T Lymphocytes in Humans by a Malaria DNA Vaccine. *Science* 1998; **282**(5388)**:** 476-480.

5. Tacket CO, Roy MJ, Widera G, Swain WF, Broome S, Edelman R. Phase 1 safety and immune response studies of a DNA vaccine encoding hepatitis B surface antigen delivered by a gene delivery device. *Vaccine* 1999; **17**(22)**:** 2826-2829.

6. Gaspar HB, Parsley KL, Howe S, King D, Gilmour KC, Sinclair J *et al.* Gene therapy of X-linked severe combined immunodeficiency by use of a pseudotyped gammaretroviral vector. *The Lancet* 2004; **364**(9452)**:** 2181-2187.

7. Hacein-Bey-Abina S, Von Kalle C, Schmidt M, McCormack MP, Wulffraat N, Leboulch P *et al.* LMO2-Associated Clonal T Cell Proliferation in Two Patients after Gene Therapy for SCID-X1. *Science* 2003; **302**(5644)**:** 415-419.

8. Hacein-Bey-Abina S, Le Deist Fo, Carlier Fdr, Bouneaud Cc, Hue C, De Villartay J-P *et al.* Sustained Correction of X-Linked Severe Combined Immunodeficiency by ex Vivo Gene Therapy. *New England Journal of Medicine* 2002; **346**(16)**:** 1185-1193.

9. Hacein-Bey-Abina S, von Kalle C, Schmidt M, Le Deist Fo, Wulffraat N, McIntyre E *et al.* A Serious Adverse Event after Successful Gene Therapy for X-Linked Severe Combined Immunodeficiency. *New England Journal of Medicine* 2003; **348**(3)**:** 255-256.

10. Raper SE, Yudkoff M, Chirmule N, Gao G-P, Nunes F, Haskal ZJ *et al.* A Pilot Study of In Vivo Liver-Directed Gene Transfer with an Adenoviral Vector in Partial Ornithine Transcarbamylase Deficiency. *Human Gene Therapy* 2002; **13**(1)**:** 163-175.

11. Raper SE, Chirmule N, Lee FS, Wivel NA, Bagg A, Gao G-p *et al.* Fatal systemic inflammatory response syndrome in a ornithine transcarbamylase deficient patient following adenoviral gene transfer. *Molecular Genetics and Metabolism*; **80**(1-2)**:** 148-158.

12. Atchison RW, Casto BC, Hammon WM. Adenovirus-Associated Defective Virus Particles. *Science* 1965; **149**(3685)**:** 754-756.

13. Linden RM, Winocour E, Berns KI. The recombination signals for adeno-associated virus site-specific integration. *Proceedings of the National Academy of Sciences* 1996; **93**(15)**:** 7966-7972.

14. Samulski RJ, Zhu X, Xiao X, Brook JD, Housman DE, Epstein N *et al.* Targeted integration of adeno-associated virus (AAV) into human chromosome 19. 1991.

15. Ponnazhagan S, Erikson D, Kearns WG, Zhou SZ, Nahreini P, Wang X-s *et al.* Lack of Site-Specific Integration of the Recombinant Adeno-Associated Virus 2 Genomes in Human Cells. *Human Gene Therapy* 1997; **8**(3)**:** 275-284.

16. Weitzman MD, KyÃ¶stiÃ¶ SR, Kotin RM, Owens RA. Adeno-associated virus (AAV) Rep proteins mediate complex formation between AAV DNA and its

integration site in human DNA. *Proceedings of the National Academy of Sciences* 1994; **91**(13)**:** 5808-5812.

17. Hermonat PL, Muzyczka N. Use of adeno-associated virus as a mammalian DNA cloning vector: transduction of neomycin resistance into mammalian tissue culture cells. *Proceedings of the National Academy of Sciences* 1984; **81**(20)**:** 6466-6470.

18. Russell DW, Alexander IE, Miller AD. DNA synthesis and topoisomerase inhibitors increase transduction by adeno-associated virus vectors. *Proceedings of the National Academy of Sciences* 1995; **92**(12)**:** 5719-5723.

19. Samulski RJ, Chang LS, Shenk T. Helper-free stocks of recombinant adeno-associated viruses: normal integration does not require viral gene expression. *J Virol* 1989; **63**(9)**:** 3822-3828.

20. Summerford C, Samulski RJ. Membrane-Associated Heparan Sulfate Proteoglycan Is a Receptor for Adeno-Associated Virus Type 2 Virions. *J Virol* 1998; **72**(2)**:** 1438-1445.

21. Sanlioglu S, Benson PK, Yang J, Atkinson EM, Reynolds T, Engelhardt JF. Endocytosis and Nuclear Trafficking of Adeno-Associated Virus Type 2 Are

Controlled by Rac1 and Phosphatidylinositol-3 Kinase Activation. *J Virol* 2000; **74**(19)**:** 9184-9196.

22. Wu Z, Miller E, Agbandje-McKenna M, Samulski RJ. {alpha}2,3 and {alpha}2,6 N-Linked Sialic Acids Facilitate Efficient Binding and Transduction by Adeno-Associated Virus Types 1 and 6. *J Virol* 2006; **80**(18)**:** 9093-9103.

23. Bell CL, Vandenberghe LH, Bell P, Limberis MP, Gao G-P, Van Vliet K *et al.* The AAV9 receptor and its modification to improve in vivo lung gene transfer in mice. *The Journal of Clinical Investigation*; **121**(6)**:** 2427-2435.

24. Burger C, Gorbatyuk OS, Velardo MJ, Peden CS, Williams P, Zolotukhin S *et al.* Recombinant AAV Viral Vectors Pseudotyped with Viral Capsids from Serotypes 1, 2, and 5 Display Differential Efficiency and Cell Tropism after Delivery to Different Regions of the Central Nervous System. *Mol Ther* 2004; **10**(2)**:** 302-317.

25. Auricchio A. Pseudotyped AAV vectors for constitutive and regulated gene expression in the eye. *Vision Research* 2003; **43**(8)**:** 913-918.

26. Wang L, Louboutin J-P, Nichols TC, Wilson JM. 161. Novel pseudotyped AAV vectors for hemophilia B gene therapy. *Mol Ther* 2004; **9**(S1)**:** S61-S62.

27. Fire A, Xu S, Montgomery MK, Kostas SA, Driver SE, Mello CC. Potent and specific genetic interference by double-stranded RNA in Caenorhabditis elegans. *Nature* 1998; **391**(6669)**:** 806-811.

28. Caplen NJ, Parrish S, Imani F, Fire A, Morgan RA. Specific inhibition of gene expression by small double-stranded RNAs in invertebrate and vertebrate systems. *Proceedings of the National Academy of Sciences* 2001; **98**(17)**:** 9742-9747.

29. Jackson AL, Bartz SR, Schelter J, Kobayashi SV, Burchard J, Mao M *et al.* Expression profiling reveals off-target gene regulation by RNAi. *Nat Biotech* 2003; **21**(6)**:** 635-637.

30. Jackson AL, Linsley PS. Noise amidst the silence: off-target effects of siRNAs? *Trends in Genetics* 2004; **20**(11)**:** 521-524.

31. Lin X, Ruan X, Anderson MG, McDowell JA, Kroeger PE, Fesik SW *et al.* siRNA-mediated off-target gene silencing triggered by a 7 nt complementation. Vol 33. 2005:4527-4535.

32. Qiu S, Adema CM, Lane T. A computational study of off-target effects of RNA interference. Vol 33. 2005:1834-1847.

33. Birmingham A, Anderson EM, Reynolds A, Ilsley-Tyree D, Leake D, Fedorov Y *et al.* 3 ' UTR seed matches, but not overall identity, are associated with RNAi off-targets. *Nat Methods* 2006; **3**(3)**:** 199-204.

34. Ma Y, Creanga A, Lum L, Beachy PA. Prevalence of off-target effects in Drosophila RNA interference screens. *Nature* 2006; **443**(7109)**:** 359-363.

35. Anderson E, Boese Q, Khvorova A, Karpilow J. Identifying siRNA-Induced Off-Targets by Microarray Analysis. *RNAi*. 2008, pp 45-63.

36. Fedorov Y, Anderson EM, Birmingham A, Reynolds A, Karpilow J, Robinson K *et al.* Off-target effects by siRNA can induce toxic phenotype. *RNA* 2006; **12**(7)**:** 1188-1196.

37. Wallen AJ, Barker GA, Fein DE, Jing H, Diamond SL. Enhancers of Adeno-associated Virus AAV2 Transduction via High Throughput siRNA Screening. *Mol Ther* 2011; **19**(6)**:** 1152-1160.

38. M D Hoggan NRB, and W P Rowe. Studies of small DNA viruses found in various adenovirus preparations: physical, biological, and immunological characteristics. *PNAS* 1966; **55**(6)**:** 1467-1474.

39. Bartlett JS, Samulski RJ, McCown TJ. Selective and Rapid Uptake of Adeno-Associated Virus Type 2 in Brain. *Human Gene Therapy* 1998; **9**(8)**:** 1181-1186.

40. Chao H, Liu Y, Rabinowitz J, Li C, Samulski RJ, Walsh CE. Several Log Increase in Therapeutic Transgene Delivery by Distinct Adeno-Associated Viral Serotype Vectors. *Mol Ther* 2000; **2**(6)**:** 619-623.

41. Mehendale S, van Lunzen J, Clumeck N, Rockstroh J, Vets E, Johnson PR *et al.* A Phase 1 Study to Evaluate the Safety and Immunogenicity of a Recombinant HIV Type 1 Subtype C Adeno-Associated Virus Vaccine. *AIDS Research and Human Retroviruses* 2008; **24**(6)**:** 873-880.

42. Flotte TR, Zeitlin PL, Reynolds TC, Heald AE, Pedersen P, Beck S *et al.* Phase I Trial of Intranasal and Endobronchial Administration of a Recombinant Adeno-Associated Virus Serotype 2 (rAAV2)-CFTR Vector in Adult Cystic Fibrosis Patients: A Two-Part Clinical Study. *Human Gene Therapy* 2003; **14**(11)**:** 1079-1088.

43. Moss RB, Milla C, Colombo J, Accurso F, Zeitlin PL, Clancy JP *et al.* Repeated Aerosolized AAV-CFTR for Treatment of Cystic Fibrosis: A Randomized Placebo-Controlled Phase 2B Trial. *Human Gene Therapy* 2007; **18**(8)**:** 726-732.

44. Aitken ML, Moss RB, Waltz DA, Dovey ME, Tonelli MR, McNamara SC *et al.* A Phase I Study of Aerosolized Administration of tgAAVCF to Cystic Fibrosis Subjects with Mild Lung Disease. *Human Gene Therapy* 2001; **12**(15)**:** 1907-1916.

45. Manno CS, Chew AJ, Hutchison S, Larson PJ, Herzog RW, Arruda VR *et al.* AAV-mediated factor IX gene transfer to skeletal muscle in patients with severe hemophilia B. *Blood* 2003; **101**(8)**:** 2963-2972.

46. Brass AL, Dykxhoorn DM, Benita Y, Yan N, Engelman A, Xavier RJ *et al.* Identification of Host Proteins Required for HIV Infection Through a Functional Genomic Screen. *Science.* Vol 319. 2008:921-926.

47. König R, Zhou Y, Elleder D, Diamond TL, Bonamy GMC, Irelan JT *et al.* Global Analysis of Host-Pathogen Interactions that Regulate Early-Stage HIV-1 Replication. 2008; **135**(1)**:** 49-60.

48. Teresa IN, Hongmei M, Tami P-M, Yupeng H, Gennadiy K, Preethi K *et al.* Identification of host genes involved in hepatitis C virus replication by small interfering RNA technology. *Hepatology* 2007; **45**(6)**:** 1413-1421.

49. Tai AW, Benita Y, Peng LF, Kim S-S, Sakamoto N, Xavier RJ *et al.* A Functional Genomic Screen Identifies Cellular Cofactors of Hepatitis C Virus Replication. *Cell Host & Microbe* 2009; **5**(3)**:** 298-307.

50. Supekova L, Supek F, Lee J, Chen S, Gray N, Pezacki JP *et al.* Identification of Human Kinases Involved in Hepatitis C Virus Replication by Small Interference RNA Library Screening. *Journal of Biological Chemistry* 2008; **283**(1)**:** 29-36.

51. Krishnan MN, Ng A, Sukumaran B, Gilfoy FD, Uchil PD, Sultana H *et al.* RNA interference screen for human genes associated with West Nile virus infection. *Nature* 2008; **455**(7210)**:** 242-245.

52. Clemente R, Sisman E, Aza-Blanc P, de la Torre JC. Identification of Host Factors Involved in Borna Disease Virus Cell Entry Through a siRNA Functional Genetic Screen. *J Virol***:** JVI.02274-02209.

53. Barker GA, Diamond SL. RNA Interference Screen to Identify Pathways That Enhance or Reduce Nonviral Gene Transfer During Lipofection. *Mol Ther* 2008; **16**(9)**:** 1602-1608.

54. Tusher VG, Tibshirani R, Chu G. Significance analysis of microarrays applied to the ionizing radiation response. *Proceedings of the National Academy of Sciences of the United States of America* 2001; **98**(9)**:** 5116-5121.

55. Pesole G, Liuni S, Grillo G, Licciulli F, Larizza A, Makalowski W *et al.* UTRdb and UTRsite: specialized databases of sequences and functional elements of 5â€² and 3â€² untranslated regions of eukaryotic mRNAs. *Nucleic Acids Res* 2000; **28**(1)**:** 193-196.

56. Grillo G, Turi A, Licciulli F, Mignone F, Liuni S, Banfi S *et al.* UTRdb and UTRsite (RELEASE 2010): a collection of sequences and regulatory motifs of the untranslated regions of eukaryotic mRNAs. *Nucleic Acids Res*; **38**(suppl 1)**:** D75-D80.

57. Douglas Zhang X, Yang XC, Chung N, Gates A, Stec E, Kunapuli P *et al.* Robust statistical methods for hit selection in RNA interference high-throughput screening experiments. *Pharmacogenomics* 2006; **7**(3)**:** 299-309.

58. A Biron C. Initial and innate responses to viral infections -- pattern setting in immunity or disease. *Current Opinion in Microbiology* 1999; **2**(4)**:** 374-381.

59. Perry AK, Chen G, Zheng D, Tang H, Cheng G. The host type I interferon response to viral and bacterial infections. *Cell Res* 2005; **15**(6)**:** 407-422.

60. Taniguchi T, Takaoka A. The interferon-[alpha]/[beta] system in antiviral responses: a multimodal machinery of gene regulation by the IRF family of transcription factors. *Current Opinion in Immunology* 2002; **14**(1)**:** 111-116.

61. Biron CA. Role of early cytokines, including alpha and beta interferons (IFN-[alpha]\[beta]), in innate and adaptive immune responses to viral infections. *Seminars in Immunology* 1998; **10**(5)**:** 383-390.

62. Darnell Jr JE, Kerr IM, Stark GR. Jak-STAT pathways and transcriptional activation in response to IFNs and other extracellular signaling proteins. *Science* 1994; **264**(5164)**:** 1415-1421.

63. Khabar KSA, Siddiqui YM, Al-Zoghaibi F, Al-Haj L, Dhalla M, Zhou A *et al.* RNase L Mediates Transient Control of the Interferon Response through Modulation of the Double-stranded RNA-dependent Protein Kinase PKR. *Journal of Biological Chemistry* 2003; **278**(22)**:** 20124-20132.

64. Kimball SR. Eukaryotic initiation factor eIF2. *The International Journal of Biochemistry & Cell Biology* 1999; **31**(1)**:** 25-29.

65. Yoshida J, Mizuno M, Nakahara N, Colosi P. Antitumor Effect of an Adeno-associated Virus Vector Containing the Human Interferon-β Gene on Experimental Intracranial Human Glioma. *Cancer Science* 2002; **93**(2)**:** 223-228.

66. Streck CJ, Dickson PV, Ng CYC, Zhou J, Hall MM, Gray JT *et al.* Antitumor efficacy of AAV-mediated systemic delivery of interferon-[beta]. *Cancer Gene Ther* 2005; **13**(1)**:** 99-106.

67. Shih C-S, Laurie N, Holzmacher J, Spence Y, Nathwani A, Davidoff A *et al.* AAV-mediated Local Delivery of Interferon-β for the Treatment of Retinoblastoma in Preclinical Models. *NeuroMolecular Medicine* 2009; **11**(1)**:** 43-52.

68. Chen JH, Ho C-T. Antioxidant Activities of Caffeic Acid and Its Related Hydroxycinnamic Acid Compounds. *Journal of Agricultural and Food Chemistry* 1997; **45**(7)**:** 2374-2378.

69. Mah C, Qing K, Khuntirat B, Ponnazhagan S, Wang X-S, Kube DM *et al.* Adeno-Associated Virus Type 2-Mediated Gene Transfer: Role of Epidermal Growth Factor Receptor Protein Tyrosine Kinase in Transgene Expression. *J Virol* 1998; **72**(12)**:** 9835-9843.

70. Zhong L, Zhao W, Wu J, Li B, Zolotukhin S, Govindasamy L *et al.* A Dual Role of EGFR Protein Tyrosine Kinase Signaling in Ubiquitination of AAV2 Capsids and Viral Second-strand DNA Synthesis. *Mol Ther* 2007; **15**(7)**:** 1323-1330.

71. Yarden Y, Schlessinger J. Self-phosphorylation of epidermal growth factor receptor: evidence for a model of intermolecular allosteric activation. *Biochemistry* 1987; **26**(5)**:** 1434-1442.

72. Labieniec M, Gabryelak T, Falcioni G. Antioxidant and pro-oxidant effects of tannins in digestive cells of the freshwater mussel Unio tumidus. *Mutation Research/Genetic Toxicology and Environmental Mutagenesis* 2003; **539**(1-2)**:** 19-28.

73. Labieniec M, Gabryelak T. Interactions of tannic acid and its derivatives (ellagic and gallic acid) with calf thymus DNA and bovine serum albumin using spectroscopic method. *Journal of Photochemistry and Photobiology B: Biology* 2006; **82**(1)**:** 72-78.

74. Whitley AC, Stoner GD, Darby MV, Walle T. Intestinal epithelial cell accumulation of the cancer preventive polyphenol ellagic acid--extensive binding to protein and DNA. *Biochemical Pharmacology* 2003; **66**(6)**:** 907-915.

75. Narayanan BA, Geoffroy O, Willingham MC, Re GG, Nixon DW. p53/p21(WAF1/CIP1) expression and its possible role in G1 arrest and apoptosis in ellagic acid treated cancer cells. *Cancer Letters* 1999; **136**(2)**:** 215-221.

76. Sud'ina GF, Mirzoeva OK, Pushkareva MA, Korshunova GA, Sumbatyan NV, Varfolomeev SD. Caffeic acid phenethyl ester as a lipoxygenase inhibitor with antioxidant properties. *FEBS Letters* 1993; **329**(1-2)**:** 21-24.

77. Aruoma OI, Halliwell B, Hoey BM, Butler J. The antioxidant action of N-acetylcysteine: Its reaction with hydrogen peroxide, hydroxyl radical, superoxide, and hypochlorous acid. *Free Radical Biology and Medicine* 1989; **6**(6)**:** 593-597.

78. Sun Y, Bian J, Wang Y, Jacobs C. Activation of p53 transcriptional activity by 1,10-phenanthroline, a metal chelator and redox sensitive compound. *Oncogene* 1997; **14**(4)**:** 385.

79. Alexander IE, Russell DW, Miller AD. DNA-damaging agents greatly increase the transduction of nondividing cells by adeno-associated virus vectors. *J Virol* 1994; **68**(12)**:** 8282-8287.

80. Yalkinoglu AÖ, Heilbronn R, Bürkle A, Schlehofer JR, zur Hausen H. DNA Amplification of Adeno-associated Virus as a Response to Cellular Genotoxic Stress. *Cancer Research* 1988; **48**(11)**:** 3123-3129.

81. Kastan MB, Onyekwere O, Sidransky D, Vogelstein B, Craig RW. Participation of p53 Protein in the Cellular Response to DNA Damage. *Cancer Research* 1991; **51**(23 Part 1)**:** 6304-6311.

82. Arris CE, Boyle FT, Calvert AH, Curtin NJ, Endicott JA, Garman EF *et al.* Identification of Novel Purine and Pyrimidine Cyclin-Dependent Kinase Inhibitors with Distinct Molecular Interactions and Tumor Cell Growth Inhibition Profiles. *Journal of Medicinal Chemistry* 2000; **43**(15)**:** 2797-2804.

83. Wang X. miRDB: A microRNA target prediction and functional annotation database with a wiki interface. *RNA* 2008; **14**(6)**:** 1012-1017.

84. Wang X, El Naqa IM. Prediction of both conserved and nonconserved microRNA targets in animals. *Bioinformatics* 2008; **24**(3)**:** 325-332.